ROLE OF RGDSK HELICAL ROSETTE NANOTUBES (RGDSK-HRNs) IN INTESTINAL MUCOSAL IMMUNE RESPONSE TO *E. COLI* INFECTION

A Thesis Submitted to the

College of Graduate and Postdoctoral Studies

In Partial Fulfillment of the Requirements

For the Degree of Doctor of Philosophy

In the Department of Veterinary Biomedical Sciences

University of Saskatchewan

Saskatoon

By

LE NGUYEN PHUONG KHANH

PERMISSION TO USE

In presenting this thesis in partial fulfillment of the requirements for a Postgraduate degree from the University of Saskatchewan, I agree that the Libraries of this University may make it freely available for inspection. I further agree that permission for copying of this thesis in any manner, in whole or in part, for scholarly purposes may be granted by the professor or professors who supervised my thesis work or, in their absence, by the Head of the Department or the Dean of the College in which my thesis work was done. It is understood that any copying or publication or use of this thesis or parts thereof for financial gain shall not be allowed without my written permission. It is also understood that due recognition shall be given to me and to the University of Saskatchewan in any scholarly use which may be made of any material in my thesis.

Requests for permission to copy or to make other uses of materials in this thesis in whole or part should be addressed to:

Head of the Department of Veterinary Biomedical Sciences

Western College of Veterinary Medicine

#52 Campus Drive, University of Saskatchewan

Saskatoon, Saskatchewan, S7N 5B4, Canada

OR Dean

College of Graduate and Postdoctoral Studies

University of Saskatchewan

116 Thorvaldson Building, 110 Science Place

Saskatoon, Saskatchewan, S7N 5C9, Canada

ABSTRACT

Integrin αvβ3 is a transmembrane receptor recognizing arginine-glycine-aspartic acid (RGD) tripeptide. However, the expression and functions of integrin αvβ3 in intestinal epithelium in diarrhea, particularly due to *E. coli* infection, have been poorly understood. Therefore, we performed a series of experiments to fill the gap information.

We found that integrin αvβ3 is localized on the plasma membrane, the cytoplasm, and the nucleus of IPEC1 cells. The expression of integrin αvβ3 on IPEC1 decreased at 15 minutes but returned to normal after 90 minutes of infection with *E. coli* F4 ($P<0.05$). The light, fluorescent and electron microscopy, western blots, and 96-well plate binding assays showed the presence of integrin αvβ3-like protein domain in *E. coli* F4. The data from binding assays on 96-well plates also suggests that *E. coli* F4 may have an RGD-like sequence binding to host integrin αvβ3.

Immunohistochemistry showed normal porcine jejuna strongly expressed integrin αvβ3 in the nucleus and the apical surface of epithelia as well as crypts. Integrin αvβ3 expression was decreased in the epithelium but increased in the vascular endothelium of the jejunum infected with *E. coli* or *E. coli* associated with *Salmonella* ($P<0.05$). Immunogold electron microscope confirmed the presence of integrin αvβ3 in the porcine jejunal epithelium and *E. coli*.

Flow cytometry showed that RGDSK-HRNs did not significantly increase dead IPEC1. RGDSK-HRNs improved IPEC1 cell survival upon *E. coli* infection compared with *E. coli* infection alone group ($P<0.05$). Western blot showed that in *E. coli* infection, RGDSK-HRNs-FITC significantly decreased the level of p-p53 compared with monoclonal anti-integrin αvβ3 antibody treatment, and the level of p-p38MAPK compared with RGDSK-FITC group ($P<0.05$).

The data from *ex vivo* villus adhesion assays showed that RGDSK-HRNs-FITC significantly reduced the number of *E. coli* adhering to villi for up to 12 hours compared with the *E.*

coli-only challenged group ($P<0.05$). Both RGDSK-FITC peptide and monoclonal anti-integrin αvβ3 antibody were effective in inhibiting the *E. coli* binding to villi for up to 24 hours compared with the *E. coli*-only challenged group ($P<0.05$). Consistently, in the *in vivo* porcine gut loop model, RGDSK-HRNs-FITC significantly decreased the number of *E. coli* binding to villi compared with *E. coli* treatment group ($P<0.05$). RGDSK-HRNs-FITC did not significantly decrease the number of *E. coli* colonies in the supernatant.

In conclusion, our study highlighted that integrin αvβ3 was involved in *E. coli* colonization in the porcine intestine. Also, the novel RGDSK-HRNs-FITC could inhibit the attachment of *E. coli* to the epithelium, suggesting a potential intervention in combination with antimicrobial and other treatments for *E. coli* infection in the future.

ACKNOWLEDGMENTS

I would not have completed the Doctor of Philosophy program without the help of many people. It is hard to describe how important they are throughout these years and my future life.

I would like to sincerely express my gratitude to my primary supervisor, Dr. Baljit Singh, for being a fantastic mentor. I am thankful to him very much for his important intellectual and stipend support, his constant encouragement, as well as his time helping me even on weekends or holidays.

I would like to sincerely thank my co-supervisor, Dr. Volker Gerdts, for his help and advice, especially on the gut loop model, throughout my Ph.D. program.

I would like to thank my advisory committee members (Dr. Hicham Fenniri, Dr. Elemir Simko, and Dr. Gurpreet Aulakh), as well as graduate chairs (Dr. Daniel MacPhee, Dr. Ali Honaramooz, Dr. Karen Machin, and Dr. Gillian Muir) for their valuable advice, help, and contributions to my program. I would like to sincerely thank the external examiner, Dr. Caroline Duchaine, for her time on my thesis defense day.

Special sincere thanks need to be given to Saskatchewan Agriculture Development Fund (ADF), Natural Science and Engineering Research Council (NSERC), Integrated Training Program in Infectious Disease - Food Safety and Public Policy at the University of Saskatchewan, Western College of Veterinary Medicine Graduate Student Scholarship, Department of Veterinary Biomedical Sciences Devolved Graduate Scholarship for the funding of the project and stipend support.

I also greatly appreciate the help of staff and faculty members at the Department of Veterinary Biomedical Sciences, Western College of Veterinary Medicine, Molecular Microbiology Laboratory, the Westgen Research facilities, Glassware and Media Preparation (Dr. Janet Hill, Dr.

John Harding, Dr. Susan Detmer, Dr. Susantha Gomis, Ms. Noreen Rapin, Mr. Jim Gibbons, Ms. Vivian Pulga, Ms. Susan Cook, Ms. Kim Tran, Eiko Kawamura, LaRhonda Sobchishin, Fernando Champika, Mrs. Pollard Cindy, Mrs. Cheryl Hack, Mrs. Painchaud-Rattai Elise, Chelsea Nafe, Samantha Ekanayake, Angie Turner, Benjamin Elwood, Mr. Nesbitt Darren, Shanna Banman, Ms. Sarah Caldwell, …), at VIDO (Dr. Walker Stew, Dr. Elsie Parson, Dr. Maria Fuchs, Dr. Jan Erickson, Dr. Colette Wheler, Dr. Tiffany Matejka, Dr. Meurens Francois, Dr. Heather Wilson, Jill, Kerby, Raf Jamil), at Prairie Diagnostic Services Inc. (Dr. Yanyun Huang), and at other colleges (Dr. Call Douglas at Washington State University, Dr. Eric Cox at Gent University, Dr. George Katselis at The College of Medicine at The University of Saskatchewan).

I'd further like to acknowledge for the help of the former and current members in Professor Baljit Singh's lab to me to overcome difficulties in my academic and personal life: Dr. Stacy Anderson, Dr. Abdul Lone, Dr. David Schneberger, Dr. Nicole House, Dr. Yadu Balachandran, Dr. Amanda Nascimento, Sushmita Maltare, Jacqueline Harrison, Jasmine Hui, Cuong Quach, Hiroko, Jessica Brocos Duda, and Manpreet Kaur, …

I would like to sincerely thank my professors and colleagues at the Faculty of Animal Science and Veterinary Medicine, Nong Lam University (The University of Agriculture and Forestry), Ho Chi Minh City, Vietnam, for their help and allowing me on-leave to pursue the Ph.D. degree in Canada. I would like to thank all my friends for their help in my academic and personal life both prior to and during my Ph.D. program.

Last but not least, I am under an obligation to my parents (Mr. Le Van Tin, Mrs. Nguyen Thi Kim Lien), parents-in-law (Mr. Quach Anh Hao, Mrs. Pham Thi Dau), my family (Husband Quach Chi Cuong, sons Quach Le Hieu Thong, and Quach Le Andrew) and brothers Le Tin Vinh Quang, Quach Anh Khoa, and Quach Diem Phuong for their help, and support for my career goals.

TABLE OF CONTENTS

Page

LIST OF FIGURES

Page

LIST OF ABBREVIATIONS

BSA:	Bovine Serum Albumin
cfu:	colony forming unit
CHO:	Chinese Hamster Ovary
CHOB3:	Chinese hamster ovary B3 cells
CHOB3C5:	Chinese hamster ovary B3C5 cells
eae:	*E. coli* attaching and effacing
E. coli:	*Escherichia coli*
ECM:	Extracellular Matrix
EGFR:	Epithelial Growth Factor Receptor
ETEC:	Enterotoxigenic *Escherichia coli*
FACS:	Fluorescence-Activated Cell Sorting
FAK:	Focal Adhesion Kinase
FBS:	Fetal Bovine Serum
gB:	glycoprotein B
gH:	glycoprotein H
H bond:	Hydrogen bond
HRNs:	Helical Rosette Nanotubes
HUVECs:	Human Umbilical Vein Endothelial Cells
IHC:	Immunohistochemistry
im.:	intramuscularly
IPEC1:	Intestinal Porcine Epithelial 1 Cell Line
IRS1:	Insulin Receptor Substrate 1

kDa:	kilodaltons
LPS:	Lipopolysaccharide
LT:	Heat-Labile toxin
MAPK:	Mitogen-Activated Protein Kinase
NY-1:	New York 1 virus (Hantavirus)
PBS:	Phosphate-buffered saline
PDGF:	Platelet-Derived Growth Factor
PDS:	Prairie Diagnostic Services Inc.
PHV:	Prospect Hill virus (Hantavirus)
PI3:	phosphoinositide 3 (kinase)
PK:	Protein Kinase
PKA:	Protein Kinase A
RGD:	arginine-glycine-aspartic acid (amino acid)
RGDSK:	arginine - glycine - aspartic acid – serine – lysin (amino acid)
SNV:	Sin Nombre virus (Hantavirus)
ST:	Heat-Stable toxin
TBL:	Twin Base Linker (aminobutane linker molecule)
TLRs:	Toll-Like Receptors
TSB:	Tryptone Soya Broth
VEGF:	Vascular Endothelial Growth Factor
VIDO-InterVac:	Vaccine and Infectious Disease Organization-International Vaccine Centre
VTEC:	Verotoxin-producing *E. coli*

CHAPTER 1. INTRODUCTION

The financial losses due to intestinal diseases are in billions of dollars every year in Canada (95) and America (74). Moreover, infectious diarrhea caused more than 2 million deaths in children below five years old in many countries, such as Nigeria, Congo, Pakistan, India, and China (20). The intestine is a unique organ of the body that is continuously exposed to the environment through food (160). In addition to the resident microbiome, the intestine also has the potential of entry for pathogens from the environment, such as *E. coli* (19). Although *E. coli* has been studied for many decades, the recent interventions cannot wholly control intestinal diseases and foodborne illness due to *E. coli* because of the continual change of *E. coli* characteristics (mutations), and multiple virulence factors (34, 35, 185, 247).

Integrin αvβ3 recognizes Arg-Gly-Asp (RGD), and plays an essential role in cell adhesion to the extracellular matrix, cell signalling transduction, cell-cell interaction, cell survival, angiogenesis and leukocyte migration (98, 121, 159, 199, 220, 260). The integrin αvβ3 integrates the external milieu with the intracellular cytoskeleton (98, 227, 231, 243). Dysregulating integrin αvβ3 signal can disrupt tissue homeostasis, and contribute to important stages in the pathogenesis of many diseases (17, 62, 121, 199, 255, 260), such as diabetes (171), hyperglycemia (171), osteoporosis (101), angiogenesis (199), tissue repair (199), tumour growth (5, 199), and rheumatoid arthritis (260). Integrin αvβ3 also appears to be the receptor for a wide range of virus families such as rotavirus, coxsackievirus A9, parechovirus 1, and tat protein of HIV (243).

Recently, a wide range of applications of nanotechnology in drug development and delivery has been studied (132). The helical rosette nanotubes (HRNs), invented by Dr. Hicham Fenniri in 2001 (39, 63, 64), are one of the highly novel nanomaterials known till now. These nanotubes are synthesized from guanine-cytosine (G∧C) motif building blocks through a rapid

hierarchical self-assembly process in water, becoming a novel metal-free, organic, water-soluble, tunable, biologically-inspired, and biocompatible nanomaterial (63, 64, 223). Scientists have found numerous potential applications of HRNs, notably in the medical areas such as potential targeted drug delivery for chondrification, bone regeneration, and cancer (39, 134, 224, 268-270). Recently, RGD peptide sequences have been integrated into nanomaterials to bio-functionalize them (83, 125, 155). In our study, Arg-Gly-Asp-Ser-Lys (RGDSK) peptide-functionalized helical rosette nanotubes (RGDSK-HRNs-FITC) were designed to target integrins for specific medical and biological applications by RGDSK, and can be visualized under a fluorescent microscope by FITC (39, 225). In 2017, House and colleagues performed an isolated perfused lung model in male Sprague-Dawley rats where intravascular RGDSK-HRNs-FITC administration reduced cell activation measured through the elaboration of adhesion molecules and ROS production (99).

However, to our knowledge, the effects of RGDSK-HRNs-FITC on the adhesion of *E. coli* to gut epithelium via interactions with integrin αvβ3 have not been investigated. Therefore, in this study, we tested the hypothesis that RGDSK-HRNs-FITC would localize along the integrin αvβ3 and block the attachment of *E. coli* to porcine jejunum.

CHAPTER 2. REVIEW OF THE LITERATURE

2.1. INTEGRINS

In 1986, integrins were named by Dr. Hynes as an integral complex of type I glycoproteins on the cell surfaces to connect the extracellular matrix and the cytoskeleton (102, 231, 243). The adhesion of the extracellular matrix to the cell via these integrins receptors is critical for cell integrity (90). For more than three decades, the structure, biology, and therapeutic applications of integrins have been widely studied (29, 187). In 2016, commercial drugs, mostly α4-series integrins inhibitors such as vedolizumab to treat ulcerative colitis and Crohn's disease, made more than three billion U.S. dollars (187).

Horton and co-authors described that integrins are a superfamily of heterodimeric transmembrane receptors composing of two subunits, α and β (98). Twenty-four heterodimers of integrins are reported from the mixture of eighteen subunits α including α1- α11, αE, αv, αIIb, αL, αM, αX, and αD and eight subunits β including β1- β8 (17, 29, 229, 243). The reasons for the specific pair of subunit such as αv with β1, β3, β5, β6, β8 but not with β2, β4, or β7 are unknown (11). Each integrin heterodimer is formed by the extended structure of α and β chains in building an N-terminal globular head portion (98). The extracellular domain of integrins has a cysteine-rich segment, and the cytoplasmic domain has a tyrosine residue which can be phosphorylated by tyrosine kinase (231). The tail of both α and β chains connects with the cytoskeleton by their intracellular C-termini (98, 243).

Scientists have described the activity of integrins in transducing signalling. Each subunit of integrins has an extracellular domain, a single transmembrane region, and a short cytoplasmic domain (8). The extracellular domain, known as a ligand-binding site, can bind various extracellular matrix proteins (26, 137) to transmit signals from outside into the cell interior and vice versa

to the affinity of their ligand-binding site (11, 29, 229, 266). Although smaller than the extracellular domains, the cytoplasmic domains activate integrins by their association with adaptor proteins, including tyrosine kinases (26, 137), actin-binding proteins (26, 137), Src, focal adhesion kinase, integrin-linked kinase, kindlin, paxillin, talin, and vinculin (103, 170). Consequently, these interactions rearrange cytoskeleton, thus affecting not only the structure and function of extracellular domains but also cell migration (103). The activation state of the integrins is characterized by the separation, twisting, pistoning, and hinging of their tails (103).

The binding ability of each integrin depends on its affinity to different integrin ligands. The integrins can bind to extracellular matrix ligands, cell-surface ligands, and soluble ligands (229). For example, αv integrins have high-affinity binding to fibronectin, one of the extracellular matrix proteins (179). Moreover, eight out of 24 integrins in total recognize aminoacid Arginine-Glycine-Aspartic acid (RGD) triad in the native ligands (17, 199), known as a general integrin-binding motif (29). These integrins are five αv integrins, two β1 integrins (α5β1, α8β1), and αIIbβ3 (29, 196). Some extracellular matrix ligands exposed their RGD sequence upon denaturation or proteolytic cleavage to bind these integrins (17). The RGD amino acid sequence may contain different specificity interaction with many receptors but through the same mechanism (184, 196). The molecular mechanisms involving the RGD sequence have been studied for many decades (184). Recently, RGD-containing peptides and mimics have been studied to develop new therapeutics for diseases via targeting integrins (196). Scientists have developed a radio-labelled form such as RGD-mimetic to determine accurate affinity and binding kinetics to integrins, not only αvβ3 but also αvβ1, αvβ5, αvβ8, α5β1, and α8β1) (89).

The integrins with a highly bent physiologic conformation have a low affinity for binding biological ligands (230). The affinity of integrins for binding to ligands may also depend on

kindlins, also known as fermitins (194). In general, this kindlins family binds to the tail of β integrin to activate the integrin. Consequently, this activated integrin can bind to a ligand, so the cell adheres, spreads, and migrates (194). Among three kindlins, kindlin-2, which binds to the tails of integrin β3, is expressed ubiquitously, notably in striated and smooth muscle cells.

The integrins are expressed in many species such as mammals, chicken, zebrafish, sponges, the nematode *Caenorhabditis elegans* (two alpha and one beta subunits, forming two integrins) and the fruit-fly *Drosophila melanogaster* (five alpha and one beta, forming five integrins) (17, 29, 229, 243). The expression of integrins is enhanced by some cytokines such as transforming growth factor (TGF)-β1 (93, 170, 187), and a growth inhibitor of normal hepatocytes and HCC cells that induces apoptosis and cellular senescence in the liver (166). The sizes of integrin α subunits vary from 120-180 kDa, containing seven repetitions of 60 amino acid tandem (98). The integrin β chains have sizes varying from 90-110 kDa (98). In 1985, Pytela and colleagues described integrins as the specific vitronectin receptor, having 125 kDa and 115 kDa molecular weight, bound to Arg-Gly-Asp tripeptides in vitronectin while the specific fibronectin receptor has 140 kDa molecular weight protein in human MG-63 osteosarcoma cell line (184). The authors classified that these two different receptors expressed at the cell surface (184). They also mentioned that the RGD containing peptides possibly had one binding site interfering with the fibronectin receptor and another specifically interacting with the vitronectin receptor (184).

The integrin functions show their involvement in cancer (αvβ6) (89), fibrosis (αvβ6) (89), thrombosis, inflammation, and pathogenesis of some diseases due to their interaction with their ligands and cytokines such as activating TGFβ (187). In detail, integrins were found as signalling molecules in tumour stroma remodeling, the survival, proliferation, differentiation, migration, and

invasion of cancer cells (90). The survival of different cell-types is dependent on the regulation of cellular processes through interactions of specific ligands with integrins (90, 93, 170).

The association of integrins with extracellular matrix supports the survival of a variety of cell types. For example, during serum starvation culture condition, Caco-2 gut epithelial cells, ureteral epithelial cells, and human umbilical vein endothelial cells (HUVECs) showed more nuclear fragmentation (151). In suspension without extracellular matrix, the endothelium showed both morphological and biochemical characteristics of apoptosis, including shrinking, membrane blebbing, fragmented nuclei, and apoptosis-specific gene expression (151). Additionally, scientists reported that the survival of early chick sympathetic neurons depended on the molecular interaction between the extracellular matrix and integrins (59). The extracellular matrix, particularly laminin, is responsible for mediating proliferation and development of avian sympathetic neurons (59). The laminins are also essential for the early survival and differentiation of neuronal cells (114). However, fewer live neuronal cells were observed on other extracellular matrices such as fibronectin or a substrate of molecules from heart cell-conditioned medium *in vitro* (59). Different from these above cells, Meredith and colleagues noted that without extracellular matrix coating, mesothelial cells and fibroblasts can still maintain their survival in suspension (151). It is explained that integrins stimulate actin remodeling for adhesion and survival signals via the phosphoinositide (PI) 3 kinase or mitogen-activated protein kinase (MAPK) pathway (80, 152). The absence of integrin can activate p53 or *jun* N- terminal kinase (JNK) death signals, and down-regulate Bcl-2 expression and function of the endothelium (152).

2.2. ALPHA V INTEGRINS (αv) INVOLVEMENT IN DISEASE

The αv integrins subunit is a partner of integrins β1, β3, β5, β6, β8 (22). Scientists have addressed the role of αv integrins through the use of inhibitors such as C8 (an integrin αvβ1

inhibitor) (22), DC9711 (an inhibitor of integrin αvβ6) (22), MABT207 monoclonal antibody (αvβ1, αvβ3, αvβ5, αvβ6, αvβ8) (22), SB273005 (22) and Cilengitide (16) (inhibitors of integrin αvβ3 and integrin αvβ5), and GSK3008348 small molecule (an integrin αvβ6 inhibitor in a trial study of pulmonary fibrosis) (89). In 2011, Weis and colleagues noted that integrin αv activation aggravates tumour cell invasion, growth, and metastatic spread (255). They found that blockage of integrin αv could inhibit the angiogenesis by slowing down the adhesion, migration, and proliferation of endothelium in cancer (255).

Numerous interventions to αv integrins have been developed clinically (187). For instance, a human antibody to αv integrins-abituzumab could inhibit TGFβ, consequently reducing trans-differentiating fibroblasts into myofibroblasts, and their extracellular matrix products such as collagen in scleroderma (118, 187). Although this product likely could work in the phase II trial for scleroderma, it was not feasible because of some difficulties in patient enrollment and risks such as inflammatory and cancerous development potentially associated with this drug (118, 135, 187).

Targeting αv integrins may have the potential for clinical therapeutics for most fibrotic diseases. For example, Bon and co-workers recently demonstrated that αv integrins associate with the production and accumulation of extracellular matrix proteins during the interaction with renal fibroblasts and human primary renal proximal tubular epithelia co-cultured *in vitro* (22). This association reveals a crucial role for αv integrins in the tubulointerstitial fibrosis of chronic kidney diseases causing renal failure (22). They also found that in the co-culture of renal fibroblasts with human primary renal proximal tubular epithelia, blockage of αv integrins dramatically down-regulated the levels of total spontaneous extracellular matrix proteins and individual extracellular matrix components such as fibronectin, as well as collagen I and III (22). Among these blocking

substrates, CWHM12, a pan αv integrins inhibitor, could block the full range of αv heterodimers (αvβ1, αvβ3, αvβ5, αvβ6, αvβ8) (22). This small molecule was the most effective inhibitor reducing total production and accumulation of extracellular matrix in that study (22), suggesting that individual αv integrins have varying severity effects such as on fibrotic diseases on their own (94).

Another example is that in 2013, Henderson and co-authors published a paper describing that deleting αv integrins attenuated hepatic fibrosis by carbon tetrachloride and pulmonary as well as renal fibrosis by Pdgfrb-Cre in murine models (94). Besides, this group found that the pharmacological CWHM 12 blocked αv integrins and moderated both liver and lung fibrosis in a mouse model (94). Additionally, Bagnato and colleagues previously reported that cilengitide could block both integrins αvβ3 and αvβ5, preventing the fibrosis and renal vascular abnormalities in the chronic reactive oxygen species - induced systemic sclerosis murine model (16).

In human lung fibrosis, the expression of αv integrins was increased in pneumocytes of the alveolar ducts and alveoli (97). The αv integrins were known as one of the tissue-restricted stimulators of transforming growth factor (TGF) β, an initiator of fibrosis characterized by the pathological deposition of excess extracellular matrix (97). An RGD motif in latent TGFβ binds to αv integrins, consequently activating the TGFβ (9). The TGFβ1 induced alveolar epithelial cell apoptosis, triggering epithelial - to - mesenchymal cell transition, as well as epithelial injury, and thus worsening the fibrosis (122). Therefore, αv integrins inhibition is one of the selected strategies to modulate TGFβ (97). The expression of αv integrins and integrin αvβ6 was augmented noticeably in cutaneous and lung injury, as well as bleomycin treatment (162). Blockage of the protein by low doses of monoclonal anti-αvβ6 integrin antibodies partially restricted TGFβ, lessen the fibrosis injury (hydroxyproline content in the lung, collagen reporter transgene expression), but without aggravating inflammation in murine bleomycin-induced pulmonary fibrosis model (97).

Recently, Bon and colleagues reported that the precursor form of TGFβ released latency-associated-peptide binding back to the mature TGFβ homodimer (22). This latency-associated peptide of TGFβ1 and TGFβ3 contains the RGD motif, which can activate αv integrins, including αvβ1, αvβ3, αvβ5, αvβ6, and αvβ8 (22). Other scientists have also added that integrin αvβ6 activate TGFβ (9), a centre mediator of fibrosis in many organs such as lungs (162), biliary tract (251), and kidney (145).

2.3. BETA 3 INTEGRINS (β3) INVOLVEMENT IN DISEASE

β3 integrins were found in endothelium and engaged in vascular permeability as well as the maintenance of vascular integrity (76). β3 integrins also play a part in the mechanism of virus entry, depending on the virus species, cell types, and host species (161). This was exemplified in work undertaken by Gavrilovskaya and colleagues in 1999 that hantaviruses invaded human vascular endothelium via β3 integrins as an entry receptor of the virus (75). These viruses caused hemorrhagic fever with renal syndrome and hantavirus pulmonary syndrome (75). More than ten years after that, Matthys and co-workers found that human β3 integrins have aspartic amino acid residue at position 39 (D39) in an N-terminal plexin-semaphorin-integrin domain which was required for Andes virus infection, causing a fatal hantavirus pulmonary syndrome in Syrian hamster model and humans (147). This amino acid was suggested to be crucial for Orthohantaviral entry in primates (161). However, β3 integrins are not present in *Apodemus agrarius* mouse field strain, although this mouse strain is susceptible to Hantavirus (161). A likely explanation is that the virus may use other alternate receptors to enter the primate or rodent cells of the host (161). These viruses use β3 integrins to dysregulate endothelial migration as part of the disease pathogenesis (76).

Recently, Wu and co-workers reported that the mRNA level of β3 integrins was increased upon nickel chloride ($NiCl_2$) exposure, consequently causing lung and skin cancer (262). The

authors explained that $NiCl_2$ activated TGF-β signalling, enhancing vascular endothelial growth factor (VEGF) product (262). VEGF plays a pivotal role in angiogenesis (33). This factor binds to VEGF receptors on the endothelium to promote angiogenesis in embryonic development, wound healing, and cancer (33). The VEGF contributes to the formation of new abnormal vasculature in and around the tumour, stimulating its exponential growth (33). The blood vessels in the tumour have irregular, tortuous structure and shape with dead ends. They do not develop well as venules, arterioles, and capillaries. They are malfunctioning, leaky, and hemorrhagic vessels leading to an increase in interstitial pressure, and hypoxia (33).

2.4. INTEGRIN ALPHA V BETA 3 (αvβ3)

2.4.1. Integrin αvβ3 biology

In 1985, "vitronectin receptor" was revealed firstly in human osteosarcoma (MG-63) by Dr. Pytela and co-workers as it bound to RGD containing peptide on human vitronectin plasma protein (184). One year after that, the proteins were cloned and sequenced by Dr. Suzuki and co-workers (227). After that, this class of receptors was proposed as integrin αvβ3 to highlight its function in integrating the external milieu with the intracellular cytoskeleton (98, 227, 231, 243). In 1986, Suzuki and co-workers illustrated that the αv subunit (150 kDa) comprises of a disulfide bonding a heavy chain (125 kDa) and a light chain (25 kDa) derived from a proteolytically cleaved precursor (227). The 125 kDa chain has an NH2-terminal amino acid sequence homologous with the one of lymphocyte function-associated antigen 1 (LFA-1) and macrophage antigen 1 (Mac-1), implying its function likely as adhesion receptor of leukocytes (227). These scientists also mentioned that the β3 subunit has 115 kDa molecular weight (227). However, in 1997, Horton and colleagues described that integrin αvβ3 has a bigger molecular weight of αv chain and smaller β3

chain in tissue, exhibiting many typical structures and functions as a member of the integrin superfamily (98). The integrin αv chain (160 kDa) has a 25 kDa C-terminal fragment, which is released on the proteolytic cleavage process in reduced condition (98). The integrin αv gene is revealed at 2d31-32, synthesizing 1018 amino acids with 13 N-linked glycosylation sites and four typical N-terminal repeated motifs (98). The integrin β3 chain (85 kDa) has a gene located at 17q21, synthesizing 762 amino acids (98).

2.4.2. Integrin αvβ3 expression and functions in organs

Integrin αvβ3 was expressed in osteoclasts and vascular endothelium (98). The expression of integrin αvβ3 on neovascular endothelial cells is intense (220). Similarly, its expression augmented during angiogenesis, osteosarcoma (98), and ovarian carcinoma (200). Integrin αvβ3 is also found in bronchial vasculature in the lung, epithelium of the small intestine, bile duct, and renal proximal convoluted tubules in the pig, dog, and cattle (213). Moreover, integrin αvβ3 was detected in COS-1 cells and human primary fibroblasts by FACS analysis (178). Integrin αvβ3 is also expressed on the apical uterine luminal epithelium and conceptus trophectoderm of pig and sheep, respectively (107). Through binding with secreted phosphoprotein 1, this receptor stimulates cell-cell adhesion and communication, contributing to the adherence of the conceptus to the uterus for implantation (107).

In 2000, Dr. Singh and co-authors reported that integrin αvβ3 was expressed in the vascular bed, endothelium, vascular smooth muscle, and large bronchial epithelium of normal rat lungs, implying its function in the microvascular system and airway (210). Interestingly, integrin αvβ3 was not found in the blood vessels of the liver, brain, skeletal muscle, and skin from rats, although the protein was present in other cells outside the blood vessels of these organs (210). For example, in the rat liver, the weak positive staining of integrin αvβ3 occurred in a branch of the

portal vein. In the brain, integrin αvβ3 is present in occasional cells. In skeletal muscle, integrin αvβ3 was found in connective tissue. In skin, integrin αvβ3 was observed in epithelium and connective tissue (210).

However, the absence of integrin αvβ3 on these organs above under resting conditions may change in different conditions. For example, Okada and colleagues reported that integrin αvβ3 was not found in normal basal ganglia of baboons (167). Interestingly, in the nonhuman primate model of MCA:O/R cerebral ischemia, integrin αvβ3 was present in middle cerebral artery occlusion, suggesting the function of integrin αvβ3 in this condition (167). These authors explained that in the ischemia condition, the increased expression of fibroblast growth factor could stimulate the transcription of integrin αvβ3 gene (167).

Immunohistochemistry of anterior mouse segment of eyes indicated that integrin αvβ3 is present at the trabecular meshwork, sclera, and ciliary body (62). Similarly, in human eyes, integrin αvβ3 is also observed within the inner wall of Schlemm's canal in the corneal epithelium, ciliary muscle (62). Immunofluorescence and FACS analysis confirmed the presence of integrin αvβ3 on human trabecular meshwork cells, and its expression increased in dexamethasone-induced glaucoma group (71). Activating integrin αvβ3 by AP5 antibody elevated intraocular pressure in mouse eyes (62). The enhanced intraocular pressure causes glaucoma, risking irreversible blindness (41). The deficiency of β3 integrins significantly reduced intraocular pressure, which is the fluid pressure inside the eyes (62). A small decrease of the integrin αvβ3 level could also affect the function of trabecular meshwork and decreased intraocular pressure in a tamoxifen eye drops – inducible $Cre^{+/-}\ \beta3^{flox/flox}$ mouse model (62). These results implied the critical function of integrin αvβ3 in glaucoma (62). In contrast, in 2007, Jacqueline and co-authors reported that integrin αvβ3 was not present at the retina and cornea of cats, cows, dogs, horses, pigs, and rats (175). The findings from

this observation suggested that the absence of integrin αvβ3 on the eyes of these animals could inhibit its ligands such as angiostatin from the program cell death of these cells, or it may be related to other eye diseases.

About twenty years ago, Singh and his colleagues demonstrated that integrin αvβ3 was present on the bronchiolar epithelia, and alveolar macrophages in healthy human lungs (211) as well as in the lungs of cattle, dogs, and pigs (213). Its expression is increased in macrophages in human septic lungs (211). These scientists also reported that the expression of integrin αvβ3 was induced in neutrophils and whole lung in *Streptococcus pneumonia* infected rat model (105). Interestingly, the level of integrin αv and integrin β3 subunits was decreased in *E. coli* infected rat lungs compared to normal control and *S. pneumoniae* infection groups (105). These authors explained that the levels of integrins were changed because of the crosstalk between integrins (105). In 2017, Brilha and co-workers also reported that integrin αvβ3 controlled the collagenase activity, adhesion, and migration of monocyte (27). The over-expression of integrin αvβ3 in diseases has suggested that inhibiting integrin αvβ3 activation to calm down the immune system can be a promising targeted therapy (27, 125).

Additionally, in 1995, the Bhattacharya laboratory found that integrin αvβ3 might regulate hydraulic conductivity across the pulmonary vascular barrier (239). This group reported that an antibody against integrin αvβ3 attenuated the up-regulation of lung capillary hydraulic conductivity (239). Using oil split drop technique, these scientists also reported that endothelial integrin αvβ3-vitronectin interaction enhanced transcapillary fluid, which was involved in complement-mediated pulmonary edema in rat lung (239). These results suggested that integrin αvβ3 on endothelium plays a part in cellular adherence and maintenance of vascular integrity (239).

Integrin αvβ3 plays a role in macrophage activation, osteoclast development, bone resorption, and inflammatory angiogenesis, involving the mechanism of rheumatoid arthritis and other arthropathies (260). Humanized monoclonal antibody IgG1 – Vitaxin/MEDI-522 was studied to block integrin αvβ3 from other ligands such as osteopontin and vitronectin, expecting to slow down the process of the pathogenesis of the arthropathies (260). Besides, integrin αvβ3 on osteoclast can bind RGD amino acid sequence on vitronectin, osteopontin, and bone sialoprotein. The integrin αvβ3 can manage the activity of this cell, including its adhesion, migration, bone resorption, cytoskeletal organization, and polarization (57), which is crucial for the remodeling process of the bone (101). Some nonpeptide antagonists of integrin αvβ3 was studied for preventing osteoporosis, such as 3(S)-(6-methoxypyridin-3-yl)-3-[2-oxo-3-[3-(5,6,7,8-tetrahydro-[1,8]-naphthyridin-2-yl)propyl]imidazolidine-1-yl] propionic acid 6 compound (101). This oral antagonist compound is a small molecule mimicking the structure of RGD binding site to specific integrin αvβ3 and was recommended as its good pharmacokinetics in rat, dog, and rhesus monkey (101).

Integrin αvβ3, known as vitronectin receptor, plays an essential role in cell adhesion to the extracellular matrix, cell signalling transduction, cell-cell interaction, cell survival, angiogenesis, and leukocyte migration (98, 121, 159, 199, 220, 260). Dysregulating integrin αvβ3 signal can disrupt tissue homeostasis and contribute to important stages in the pathogenesis of many diseases (121, 199, 260), for instance, tumour (5), diabetes (171), hyperglycemia (171), osteoporosis (101), angiogenesis (199), tissue repair (199), tumour growth (199), and rheumatoid arthritis (260).

Interestingly, in 2013, Gagen and co-authors reported that the activation of integrin αvβ3 by dexamethasone could inhibit the phagocytosis by regulating the integrin αvβ5-FAK-mediated pathway in human trabecular meshwork cells (71). Dexamethasone increased the level of integrin αvβ3 but not integrin αvβ5 (71). Likely, activated integrin αvβ3 and integrin αvβ5 have

antagonistic roles in phagocytosis (71). It could be explained that the activated integrin αvβ3 possibly mediated the actin cytoskeletal rearrangement and filament recruitment in phagocytosis activities (41, 71). However, in an earlier study using mouse bone marrow neutrophils and peritoneal macrophages, Friggeri and colleagues reported that high mobility group box protein 1, a protein in the extracellular milieu, could reduce the efferocytosis of macrophage to apoptotic neutrophils (68). These scientists explained that this protein could block the interaction of integrin αvβ3 on macrophage, milk fat globule EGF factor 8 opsonin, and phosphatidylserine on the surface of apoptotic neutrophils (68).

In 1995, Lawson and colleagues described that the presence of integrin αvβ3 on the leading edge is higher than that on the rear of migrating neutrophils (133). At the leading edge of migrating neutrophils, integrin αvβ3 stays along with F-actin, which is localized with talin (133). These authors also reported that integrin αvβ3 was endocytosed and recycled, which belonged to Ca(2+) and calcineurin-dependent pathway (133). Additionally, the distribution of integrin αvβ3 on the extending pseudopod helps migrating neutrophils adhering to vitronectin (133). Moreover, the tight binding of integrin αvβ3 to ligands, such as fibronectin make the polarized distribution of integrin αvβ3 (133), and facilitates the migration of cells. About ten years after that, Aulakh and co-authors added that integrin αvβ3 is distributed on the lipid raft of neutrophils (14). These scientists reported the role of integrin αvβ3 in the migration of neutrophils via its binding to RGD on angiostatin protein, which is an endogenous angiogenic inhibitor cleaved from plasminogen (14). These authors also highlighted that this binding consequently deactivated neutrophils and prevented their migration (14). Also, blocking integrin αvβ3 by LM609 antibody partially prevented the effects of angiostatin, such as recovering neutrophil polarization (14).

In the blood vessel, integrin αvβ3 promotes angiogenesis, including endothelial cell adhesion, migration, and survival under the control of kindlin-2 (141). Integrin αvβ3 is also the key mediator of smooth muscle cell filopodia formation and migration in hyperglycemia (171). Integrin αvβ3 was stimulated by thrombospondin ligand and was modulated by Rap1 (171). In detail, integrin αvβ3 is activated during hyperglycemia due to its interaction with the high level of thrombospondin, vitronectin, and osteopontin ligands secreted by the vascular smooth muscle (42). This activation leads to the stimulation of MAP kinases, resulting in the proliferation and migration of smooth muscle, mitogenic response, and atherosclerosis (42).

Integrin αvβ3 is a biomarker and a cell adhesion molecule, involved in angiogenesis and cancerous metastasis (5, 38, 53). Angiogenesis is a crucial factor for tumour growth and metastasis, depending on some signaling molecules and pathways (256). One example of this is the study carried out by Brooks and co-workers in 1994 that ligation of integrin αvβ3 induced vasculogenesis (28). Therefore, integrin αvβ3 was noticed early as a potential therapeutic target for suppressing angiogenesis in cancer (5). Antagonists of integrin αvβ3 were used to down regulate the development and spread of cancer cells (38). About three decades ago, scientists found that angiogenesis on human tumours transplanted onto the chick choriollantic membrane was disrupted by a cyclic peptide or a functional monoclonal antibody antagonist of integrin αvβ3 (28). These antagonists enhanced apoptosis of angiogenic blood vessels (28).

As mentioned above, antiangiogenics targeting selective integrin αvβ3 imply the potential of exploiting this integrin for therapeutics of pathological conditions such as cancer and inflammatory diseases. One of such is RGDechiHCit comprising of a cyclic RGD motif and two echistatin moieties (199). The disintegrin RGDechiHCit prohibits the intracellular mitogenic signalling, proliferation, and tube forming of the endothelial cell line. This disintegrin also delayed

wound healing in the murine model. However, although blocking the function of integrin αvβ3 or integrin αvβ5 may suppress neovascularization and tumour growth, others reported that deficiency of β3 integrins or β5 integrins support tumorigenesis by enhancing tumour growth, tumour angiogenesis and vascular endothelial growth factor (VEGF) – induced blood vessel growth and angiogenic response to hypoxia in a mouse model (190). Overall, it is agreed that the integrin αvβ3 promotes angiogenesis through the suppression of apoptosis in endothelial cells and the promotion of their migration through interactions with cytoskeleton.

2.4.3. Integrin αvβ3 association with other receptors

Integrin αvβ3 can bind extracellular matrix protein, comprising of fibronectin, vitronectin, von Willebrand factor, tenascin, osteopontin, fibrillin, fibrinogen, bone sialic protein, and thrombospondin (100, 243). In addition to those, integrin αvβ3 can recognize soluble ligands, including fibrinogen, cysteine-rich angiogenic protein 61, mouse connective tissue growth factor (Fisp12/mCTGF), matrix metalloproteinase, endostatin, angiostatin, tumstatin (243). The activity and role of integrin αvβ3 are complex to understand and depends on the nature of the proteins, extracellular matrix composition, organs, stage of diseases, conditions, environment (91, 121), other networks of signalling activators (62, 91) and cross-talk with other receptors (86). Weis and co-workers also mentioned that the ligation of an integrin to a specific matrix protein created a signal of cross-talk between integrins (256)

Integrin αvβ3 engaged the activities of other integrins through its interaction with the extracellular matrix. An example of this is the study performed by Blystone and co-workers in 1999 (21). The lab explained that the activation of integrin αvβ3 by binding with its ligand gave the signal to Ser752 of the β3 cytoplasmic tail to suppress the activation of calcium- and

calmodulin-dependent protein kinase II (CamKII) (21). This suppression restricted the function of integrin α5β1 on mediating both phagocytosis and migration of human peripheral blood monocyte-derived macrophages in an *in vitro* study (21). These scientists also reported that although mutation of the Ser752 residue on the β3 subunit had no impact on the ability of integrin αvβ3 binding to its ligand, this mutation still deleted the effect of integrin αvβ3 on integrin α5β1 (21).

The extracellular domain of integrin αvβ3 but not β1 integrins can interact with trans-membrane protein such as insulin receptor (202), platelet-derived growth factor receptor-β (PDGF-Rβ) (23, 202), and vascular endothelial growth factor receptor-2 (VEGF-R2) (23, 243). The PDGF-Rβ associates sufficiently with the extracellular domain of the β3 subunit, while VEGF-R2 needs αv subunit for the interaction (23). These two receptor tyrosine kinases were stimulated by growth factors, promoting the proliferation and migration of cells adhering to vitronectin through its integrin αvβ3 (23). In 1993, Juliano and co-authors noted that the importance of integrin αvβ3 as a receptor in transducing signals to the cellular interior via tyrosine phosphorylation (113). The involvement of these cell-matrix interactions in the cellular response to growth factors implicates the crucial role of integrin αvβ3 in tissue regeneration, angiogenesis, and tumour metastasis (202).

The cytoplasmic domain of integrin αvβ3 has an association with cytoplasmic intracellular proteins. For example, in 1994, Vuori and co-authors revealed that integrin αvβ3 on FG human pancreatic carcinoma cell line interacted with insulin receptor substrate 1 (IRS1) (248). The IRS1 could bind to growth factor receptor-bound protein two, as well as phosphatidylinositol-3' kinase to control insulin signalling (248). The association between integrin αvβ3 and IRS1was enhanced by insulin challenging (248). These researchers reported that the insulin treatment increased the expression of integrin αvβ3 on the FG cells plated on vitronectin, and that expression was higher than that on cells plated on collagen, a ligand more specific for integrin β1 (248).

As mentioned above, the topic "cross-talk" between the integrin αvβ3 and other integrins such as integrin α5β1 was brought up with evidence many years. For example, in 2002, a group of researchers reported that the decreased expression of integrin αvβ3 might trigger the activity of β1 integrins, activating angiogenesis in a mouse model (190). In an *in vitro* study carried by Gonzalez and co-workers in the same year, they found that blocking both integrin α3β1 and α6β1 by antibodies MKID2, and 6S6 may change the activity of integrin αvβ3 (87). Interestingly, blocking integrin αvβ3 by LM609 antibody could indirectly inhibit integrin α3β1 and α6β1 on immortalized human bone marrow endothelial cells adhering to laminin-5 ligand (87). However, entirely knocking-out the integrin αvβ3 triggered integrin α3β1and α6β1 function on angiogenesis in a mouse model (87). These results suggested that the function of integrin αvβ3 may depend on integrin α3β1 and α6β1 and vice versa. An explanation for the interaction was that integrin αvβ3, and integrin α3β1 interacted with the ligand G domain of laminin α4 subunit which distributed in the basement membrane of blood vessels, where the interaction was involved in vascular development in a mouse model (87). LM609 antibody blocking integrin αvβ3 could prevent endothelial cells from adhering to the G domain (87).

Another example of the cross-talk was described in the study of Ly and co-workers in 2003. They revealed that integrin αvβ3 was activated and responsible for mediating integrin α5β1-lacked Chinese hamster ovary B3 cells (CHOB3) adhering to and migrating on fibrinogen (144). LM609 function-blocking antibody significantly prevented CHOB3 cells binding to fibrinogen (144). The adhesive function of integrin αvβ3 on CHOB3 cells to fibronectin was not influenced even under soluble MnCl2 agonist, implying the stable and high affinity of integrin αvβ3 in these cells (144). However, MnCl2 agonist activated integrin αvβ3, enhancing the adherence of Chinese hamster ovary B3C5 (CHOB3C5) cells to fibrinogen (144). Interestingly, CHOB3C5 cells

expressing both integrin αvβ3 and integrin α5β1 have the lower adhesive ability of cells to fibrinogen compared with CHOB3 cells (144). Impressively, Chinese hamster ovary X5C5 cells without integrin αvβ3 did not bind to fibrinogen (144). The authors suggested that integrin αvβ3 mediated the cellular adhesive activity under the regulation of integrin α5β1, which depended on the cytoplasmic tail of the α chain and independent of ligand agonist binding (144).

This distinction is further explained in a study by Orr and co-workers in 2006. In an *in vitro* study of shear stress on bovine aortic endothelial cells, these scientists found that Protein Kinase (PK) A and C play a critical part in the crosstalk of integrin αvβ3 and others (86, 169). Fibrinogen and fibronectin bind to integrin αvβ3, and the simultaneous onset of flow activates the PI3-kinase with subsequent stimulation of PKCα (169). These activations lead talin to suppress integrin α2β1 (169). However, in the presence of collagen-binding to integrins, the junctional mechanoreceptor complex gets the signal from the onset of flow to activate PI3-K, subsequently stimulate integrin α2β1 (169). These actions activate matrix-specific PKA to effect on talin, resulting in suppressing integrin αvβ3 (169). Inhibiting PKA with chemical kinase inhibitor such as 14-22 myristoylated trifluoroacetate restore ligand affinity of integrin αvβ3 (169).

Reversely, integrin αvβ3 activity also depends on other integrins. For example, it is known that fibronectin binds both integrins αvβ3 and α5β1 on endothelium, providing a signal for angiogenesis (86). In 2010, Gonzalez and colleagues showed that blocking integrin α5β1 by anti-integrin β1 antibody could perturb integrin αvβ3 binding to fibronectin, eventually preventing angiogenesis (86). Additionally, the expression of β1 integrin can affect the mRNA transcription stability of β3 integrins, leading to reduced expression of integrin αvβ3 in GD25 cells derived from murine embryonal stem cells (86). Another example is that kindlin-2 is well-known as an important activator of integrin αvβ3 (216). Integrin αvβ3 expression is up-regulated in pathogen-infected

macrophages *in vitro* (10, 27, 129, 205). Several researchers reported that kindlin-2 deficiency deactivated integrin αvβ3, inhibited the recruitment of macrophages and their productions, thus reducing the resistance to therapy in breast cancer (216).

2.4.4. Integrin αvβ3 association in the pathogenesis of diseases

Integrin αvβ3 plays a crucial role in cellular development and numerous diseases (17, 62, 255). Many scientists have also revealed the importance of integrin αvβ3 for neovascularization of tumour, which is necessary for the nutrition and survival (245), growth (113), differentiation (113), proliferation (245), and metastasis (245) of tumour cells, particularly in human melanoma (243, 245). Moreover, integrin αvβ3 can recognize toxins such as disintegrins in snake venoms (243). Recently, treatments targeting integrin αvβ3 have been attractive topics to interfere with pathogens - host cell interaction to control infectious diseases (22, 218), and cancer (200).

RGD peptides have been used to target integrin αvβ3 expressed in the tumours (5, 196, 200). For example, blocking integrin αvβ3 by a high dose of RGD-labelled ultrasmall superparamagnetic iron oxide (RGD-USPIO) to decrease endocytosis and adhesion activity of glioma cells in the brain tumour (120). Dijkgraaf and colleagues also used radiolabeled cyclic RGD peptide ligands targeting integrin αvβ3 to image tumours in cancer patients, and to inhibit angiogenesis (54). In a study in 2004, radiotracers ^{125}I or ^{18}Fludeoxyglucose (^{18}F) labelled cyclic RGDyK peptide was applied in subcutaneous and orthotopic brain tumour models (38). In orthotopic MDA-MB-435 breast cancer model, 1,4,7,10-tetraaza-1,4,7,10-tetradodecane-N,N,N′ ′,N′ ″-tetraacetic acid (DOTA) and ^{64}Cu conjugated cyclic RGDyK was used to compare with ^{125}I-c(RGDyK) and ^{18}F-c(RGDyK) (38). In general, these radiotracers appear to have fast blood clearance, high tumour-to-blood, and tumour-to-muscle standard uptake ratio, which are surrogate parameters of the metabolic rate of radiotracers (38). However, ^{18}F-c(RGDyK) and ^{64}Cu- DOTA- c(RGDyK) had

lower tumour uptake than ^{125}I analogue (38). Their results implied that different radiotracers above have akin effectivity but still need to be optimized to improve their kinetics and to prolong tumour uptake *in vivo*. The ability of integrin αvβ3 binding to small-molecule ligands, radiotracer, and radiolabeled RGD peptides, such as triazole RGD mimics-base integrin αvβ3 selective radiotracer [^{3}H]ZMPZAT71 or [^{18}F]FDR-Aoa-c(RGDfK) radiotracer (bioconjugation of 18-Fluoride 5-fluoro-5-deoxyribose to aminooxyacetyl functionalized cyclo(Arg-Gly-Asp-$_{D}$-Phe-Lys)), also depends on integrin αvβ3 expression and activation status (8). For example, these bindings were increased when integrin αvβ3 was activated at the presence of Mn^{2+} or talin head domain transfection of PC3 prostate cancer cells and U87MG glioblastoma cells (8). Recently, Sartori and colleagues conjugated c(AmpRGD) peptide (alias aminoproline-base RGD cyclotetrapeptide) and a tyrosine kinase inhibitor sunitinib to target integrin αvβ3, then receptor tyrosine kinase associated with drug resistance intracellularly, consequently affect the cross-talk between integrin αvβ3 with other receptors in the cancer cells (200).

Integrin αvβ3 also appears to be the receptor for a wide range of viruses such as rotavirus, coxsackievirus A9, parechovirus 1, and tat protein of HIV (243). Integrin αvβ3 function varied depending on the virus. Adenovirus (particularly Adenovirus 2/5) used integrin αvβ3 for cell entry, signalling, and endosome escape while Herpesvirus (particularly Human Cytomegalovirus, HCMV) utilized integrin αvβ3 for cell entry and signalling (218). Integrin αvβ3 is essential for the attachment and entry of Hantavirus (particularly Sin Nombre virus, SNV), Picornavirus (Foot-and-mouth disease virus, CA9, EV9), and Reoviridae (Reovirus) (218). Recently, a study confirmed that integrin αvβ3 was a primary receptor for virulent Foot-and-mouth disease virus type O1 (164).

Numerous publications noted that various microbial pathogens exploited integrin αvβ3 to invade host cells (218). For example, in 1994, Cuzange and co-workers demonstrated that

integrin αvβ3 is a receptor for Adenovirus. This virus has an RGD motif present in one of the capsid proteins (50) is involved in the internalization of the virus into M21 melanoma cells and human Hela cervical cancer cells via interaction with integrin αvβ3 (96, 178, 259). Moreover, human cytomegalovirus (HCMV), which is a β-herpesvirus causing congenital disabilities in new-born and severe immunocompromised diseases, contains an envelope glycoprotein B (gB) and gH for efficient cell signalling, fusion, and infection (252). The gB consisted of the RX6-8DLXXF consensus sequence of metalloprotease-15, 23 (ADAM), which targeted integrin αvβ3 (218, 252) as a coreceptor with epidermal growth factor receptor (EGFR) (252). The integrin αvβ3 is trans-located to lipid rafts and plays a role in EGFR signalling (252). The ADAM has a sequence similar to the reprolysin family of snake venomases, sharing the metalloproteinase domain with matrix metalloproteinases, involving integrin αvβ3 activity in cancer (156). Moreover, Van Der Flier con-firmed before that integrin αvβ3 could play a role in cell-cell adhesion through its interaction with CD31 or with a disintegrin and metalloprotease (ADAM) 15 or with ADAM-23 (243). Parry and colleagues also reported that gH ectadomain, a virion envelope glycoprotein of Herpes simplex virus type 1 (HSV1), had essential RGD motif for virus entry via integrin αvβ3 in an experiment on monkey kidney epithelium Vero cell line and Chinese hamster ovary (CHO) cell line (174).

Hantaviruses cause diseases such as hemorrhagic fever with renal syndrome (HFRS) and hantavirus pulmonary syndrome (HPS) (75) characterized by disrupting the functions of endothe-lium and platelet, rendering clotting defects and acute pulmonary edema (218). In 1998, Gav-rilovskaya and co-workers noted that integrin αvβ3 allowed the entry of hantavirus, particularly New York 1 (NY-1) and Sin Nombre virus (SNV) via RGD interactions, into the monkey kidney epithelium Vero E6 and CHO cells (77). The hantavirus invasion was partially or entirely pre-vented by fibronectin (Prospect Hill virus, PHV), vitronectin (SNV and NY-1), or MAB1976

antibody to integrin αvβ3 (SNV and NY-1) (77). Later on, it was also shown antibodies against integrin αvβ3, or vitronectin prevented the infection of human umbilical vein endothelial cells and Vero E6 cells from HFRS-causing hantaviruses Hantaan, Seoul, and Puumala, but did not affect the nonpathogenic Hantaviruses (75). Interestingly, the surface glycoprotein of these hantaviruses did not have an RGD sequence, and RGD treatment did not inhibit the virus entry (75). These findings added information that the complex hantaviruses-integrin αvβ3 interaction may be at a specific region of integrin αvβ3, and that interaction was likely blocked sterically by vitronectin (75) or that another molecule may be acting as a bridge between the integrin and the viruses. Similarly, the antibodies to both integrin αv and β3 or vitronectin but not RGD peptide prevented Rotavirus infection of CHO cell line and monkey kidney epithelium MA-104 cell line (88, 177). Moreover, integrin αvβ3 expression was increased in African green monkey Vero E6 cells and porcine intestinal epithelial cells (IECs) infected porcine epidemic diarrhea virus (PEDV) (138). Replication of PEDV on Vero E6 cells was reduced by RGD peptide, polyclonal antibodies anti-integrin αv, and polyclonal antibodies anti-integrin β3 treatments via its interaction with integrin αvβ3 (138).

Some bacteria, such as *Staphylococcus aureus*, or their components, appear to utilize integrin αvβ3 on the epithelial surface as its receptor (58, 123, 149, 164). Cilengitide that inhibited integrin αvβ3 on human endothelial cell line reduced the attachment of *E. coli* and *Staphylococcus* to the cell (73, 149), potentially decreased the effect of these bacteria in early sepsis (73). Moreover, Kim and colleagues reported that *Shigella flexneri* effector OspE and *Salmonella* could interact with integrin-linked kinase to reinforce host cell adherence to maintain infection in a guinea pig model, thus implying that the bacteria may use integrin αvβ3 to colonize gut epithelium (123). Also, invasins such as AfaD and AfaDE tip complex, purified from bacterial fimbriae,

communicated with the mammalian host cells through integrin αvβ3 receptor (52). More than three decades ago, Charbit and colleagues described the role of RGD residues in the bacteriophage Lambda receptor of *E. coli* in the attachment to mammalian cells (36, 184). These phage receptor areas are in Lam B protein in the integral outer membrane of *E. coli* K12 suggesting a role in binding to integrins αvβ3 receptor (36, 184). It has been reported that RGD peptide could prevent *Treponema pallidum* attachment to human epithelial Hep-2 cells and human tumour HT1080 cells (236).

Moreover, integrin αvβ3 could be a receptor for fungi. For example, in 1990, a group of researchers reported that RGD peptide, a fibronectin-binding sequence, down-regulated fungus *Pneumocystis carinii* attachment to rat alveolar macrophages *in vitro* (182). The RGD sequence of Discoidin-I synthesized by *Dictyostelium discoideum* also plays a role in cell-cell cohesion process, fruiting body forming, and aggregation of the amoeba (181, 184, 217).

Taken together, the data show that integrin αvβ3 has multiple roles that regulate cell division and proliferation through its ability to generate and regulate signals that alter cell shape, migration, and adhesion (Figure 2.1). The integrin is also established as a receptor for various viruses. There are also some data, although highly limited, to suggest its role in the binding of bacteria.

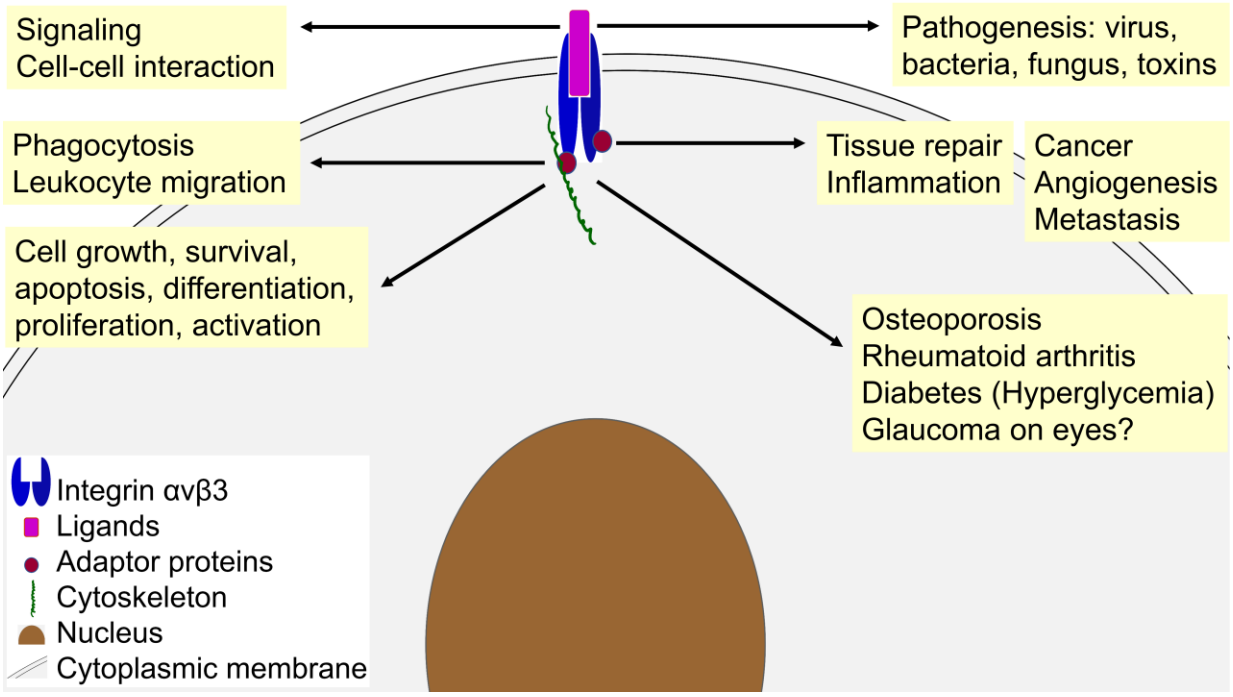

Figure 2.1. Integrin αvβ3 functions

Integrin αvβ3 functions in normal cells (left side) and pathogenesis of diseases (right side). Integrin αvβ3 binds to appropriate ligands by its extracellular domains, and adaptor proteins by its cytoplasmic domains, consequently, rearranging cytoskeleton.

2.5. HELICAL ROSETTE NANOTUBES (HRNs or RNTs)

Nanotechnology has been a rapidly growing multidisciplinary field dealing with the creation and investigation of functional materials and nano-devices by manipulating matter in the nanoscale range at approximately 1–100 nm for more than two decades (48, 132). The application of nanotechnology in drug development and delivery, such as protection from degradation, has been studied (132). Nanomaterials such as gold nanoparticles, carbon nanotubes, and magnetic nanoparticles have a large number of potential applications (131, 250). However, the use of these carbon and metallic nanoparticles is challenging due to their poor solubility, distribution, and cytotoxicity, causing biological impacts on the environment, and health such as cellular proliferation and differentiation (131, 224, 250).

The helical rosette nanotubes (HRNs) were invented by Dr. Hicham Fenniri in 2001 (39, 63, 64), and these are one of the highly novel nanomaterials known till now. The structure of the twin rosette shape of these nanotubes is more stable than single base rosette nanotubes under physiological conditions (63, 64, 223). HRNs are a novel class of metal-free, organic, water-soluble, tunable, biologically-inspired, and biocompatible nanomaterials (63, 64, 223). These nanotubes are synthesized from guanine-cytosine (G∧C) motif building blocks through a rapid hierarchical self-assembly process in water maintained by 18 hydrogen (H) bonds, which then organize to form a nanotube with a central channel of 1.1 nm. G∧C motifs self-organize into hexameric macrocycles in rosette shape to form biocompatible architectures of rosette nanotubes due to spatial arrangement of the asymmetric hydrogen-bond network in aqueous solution (64). The formed tubes are noncovalent yet kinetically stable and maintained by electrostatic, hydrophobic, and stacking interactions (63, 64).

Scientists have found numerous potential applications of HRNs, notably in the medical areas (39, 134, 224, 268-270). One of the excellent properties of the rosette nanotube is the ability to tag a variety of functional groups at the G∧C site on the surface of the tube to impart functional versatility for specific nanomedical or biological applications**.** Based on the speed and specificity of binding, the RNT can be functionalized by tagging peptides to interact with cell receptors and cell adhesion molecules, such as integrins (223). The advantages of HRNs in biocompatibility, water solubility, and tunability compared to other nano-materials make them more attractive for biomedical use (39, 63). There, however, is need to fully understand their safety for use in humans and animals (39, 134, 224, 268-270). Dr. Singh's laboratory has reported that the RNTs-1G(0) did not have significant adverse effects on the respiratory system *in vivo,* indicating their biocompatibility with mammalian system (112). This group has also studied the biology of lysine-functionalized helical rosette nanotubes (RNT-K), containing lysine at the G∧C motif. The RNT-K is about 3 nm in diameter and 50 nm to a few microns in length. The effects of this tube on macrophages were dependent on their size with smaller tubes have more inflammatory potential than the longer tubes. However, RNT-K overall did not induce any appreciable inflammatory response and cell death in macrophage cell lines (109, 111). RNT-K neither affected viability or induced inflammatory response in pulmonary epithelial cells (110). These tubes; however, induced the production of proinflammatory cytokines (IL-8, TNF-α) in human U937 macrophage cells without affecting their viability (111). Collectively, these data suggested that RNT-K could be used for biomedical applications (112).

The established roles of integrin αvβ3 as cell signalling and adhesion have resulted in major interest in the biomedical applications of RGD peptides. There, however, are challenges in cell and tissue-specific targeting of RGD compounds. Despite major advances in deciphering the

molecular structures of pathogens and the identification of their receptors, we still need more precise and better-targeting molecules to reduce the side-effects of drugs. HRNs, through their inherent ability to accept and display molecules, create new possibilities for precise targeting of drugs. (221). The Singh laboratory further investigated the potential of RNTs formed by K-RNT co-assembled with Arg-Gly-Asp-Ser-Lys-functionalized RNTs (RGDSK-RNTs) as drug delivery vehicles. The generated RNTs featuring RGDSK peptide and one K amino acid on their surface in predefined molar ratios are named K^x/$RGDSK^y$-RNT, where x and y refer to the molar ratios of K-G∧C and RGDSK-G∧C, respectively. These hybrid K/RGDSK-RNTs were of course designed to target integrins. It was reported that K^{10}/$RGDSK^1$-HRNs induced cell death genes, p38 mitogen-activated protein kinase (MAPK) phosphorylation, caspase-3 activity, and DNA fragmentation in human bronchial epithelial adenocarcinoma cells (226). These data showed that K^{10}/$RGDSK^1$-RNT could induce inflammation and apoptosis in tumour cells and thus showing their potential for use in cancer (226). The K/RGDSK-RNTs also reduced the migration of bovine neutrophils through inhibiting the phosphorylation of ERK1/2 and p38 MAPK (134). These data collectively showed the cell signals activated by K^{10}/$RGDSK^1$-HRNs in inducing death in cancer cells and modulating the chemotaxis in neutrophils.

In 2011, Suri and colleagues provided the first evidence contrary to expectations that intravenous administration of K^{90}/$RGDSK^{10}$-RNT aggravates the proinflammatory effect of an acute lipopolysaccharide (LPS) - induced lung inflammation in a mouse model (225). LPS and K^{90}/$RGDSK^{10}$-RNT treatment groups notably showed increased infiltration of neutrophils in bronchoalveolar lavage fluid compared with the saline control (225). Compared with LPS alone, the combination of LPS and K^{90}/$RGDSK^{10}$-RNT significantly increased in the expression of interleukin-1β, MCP-1, MIP-1, and KC-1 in the bronchoalveolar lavage fluid, and myeloperoxidase

activity in the lung tissues. These researchers concluded that K^{90}/$RGDSK^{10}$-RNT, in conjunction with LPS, promoted acute lung inflammation, leading to an exaggerated immune response in the lung via up-regulating P38 MAPK cascade (225). This underscores the need for further work in understanding the biology of these novel compounds.

Novel HRNs with unique physiochemical properties are posing challenges to understand the full spectrum of interactions at the nano-bio interface, particularly in the bone. In 2008, Zhang and colleagues applied K-HRNs to enhance the osteoblast adhesion for bone healing *in vitro* (269). However, they did not mention the effect of K-HRNs on the osteoclast, a different subtype of macrophages (269). The data also showed that composites of HRNs- nanocrystalline hydroxyapatite could be a possible material for bone tissue engineering applications due to HRNs ability to mimic the helical nanostructure of collagen in bone (270). RGDSK-conjugated nanotubes could enhance osteoblast adhesion and proliferation due to an increase of fibronectin by RGDSK surface chemistry and a favorable cell environment from nanoscale biomimetic features of nanotubes (268). In 2013, Childs and colleagues found that TB-RGDSK:TBL (RGDSK-HRNs) promoted the chondrogenic adhesion and differentiation of bone marrow mesenchymal stem cell from human (hMSC) on poly(l-lactic acid) scaffolds, implying a potential therapeutics for cartilage regeneration (39).

As mentioned above, RGDSK-TB is a twin G∧C – based RNTs functionalized with arginine-glycine-aspartic acid-serine-lysine (RGDSK) peptide, one of the most popular ligands that can bind integrin αvβ3 (196). The fluorescein isothiocyanate (FITC) conjugated twin G∧C – based RNTs is another valuable functional group to observe HRNs. The mixture of these two materials forms stable RGDSK-HRNs-FITC in which RGDSK functionalized group is displayed on its surface to target integrin αvβ3. Furthermore, the RGDSK-HRNs-FITC can be visualized with a

fluorescent microscope (Figure 2.2) (39, 225). The RGDSK-HRNs-FITC exploited the integrin αvβ3 to enter the endosomes of dendritic cells (99). House and colleagues performed an isolated perfused lung model in male Sprague-Dawley rats with RGDSK-HRNs-FITC intravascular administration to report minimal cell activation measured through the elaboration of adhesion molecules and ROS production (99). Further works are required to elucidate the mechanisms of action occurring when rosette nanotubes are applied to either a healthy or inflamed host/tissue.

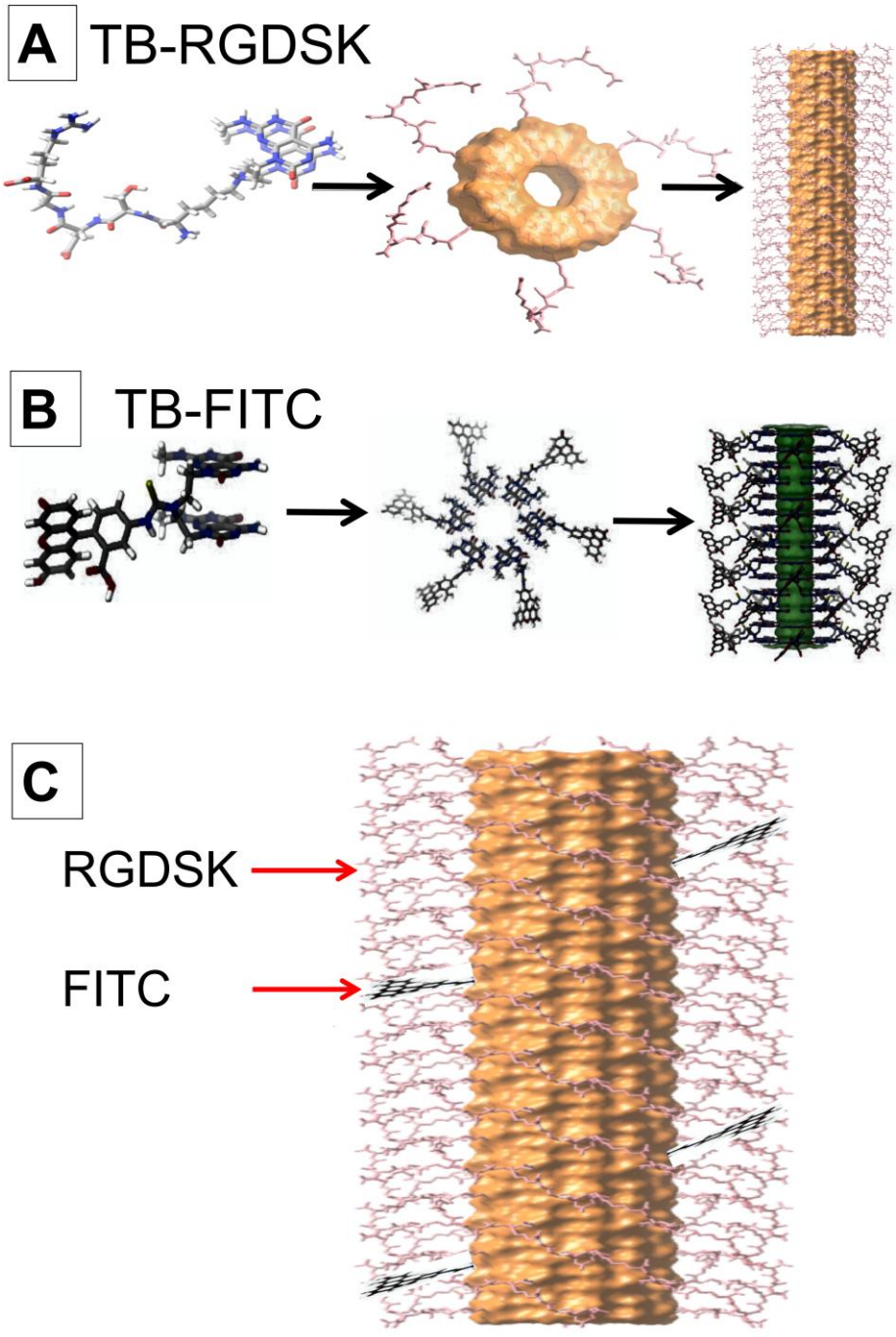

Figure 2.2. Schematic of RGDSK-HRNs-FITC

(A) RGDSK-TB modules forming RGDSK-HRNs, (B) FITC-TB modules forming FITC-HRNs, (C) the mixture of RGDSK-TB and FITC-TB modules forming RGDSK-HRNs-FITC. (used with permission of Dr. Hicham Fenniri)

2.6. BACTERIAL INTERACTION WITH THE HOST

Attachment to the specific host cell receptor is the first step of bacterial pathogen infection (32, 124). Up to date, many scientists have revealed names of cellular membrane proteins could bind and mediate the adherence of bacteria (130). In 2006, Simpson and co-workers also confirmed that bacterial – epithelial cross-talk was recognized as a fundamental feature for the colonization of bacteria in host tissues (209). Studies have been identifying the molecular adhesion receptors driving the intracellular bacteria entering non-phagocytic cells. For example, a group of scientists pointed out that the immobilized invasin of *Yersinia pseudotuberculosis* enteric bacterium targeted integrins $\alpha 3\beta 1$, $\alpha 4\beta 1$, $\alpha 5\beta 1$, and $\alpha 6\beta 1$ receptors (104).

Moreover, scientists reported that bacteria could bind to the extracellular matrix and proteins containing RGD peptide (32, 257). The extracellular matrices, comprising of collagens, glycosylated protein laminin, and fibronectin (a proteoglycan containing protein-bound glycosaminoglycan chains), are present under the epithelium, endothelium, and around connective tissue (130, 150, 257). These materials regularly interact with host cells and play a role in the metabolism and differentiation of cells (148). Therefore, by using these materials, bacteria can either directly or indirectly affect the biology of the host. For example, scientists revealed that mycobacterial isolates could interact with soluble fibronectin (189). Another example is that cell surface proteins of *Staphylococcus aureus* and *Streptococci* could bind to both fibronectin and collagens (24, 128). Of course, the extracellular matrix components, such as fibronectin, bind to integrins such as integrin $\alpha v\beta 3$, which creates a potential of applications of RGD-conjugated HRNs.

Enterobacteria with their fimbriae also could bind to extracellular matrix proteins (168, 215, 257, 258). In detail, in 1993, Collinson and colleagues reported that aggregative fimbriae SEF 17 of enteropathogenic *Salmonella* bound human fibronectin (45). Other examples in the past are

that some strains of *E. coli* under different condition could bind and activate plasminogen via its G fimbria (127), or adhered to fibronectin via its lectin-like component type 1 fimbriated CSH-50 (215), or immobilized fibronectin via its P fimbriae (258), or fibronectin and laminin via its curli (168).

2.7. E. COLI

E. coli is frequently found in the environment, food, and intestine of animals and humans (31, 233). These bacteria have been globally studied for many decades due to their unstable characteristics and multiple virulence factors (247). The non-pathogenic *E. coli* is harmless and controllable (233). Other pathogenic *E. coli* can infect many organs, such as the intestinal, urinary, and respiratory systems (115).

Pathogenic *E. coli* strains are categorized according to their elements, eliciting the host's immune response, as follows: 174 O antigens in the lipopolysaccharide layer, K antigen in the capsule, 53 H antigens in the flagellin, and F antigen in the fimbriae (31, 47). Two types of pathogenic *E. coli* are enteric pathogenic *E. coli* (also named diarrheagenic *E. coli*), and extraintestinal pathogenic *E. coli* (ExPEC) such as subgroup uropathogenic *E. coli* (UPEC), infecting urinary (31, 47). Enteric pathogenic *E. coli* includes enteropathogenic *E. coli* (EPEC), Shiga toxin-producing *E. coli* (STEC edema disease), Verocytoxin-producing *E. coli* (VTEC) such as enterohemorrhagic *E. coli* O157:H7 (EHEC), enteroaggregative *E. coli* (EAEC), enterotoxigenic *E. coli* (ETEC), diffusely adherent *E. coli* (DAEC), adherent invasive *E. coli* (AIEC), enteroinvasive *E. coli* (EIEC) (31, 47).

Adhesive factors and toxins are two virulent factors taking part in the diseases. For example, VTEC has *E. coli* attaching and effacing (*eae*) gene, which was found in many isolates from severe diarrheal cases in cattle and humans (143). The *eae* gene in enterohemorrhagic *E. coli*

promotes its attachment to and desquamation of colonic epithelial cells with consequent recruitment of inflammatory cells and edema formation (56). Another example is that *E. coli* O101 strain possesses a Shiga-like toxin, causing hemorrhagic colitis and hemolytic-uremic syndrome in humans (66). *E. coli* O101 infected pigs could be a reservoir transmitting the bacteria to humans (30, 66).

The adhesive properties of *E. coli* are complex to understand. The majority of the strains of commensal and pathogenic *E. coli* possess type 1 fimbriae (70). When one adhesive receptor is inhibited, other specific adhesive receptors could be activated and compensated for each other (F4, F41, F1, …) (70). In 1982, Gaastra and colleagues illustrated that the typical composition of adhesion subunits of *E. coli* F4 (K88) had arginine (R), glycine (G), aspartic acid (D), serine (S), and lysine (K) (70). The amino acid sequences of fimbriae for the adhesive function are varied and unclear, depending on the strains of *E. coli*, phase variation, evolution, and environmental conditions such as temperature and growth media (70).

Among *E. coli* related diseases, *E. coli* infection outbreak associating with food poisoning, and persistent diarrhea with a high mortality rate has occurred in both developing countries and developed countries (20, 34, 35, 60, 185). Enterotoxigenic *E.coli* (ETEC) is the most common bacteria causing diarrhea in animals (31)and humans (240). ETEC can penetrate the mucus layer, then use flagella, fimbria, or F4 (K88) to bind directly to the luminal surface of enterocytes to colonize in the small intestine (240) (Figure 2.3).

F4 positive (F4+) *E. coli*, also named *E. coli* K88, was firstly reported in Ireland and Germany (70, 197). *E. coli* F4 is associated with both pre-weaning and post-weaning diarrhea in pigs (61, 222). Diarrhea occurs after one to five days of *E. coli* infection when the *E. coli* population is more than 10^9 in pigs (222). Post-weaning diarrhea by *E. coli* is characterized by watery

feces and decreased performance, causing an economic loss for the swine industry. *E. coli* F4 colonizes in the small intestine and release enterotoxins such as heat-stable toxin (ST) and heat-labile toxin (LT) to stimulate epithelial cells to secrete fluid into the lumen of the gut through the cystic fibrosis transmembrane conductance regulator (CFTR), causing enteritis (31, 61, 70). It was reported that *E. coli* F4ab and *E. coli* F4ac could agglutinate erythrocytes of guinea pigs, but F4ac antigen could not agglutinate chicken erythrocytes (70).

In 1982, Gaastra and co-authors described F4 antigen as thin, flexible threads, having a fimbria-like structure with 2.1 nm diameter and covered with filamentous appearance material (70). These researchers noted that the F4 fimbrial adhesion was maintained via hydrophobic or electrostatic interactions between adjacent subunits in F4 fimbriae but not the disulfides bridges (70). Although fimbriae have been found to play an essential role in the attachment of *E. coli* F4, the receptor for F4 antigen adhesion, the interaction of F4 with other receptors, and the detailed mechanism of adhesion is not yet fully understood (70).

In 1999, Francis and co-authors reported that receptors in brush borders of host cells for F4 fimbriae on *E. coli* are an intestinal mucin-type sialoglycoprotein (IMTGP), intestinal transferrin (GP74), and an intestinal neutral glycosphingolipid (IGLad) (65). It is explained that variable glycolipids and glycoprotein receptors with varied sizes in the intestinal mucus and brush border membranes are due to *E. coli* F4 variants, swine breeds, and different sites of attachment in the small intestine. Moreover, Jin and colleagues reviewed in 2000 that receptors in brush border were age-independent (106).

In addition to enterotoxins, ETEC has other factors including O serogroup on lipopolysaccharide, H serogroup on flagella, colonization factor antigens (CFAs), and other adhesive factors on fimbria of ETEC surface (261). CFAs play an essential role in allowing ETEC to adhere to

epithelial cells of the small intestine, and also serve as virulence factors (261). In 2006, Simpson and colleagues described that the adhesive forces were strong enough to resist the flushing action of the gut peristalsis (209). These scientists also mentioned that these interactions contribute to the pathogenicity of *E. coli*, leading to immune-mediated gut disorders (209).

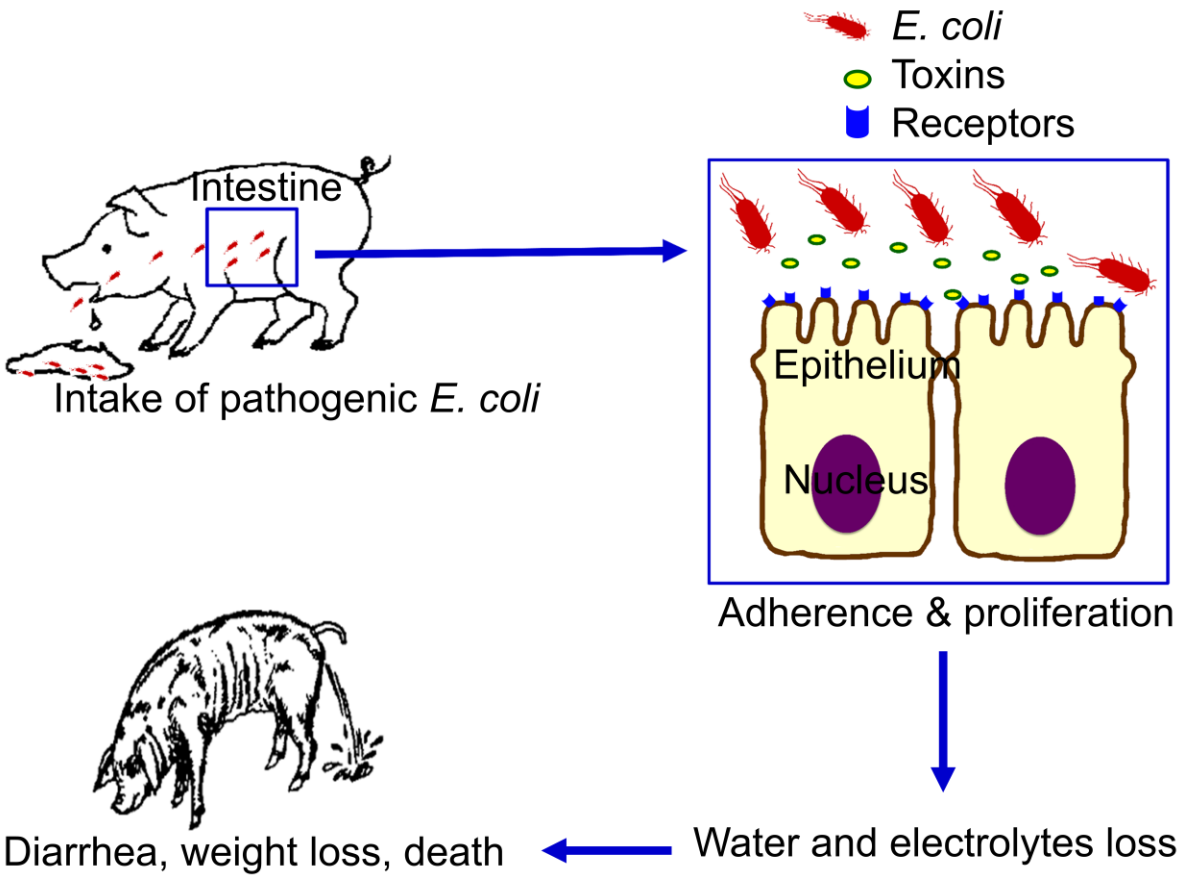

Figure 2.3. Enterotoxigenic E. coli infection

In general, the intestinal mucosa is lined by a single layer of epithelium, allowing the absorption of nutrients. This layer also forms the frontline barrier against the entry of pathogens into the host systems. The initial adhesion of the microbes with the gut epithelium is the first stage in the pathogenesis of gut diseases. The adherent bacteria and their enterotoxins such as a heat-labile toxin (LT), and a heat-stable toxin (ST), leads to electrolyte and fluid efflux through the cystic fibrosis transmembrane conductance regulator (CFTR). This reaction causes water and electrolyte loss into the intestinal lumen, leading to diarrhea, dehydration, weight loss, and death.

However, till now, most interventions cannot completely control intestinal diseases and foodborne illness worldwide due to *E. coli* infection (37, 40, 119, 139, 158, 206, 208, 209, 234, 263, 273). Therefore, many studies on this public health concern have been ongoing to decipher better knowledge at the molecular and cellular levels. For example, a few years ago, Garas and co-workers reported that milk from human lysozyme transgenic goats could protect piglets from ETEC infection in term of less severe diarrhea, fewer bacteria translocated into the mesenteric lymph nodes, lower mucin 1, and higher tumour necrosis factor – α (72). Moreover, many scientists recommended that obstructing the receptor adhesion sites to inhibit the primal step of *E. coli* attachment to the intestine, particularly epithelium, can lead to the development of novel interventions to modify this enterotoxigenic pathogen-induced diarrhea (106).

There was no data to demonstrate that prokaryotes expressed integrins (203). Therefore, *E. coli* was used for many specific protein productions. For example, in some studies, *E. coli* MG1655 and *E. coli* EC410 were transformed with vectors to produce RGD containing peptide and recombinant integrin αvβ3, respectively (203, 228). However, recently, scientists reported that integrins were involved in activities of *E. coli*. For example, in 2003, in an *in vitro* experiment on HeLa cell line, Laarmann and co-workers suggested that integrin αv (CD51) was the potential receptor of adhesin involved in diffuse adherence-I (AIDA-I) protein of *E. coli* K12 (130). These researchers discussed that integrin αv and AIDA-I interaction could mediate the attachment of *E. coli* to mammalian cells (130). Another example is the study of De Greve and co-workers in 2007 (46, 52). Their laboratory revealed that Invasins, such as AfaD and AfaDE tip complex, were found on pathogenic *E. coli* strains, causing chronic diarrhoeal and urinary tract infections such as cystitis and pyelonephritis (46, 52). These Invasins could communicate with the mammalian host cells through integrins αvβ3 and α5β1 receptor (46, 52). Moreover, Hemolysin (HlyA) toxin from

uropathogenic *E. coli* was mediated by β2 integrins in U-937 human monocytic cell line, demonstrating the involvement of β2 integrins in the sensitivity of the cell to toxins from *E. coli* (191).

Till now; however, there are no data on the expression and role of integrin αvβ3 on *E. coli* bacteria. This integrin may play a role in the attachment of *E. coli* to gut epithelium as one of the first steps towards colonization. Considering that the gut epithelia in pig and calf express the integrin αvβ3, it is crucial to examine the expression of this integrin on *E. coli* and to understand its role in E. coli adhesion to gut epithelium.

2.8. GUT LOOP MODEL

One of the major health issues in animals and humans globally is intestinal diseases. The intestine interacts with the environment through the handling of the food traveling through it (2, 237). Therefore, the mucosal immune system of the intestine is critical since this organ is exposed to many pathogens. The intestine is protected by many factors, including the intestinal microbiota, mucus layer, surface epithelium, and immune cells (165, 176). The complex activities and interaction of these factors influence the dynamic ecosystem, condition, and functions of the intestine in defending pathogens (165). For example, the intestinal microbiota, known as commensal microorganisms, resides in numerous pits to protect the host substances from the colonization of external pathogenic organisms (2, 165, 237). Besides that, the unique and heterogeneous epithelial lining of the intestine is the first barrier that has a well-developed system to manage the bacterial populations in the gut (2, 237). Moreover, pathogens are recognized by intestinal epithelial cells and immune cells via pattern-recognition receptors such as Toll-like receptors (TLRs) and intracellular Nod-like receptors. Among TLRs, TLR4 has important functions on the trigger of the inflammatory response and being able to sense bacteria (246). TLR4 likely transduces lipopolysaccharide (LPS) signal across the plasma membrane (180).

The usage of animal models is applicable for scientific research and cannot be replaced by any alternative methods to study the intestinal mucosal immune system, pathogenesis, and new interventions for intestinal infectious diseases (6, 195). Appropriate animal models provide possibilities for further clinical studies in humans (117). It is generally understood that discoveries of new therapeutics made in rodent models usually fail to translate to other species, including domestic animals and humans. Therefore, the availability of physiologically relevant animal models is critical to investigate biological phenomena to advance our knowledge and develop better drugs and vaccines (117).

Among animal models, large animals have been used for many years for preclinical research because outcomes from these animals are close to and can be predicted in clinical studies on humans. For example, pigs, dogs, lambs, bovines, and horses are the superior resources for efficiently studying nutrition, biomedicine, microbiology, immunopathology, or particularly host-pathogen interaction (6, 7, 117, 165, 195). Besides non-human primates, pigs have recently been used in many *in vivo* preclinical models because of their similarities with humans regarding their biological development (117, 195). Pigs have a similar immune system and pathogen susceptibility when compared to human (154). Another reason is that pigs likely have similar genetic homology, physiology, and anatomy as humans (79, 154, 165, 195). Besides that, other advantages are the availability of pigs, and the ready immunological toolbox of the pig for feasible experimental design (116).

Dr. Volker Gerdts and his colleagues have developed a gut loop model to study the interaction of pathogens and epithelium, as well as other immune cells in pigs, sheep, and lambs (51, 78, 153) (Figure 2.4). This superior model can analyze mucosal immune responses and the effect of multiple treatments to identical, independent segments of the intestine in the same animal,

reducing the variability associated with large outbred animals, and eliminating genetic variability (78). Because of animal ethics and the effort of minimizing the number of animals used for experiments, the gut loop model is suitable for many research aims. For example, in 2002, Dr. Mutwiri and co-workers applied the gut loop model in lambs to test three different porcine serum albumin encapsulated in alginate microspheres (163). Each loop provided independent but identical sites for testing the mucosal immune responses (163). They found that these porcine serum albumins enhanced antibody-secreting cells in humoral immune responses but not T-cell responses (163). Another example is that in 2009, Meurens and co-workers applied the gut loop model in pigs to study the host's response to *Salmonella* Typhimurium infection (153). In that study, the *Salmonella* treated loops displayed the specific response of the host intestine to *Salmonella* infection compared with normal control loops (153). The *Salmonella*-infected group had a higher level of inflammatory cytokine mRNA (IL6, IL8/CXCL8, and TNFα), as well as T-helper type 1 cytokine mRNA (IL12p53, IL12p40, IL27p28, and IFN gamma) than normal control group (153). Moreover, in 2011, Vandenbroucke and co-workers applied the loop model in porcine ileum to study the interaction between mycotoxin deoxynivalenol and *Salmonella* Typhimurium (244). They found that deoxynivalenol induced the susceptibility of the intestinal epithelium to *Salmonella* Typhimurium infection (244).

Taken together, the gut loop model has been widely applied in many projects because the potential advantages outweigh the disadvantages.

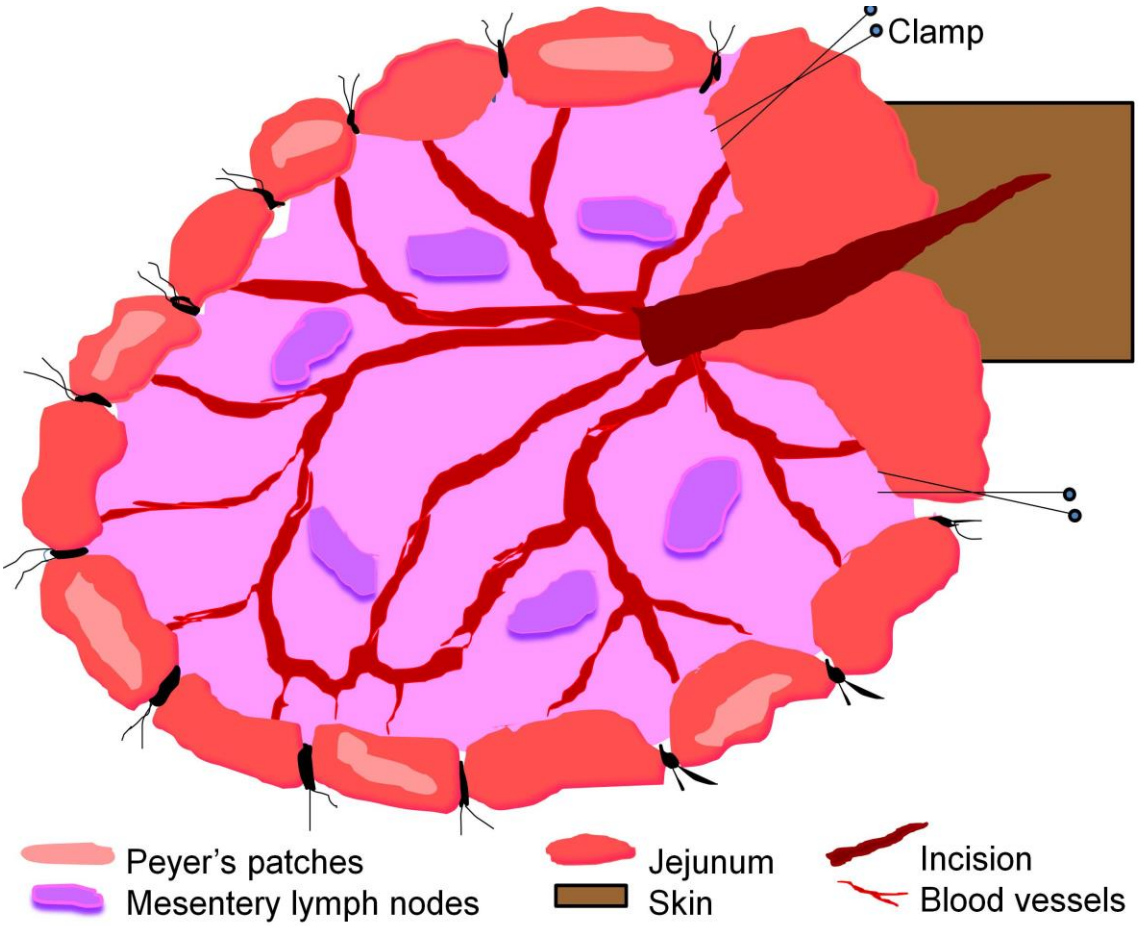

Figure 2.4. Schematic diagram of the porcine gut loop model

Schematic representation of surgically created sections for the experiment, which were named loops. The rest of the sections between loops were named interspaces. The intestine was segmented, and two ends of each segment were tightened. The continuity of the intestinal system was re-established by end-to-end anastomosis. These loops were independent, identical with the same length, and condition for analyzing mucosal immune responses in vivo. Then the intestine was returned to the abdominal cavity which was then closed in three layers.

CHAPTER 3. OBJECTIVES AND HYPOTHESES

3.1. Objectives and rationales

RGD peptides bind to integrin αvβ3 expressed on various cells, including intestinal epithelial cells (39). We have been exploring the functions of novel helical rosette nanotubes (HRNs) in inflammation. Recently, we have developed HRNs that are conjugated to RGDSK peptides that bind to integrin αvβ3. Building on these studies, I propose to investigate the interactions of RGDSK-HRNs with integrin αvβ3 in the context of interactions of *E. coli* with the intestinal epithelium, specifically the binding of *E. coli* to the jejunal epithelium. This study aims to contribute fundamental knowledge to the biology of RGDSK-HRNs and their applications in therapeutics of infectious diseases.

1. Determine the expression of integrin αvβ3 in the intestinal porcine epithelial cell line 1 (IPEC1) and *E. coli* upon infection.
2. Investigate the functions of RGDSK-HRNs in blocking the attachment of *E. coli* to IPEC1 *in vitro* and porcine villi *ex vivo*.
3. Explore the effect of RGDSK-HRNs exposure on apoptosis and survival of IPEC1 upon *E. coli* infection.
4. Investigate the effects of RGDSK-HRNs on *E. coli* infection in a porcine gut loop model.

3.2. Hypotheses

1. Integrin αvβ3 is expressed in IPEC1, and its expression will change upon *E. coli* infection.
2. RGDSK-HRNs will bind to integrin αvβ3 expressed in IPEC1 and block the attachment of *E. coli* to IPEC1.
3. RGDSK-HRNs enhance the apoptosis of intestinal epithelium upon *E. coli* infection.

4. RGDSK-HRNs inhibit *E. coli* attachment to the mucosal membrane *in vivo*.

CHAPTER 4. INTEGRIN αvβ3 EXPRESSION IN THE INTESTINAL PORCINE EPITHELIAL 1 CELL LINE (IPEC1) UPON *E. COLI* INFECTION *IN VITRO*

We performed immunohistochemistry to confirm the expression of integrin αvβ3 in the normal porcine gastrointestinal tract, as reported previously in Dr. Singh's lab (213). We found that integrin $\alpha_v\beta_3$ was expressed in the epithelium (Figure 9.1 in supplemental results). However, up to date, there are no data on the role of integrin αvβ3 in the intestinal epithelium, especially in *E. coli* infection. Therefore, we used intestinal porcine epithelial cell line 1 (IPEC1) and *E. coli* F4 to find the gap information. This chapter focused on determining the expression of integrin αvβ3 in IPEC1 and *E. coli* F4 upon infection *in vitro*.

4.1. ABSTRACT

Integrin αvβ3 is expressed in endothelium, epithelium, and various immune cells such as neutrophils, macrophages, and platelets. It binds to bacteria, viruses, and acute-phase proteins such as vitronectin. However, there are no data on the expression of integrin αvβ3 in *E. coli*, and its role in adhesion to the intestinal epithelium that expresses integrin αvβ3. Therefore, we used porcine intestinal epithelial cell line 1 (IPEC1) and *E. coli* F4 to explore the hitherto unknown expression of integrin αvβ3 *in vitro* with fluorescent and electron immunocytochemistry, immunoprecipitation, and western blots.

Integrin αvβ3 was localized on the plasma membrane, the cytoplasm, and the nucleus of IPEC1 cells. The expression of integrin αvβ3 in IPEC1 decreased at 15 minutes but returned to normal after 90 minutes of infection with *E. coli* F4 ($P<0.05$). Immuno-gold quantification showed changes in the subcellular expression of integrin αvβ3 in IPEC1. The light, fluorescent and electron microscopy, and western blots showed the novel expression of integrin αvβ3 in *E. coli* F4. The presence of this protein was confirmed by a 96-well plate binding assay, and preliminary mass

spectrometry analysis. In conclusion, these are the first data to show the expression of integrin αvβ3 on intestinal epithelium infected with *E. coli*. These results suggest that this protein may play a role in *E. coli* infection.

Key Words: integrin αvβ3, intestinal epithelium, *E. coli*

4.2. INTRODUCTION

Enterotoxigenic *Escherichia coli* (ETEC) is one of the common causes of diarrheal diseases worldwide in humans and animals (4, 20). ETEC infection has a high economic impact on swine production, poses a threat to pork food products, and is an important public health concern (204, 238, 249, 261). For example, *E. coli* F4 causes neonatal and post-weaning diarrhea in pigs (69). However, treatment for enteric diseases is challenging because of the emergence of antibiotic resistance, the side effects of prolonged medication, and multiple virulence factors in enterotoxins (60, 186, 271). Because of the ongoing morbidity, mortality, and economic losses, there is a pressing need to develop better protocols to manage the impact of enteric infections in humans and animals.

The mechanisms of the induction of diarrhea by enteric pathogens are not fully understood. In general, the intestinal mucosa is lined by a single layer of epithelium, allowing the absorption of nutrients and sampling of the antigens. This barrier forms the frontline offense against the entry of pathogens into the host systems; for example, it prevents many normally-resident bacteria such as *Clostridium perfringens* and *E. coli* from entering the gut. The epithelia are activated by both bacterial adherence and through interaction with bacterial molecules such as toxins. Therefore, the initial adhesion of the microbes to the gut epithelia is the first stage in the pathogenesis of the gut disease (136, 157).

Recent studies have been identifying the molecular adhesion receptor driving the entry of bacteria into non-phagocytic cells (104, 164). Integrin α*3*β*1,* α*4*β*1,* α*5*β*1, and* α*6*β*1* can bind the immobilized invasin of *Yersinia pseudotuberculosis* enteric bacterium (104). β2 integrins in U-937 human monocytic cell line mediated hemolysin (HlyA) toxins from uropathogenic *E. coli*, demonstrating the involvement of β2 integrins in the sensitivity of the cell to toxins from *E. coli* (191).

Integrin αvβ3 expressed on epithelial cell surfaces is known to act as a receptor for some bacteria and viruses (123, 164), including adenoviruses (50). In 2008, Tchesnokova and colleagues reported that *E. coli* K12 had an integrin-like allosteric site on FimH, an adhesive subunit of type 1 fimbriae of *E. coli* (232). However, there are no data on the expression of integrin αvβ3 on *E. coli* and its role in the attachment of *E. coli* to the intestinal epithelium. Therefore, in this paper, we explored the hitherto unknown expression of integrin αvβ3 on *E. coli* and the intestinal porcine epithelial 1 cell line (IPEC1)**.** The results support our hypothesis that *E. coli* F4 has integrin αvβ3-like protein. Also, integrin αvβ3 is expressed on IPEC1, and its expression on IPEC1 decreased upon *E. coli* F4 infection.

4.3. MATERIALS AND METHODS

4.3.1. Materials

pFPV-tdTomato plasmid was a generous gift from the laboratory of Professor Douglas Call, Washington State University, USA. *E. coli* DH5α was obtained from Professor Janet Hill's laboratory at the University of Saskatchewan, Canada.

E. coli F4 strain EC52, serotype O101:K30+:K99- and IPEC1 were gifts from Dr. Francois Meurens and Dr. Heather L. Wilson at Vaccine and Infectious Disease Organization -

International Vaccine Centre (VIDO-InterVac). IPEC1 cells were developed from the jejunum of unsuckled, mixed-bred piglets less than 12 hours old (85). IPEC1 cells were cultured in 75 cm^2 flask in Dulbecco's Modified Eagle Medium/Nutrient Mixture F-12 at 37ºC in a humidified 5% CO_2 incubator (84, 126).

Mouse MAB1976 monoclonal integrin αvβ3 antibody (clone LM609, Chemicon Inc., Temecula, USA), rabbit polyclonal antibody anti-integrin beta 3 (EMD Millipore, Temecula, USA), Rabbit anti-human integrin αv polyclonal antibody (EMD Millipore, Temecula, USA), Alexa Fluor 633 conjugated secondary antibody polyclonal goat anti-mouse immunoglobulins (Thermo Fisher, Rockford, USA). RGDSK-FITC (American peptide company, Sunnyvale, CA 94086, USA), secondary polyclonal goat anti-rabbit immunoglobulins/HRP (Dako), Bio-plex cell lysis kit (Bio-rad, Mississauga, ON, Canada), SureBeads™ magnetic beads immunoprecipitation kit (Bio-rad, Mississauga, ON, Canada), Detergent Compatible (DC) Bradford protein assay kit (Bio-rad, Mississauga, ON, Canada) were purchased commercially.

4.3.2. pFPV::tdTomato plasmid transformation to visualize *E. coli* under a confocal microscope

The visualization of *E. coli* under the confocal microscope was based on pFPV::tdTomato fluorescent protein. *E. coli* strain DH5α and F4 were treated with morpholinopropanesulfonic acid, rubidium chloride, and calcium chloride to become chemically competent cells. After that, pFPV::tdTomato plasmid was transformed into competent *E.coli* by heat shock following a previous standard method (198). The transformant *E. coli* was selected on Luria broth agar having ampicillin. Successful pFPV::tdTomato plasmid transformed *E. coli* had red fluorescence upon 554nm excitation. *E. coli* was stored in -80ºC freezer till further use.

4.3.3. *E. coli* preparation

E. coli F4 having pFPV::tdTomato fluorescence protein was cultured for 18 hours on Luria broth supplemented with ampicillin. The concentration of bacteria was determined by adjusting the optical density at 620nm (OD_{620}) to 1 to achieve $4x10^9$ CFU/ml as determined by prior CFU counting. *E. coli* was centrifuged at 16,200 xg for 5 minutes, followed by a wash in 0.1M PBS supplemented with ampicillin at pH=7.4. Serial dilution was done to reach the desired concentration of the bacteria for the assay later, according to previously cited (126).

4.3.4. Immuno-gold electron microscopy for integrin αvβ3

E. coli F4 and *E. coli* DH5α were cultured overnight in tryptone soya broth (TSB) medium. *E. coli* was washed three times in 0.1M PBS and resuspended in 0.1M PBS for immunogold staining for integrin αvβ3. For challenging IPEC1, *E. coli* F4 was resuspended in DMEM/F12 medium without serum. The experiment was performed in 1.5ml microcentrifuge tubes. For control experiments, IPEC1 ($1x10^6$/ml) were challenged with 10^8 *E. coli* F4 or DMEM/F12 medium only for 15 minutes. Healthy IPEC1, IPEC1 exposed to *E. coli* F4 for 15 minutes, *E. coli* F4, and *E. coli* DH5α only were fixed in 2% paraformaldehyde and 0.1% glutaraldehyde in 0.1M sodium cacodylate buffer for 3 hours at 4°C. The samples were pelleted in 1% agarose, dehydrated, and infiltrated in acrylic LR white resin. Next, the samples were sectioned at 100nm thickness on nickel grids. The non-specific bindings were blocked by BSA 1% in Tris-buffered saline before one-hour incubation in the anti-integrin αvβ3 antibody (50µg/ml). The sample stained without primary antibody served as a negative control.

After three washes in Tris-buffered saline, the sections were incubated for one hour in a 15 nm gold-conjugated anti-mouse secondary antibody (1:100). Aqueous uranyl acetate served as

an indicator of negative staining. Besides, we used Reynold's lead citrate to enhance the electron-scattering properties of biological components inside the cells. The electron micrographs were imaged using a transmission electron microscope (Hitachi HT7700 - XFlash 6T160, Germany) operated at 80KV. The gold particles positive integrin αvβ3 in the nuclei, cytoplasm, and plasma membrane of ten cells were objectively counted for statistical analysis.

4.3.5. Immunoprecipitation and western blot for integrin αvβ3

IPEC1 at $1x10^6$ cells concentration were seeded into 25 cm^2 flasks. The cells became confluent after overnight incubation, and these were challenged with 1ml of 10^8 *E. coli* F4 for 15, 30, 60, 90 minutes. The supernatant from the experiment was collected and stored at -80ºC for future use. Cells were lysed and immunoprecipitated for integrin αvβ3 following manufacturer's protocols (Bio-rad, Mississauga, ON, Canada). Briefly, the treatment reaction was stopped by adding ice-cold wash buffer to the cells. Samples were homogenized by adding a lysing solution. The protein concentrations of samples were measured by using a detergent compatible Bradford protein assay kit (Bio-rad, Mississauga, ON, Canada). The samples were diluted to have the same protein concentration, and the same amount of total protein for immunoprecipitation. The general principle is that integrin αvβ3 protein in samples binds magnetic beads-conjugated monoclonal anti-integrin αvβ3 antibody, followed by their pull-down by the magnet in the rack. The elution of integrin αvβ3 was finished in 1X Laemmli buffer boiling 70ºC in 10 minutes. The beads were magnetized, and the eluent was collected into a new vial.

The western blot procedure was appropriately modified from a previous protocol (105). We first probed for integrin αv (n = 4 each group for IPEC1 experiment, n=3 times for *E. coli* lysates). The membranes were incubated with rabbit anti-human integrin αv polyclonal antibody (1:750, EMD Millipore, Temecula, USA), and secondary polyclonal goat anti-rabbit

immunoglobulins/HRP (1:2000, Dako). Incubation without primary antibody served as a negative control. The detection of proteins was accomplished by Amersham ECL western blotting detection reagents kit (GE Healthcare, Freiburg, Germany). Finally, the membranes were scanned using Bio-rad ChemiDoc MP Imaging system scanner and Imagelab 5.2.1 software (Bio-rad, Mississauga, ON, Canada). For detecting integrin β3, the probed membrane was stripped with the blot restore membrane rejuvenation kit (Millipore, Billerica, MA, USA) before being re-probed with rabbit polyclonal antibody anti-integrin β3 (1:750, EMD Millipore, Temecula, USA) and secondary polyclonal goat anti-rabbit immunoglobulins/HRP. About semi-densitometric quantification, we used ImageJ software to evaluate the relative density of integrin αv, integrin β3 in all groups, and compared with a loading control.

4.3.6. Immunofluorescent staining integrin αvβ3 on IPEC1

For immunofluorescent staining, $2x10^5$ IPEC1/well were seeded into 24-well plates with a cover slide at the bottom. After being confluent overnight, IPEC1 cells were washed by 1 ml per well of fresh DMEM/F12 without serum. Cells were then treated with 10^7 *E. coli* F4/ml resuspended in medium. Medium without bacteria was used for normal healthy control. Samples were fixed by 4% paraformaldehyde. Non-specific binding was blocked by 10% BSA. The samples were incubated in monoclonal integrin αvβ3 antibody (1:50, clone LM609, Chemicon Inc., Temecula, USA.) then in Alexa flour 633-conjugated goat anti-mouse IgG secondary antibody (1:100). Cells were incubated for 5 minutes in 0.33µg/ml DAPI for staining the DNA of nuclei. We imaged the samples by using a confocal scanning laser microscope Leica TCS SP5 LSCM, with a 63× objective lens under oil immersion. Negative controls for the specificity of primary, secondary antibody, and protocol include mouse IgG1 isotype control, the omission of primary antibody, or both primary antibody and Alexa flour 633-conjugated secondary antibody.

4.3.7. Immunocytochemistry staining integrin αvβ3 for *E. coli*

E. coli F4 and *E. coli* DH5α were cultured overnight in tryptone soya broth (TSB) medium. Both strains of *E. coli* were washed three times in 0.1M PBS. Then the bacteria were cytospun on microscope slides and fixed in 4% paraformaldehyde. Endogenous peroxidase, and non-specific binding to samples were blocked by 3% H_2O_2 in PBS and 1% BSA in PBS, respectively. To confirm whether these strains of *E. coli* had an integrin αvβ3-like protein, samples were incubated with monoclonal anti-integrin αvβ3 antibody (clone LM609, Chemicon Inc., Temecula, USA.) and appropriate polyclonal anti-mouse immunoglobulins/HRP secondary antibody. The color development from HRP of secondary antibody was carried out with Vector® VIP peroxidase substrate kit. Samples that were stained with isotype antibody matching control (mouse IgG) instead of the primary antibody or were omitted primary antibody served as negative controls.

4.3.8. *In vitro* anti-integrin αvβ3 antibody binding assay

In vitro anti-integrin αvβ3 antibody binding assay was modified from previous protocols (27, 149) to examine whether *E. coli* has an integrin αvβ3-like protein domain which can be blocked by RGDSK peptide. In brief, 96-well high binding plates were precoated overnight with 50µl of 5µg/ml mouse monoclonal integrin αvβ3 antibody (clone LM609, EMD Chemicon Inc., Temecula, USA.) in 100 mM HCO_3^-/CO_3^{2-} coating buffer. Coating buffer only was used as a negative control. The wells were washed gently with 100µl of 0.1% sterile Tween-TBS then were incubated in 1% BSA to prevent non-specific binding. *E. coli* F4 having pFPV::tdTomato fluorescence protein was added at seven different concentrations (50 µl of $10x10^6$, $5x10^6$, $2.5x10^6$, $1.25x10^6$, $0.62x10^6$, $0.31x10^6$, $0.15x10^6$ CFU per well). After a one-hour incubation, unbound *E. coli* was removed by rinsing with PBS ampicillin. Binding *E. coli* on the bottom of the 96-well

plate was fixed in 2% paraformaldehyde. pFPV::tdTomato fluorescence from binding *E. coli* was measured at 530nm excitation /570nm emission in POLAR Start OPTIMA microplate fluorescence reader. Fluorescence intensity was adjusted with the background fluorescence of the wells without adding *E. coli*. The experiment was repeated four times.

In vitro, anti-integrin αvβ3 antibody binding assay was again modified from previous protocols (27, 149) to examine whether *E. coli* has a protein domain similar to integrin αvβ3. In brief, 96-well high binding plates were precoated overnight with 50µl of 6 different concentration (5µg/ml, 2.5 µg/ml, 1.25 µg/ml, 0.625 µg/ml, 0.3 µg/ml, 0.15 µg/ml) of mouse monoclonal integrin αvβ3 antibody (clone LM609, EMD Chemicon Inc., Temecula, USA) in 100 mM HCO3/CO3 coating buffer. Coating buffer only was used as a negative control. The wells were washed gently with sterile 100µl of 0.1%Tween-TBS then were incubated in 1% BSA to prevent non-specific binding. *E. coli* F4 having pFPV::tdTomato fluorescence protein was added (50 µl of $5x10^6$ CFU/ml per well). After one-hour incubation, non-adhering *E. coli* was removed by rinsing with PBS ampicillin. Bound *E. coli* was fixed in 2% paraformaldehyde. pFPV::tdTomato fluorescence from bound *E. coli* was measured at 530nm excitation /570nm emission in POLAR Start OPTIMA microplate fluorescence reader. Fluorescence intensity was adjusted with background fluorescence from well without adding *E. coli*. The experiment was repeated three times.

4.3.9. Mass spectrometry analysis

E. coli lysis and the immunoprecipitation for integrin αvβ3 protocols were followed as per manufacturer's protocols as a briefly described protocol above (Bio-rad, Mississauga, ON, Canada). The immune-precipitates were sent to the Canadian Centre for Health and Safety in Agriculture (CCHSA) Mass Spectrometry Laboratory, the University of Saskatchewan for amino acid sequencing following a previous protocol (55). In brief, *in-gel* protein bands were digested using

trypsin buffer. Trypsin digestion reaction was quenched by adding trifluoroacetic acid (TFA), and tryptic peptides were extracted from gel samples using TFA in acetonitrile. After that, samples were transferred to a mass spectrometry vial for liquid chromatography-tandem mass spectrometry (LC-MS/MS) analysis. An Agilent 6550 iFunnel quadrupole time-of-flight (QTOF) mass spectrometer, equipped with an Agilent 1260 series liquid chromatography instrument, and an Agilent Chip Cube LC-MS interface analysed all mass spectrum.

The chromatographic peptide separation was accomplished using a high-capacity Agilent C18 Polaris Chip. The spectral data were converted to a mass/charge data format using Agilent MassHunter Qualitative Analysis Software and were processed against the SwissProt Human database (UniProt release 2017_09), using Spectrum Mill as the database search engine. Search parameters included a fragment mass error of 50 ppm, a parent mass error of 20 ppm, trypsin cleavage specificity, carbamidomethyl as a fixed modification of cysteine and oxidized methionine as a variable modification. The spectrum Mill validation was performed at peptide and protein levels (1% false discovery rate).

4.3.10. Statistical analysis

We used the GraphPad Prism version 5.04 software (San Diego, CA, USA.) to analyse data. Quantitative results were expressed as mean ± SEM, and error bars represented standard error. The normal distribution of residuals was tested by histogram and Shapiro-Wilk test. Data were analyzed by Analysis Of Variance (ANOVA), followed by Bonferroni multiple comparison test. A significant difference was set when the critical value of α was below or equal to 0.05 as (two-tailed, $p<0.05$).

4.4. RESULTS

4.4.1. Integrin αvβ3 expression on IPEC1 decreased upon *E. coli* infection

To understand the role of integrin αvβ3 and how integrin αvβ3 interact with bacteria, we performed immunofluorescent staining for the integrin on IPEC1. The results showed that integrin αvβ3 was expressed in the nucleus, cytoplasm, and plasma membrane of IPEC1 (Figure 4.1). The expression of integrin αvβ3 in IPEC1 cells decreased upon *E. coli* F4 infection (Figure 4.1).

To further understand the fine distribution of integrin αvβ3 on the cells, we performed immuno-gold electron microscopy on normal IPEC1 cells, and *E. coli* F4 infected IPEC1 cells. The immuno-gold staining data were consistent with the confocal results. Normal IPEC1 had approximately double the number of gold particles for integrin αvβ3 in all compartments than the cells exposed to *E. coli* F4. (Figure 4.2). Densitometry semi-quantification from immunoprecipitation and western blot showed that the expression of integrin αvβ3 on IPEC1 decreased at 15 minutes and returned to normal after 30, 60, and 90 minutes *E. coli* F4 infection (Figure 4.3).

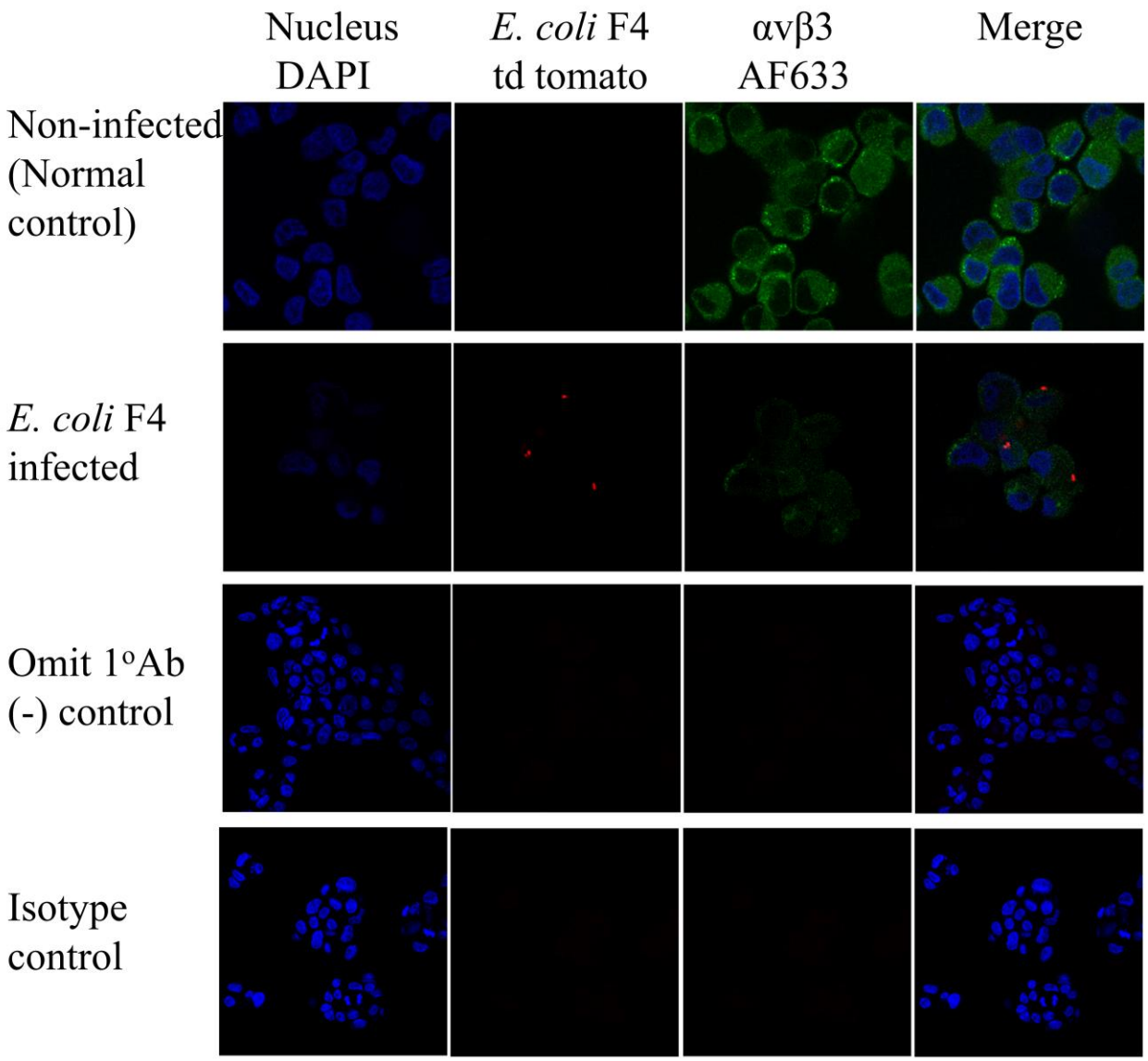

Figure 4.1. Immunofluorescent staining of integrin αvβ3 on IPEC1

Negative controls stained with BSA instead of integrin αvβ3 antibody (3rd row from top), IgG1 isotype control (last row from top) shows only DAPI blue color of the nucleus. Intense staining (green) for integrin αvβ3 is observed in normal IPEC 1 control (1st row on top). The intensity of positive staining in IPEC1 decreased upon E. coli F4 infection (2nd row from top). Green: Integrin αvβ3; Red: pFPV::td tomato E. coli F4; Blue: DAPI.

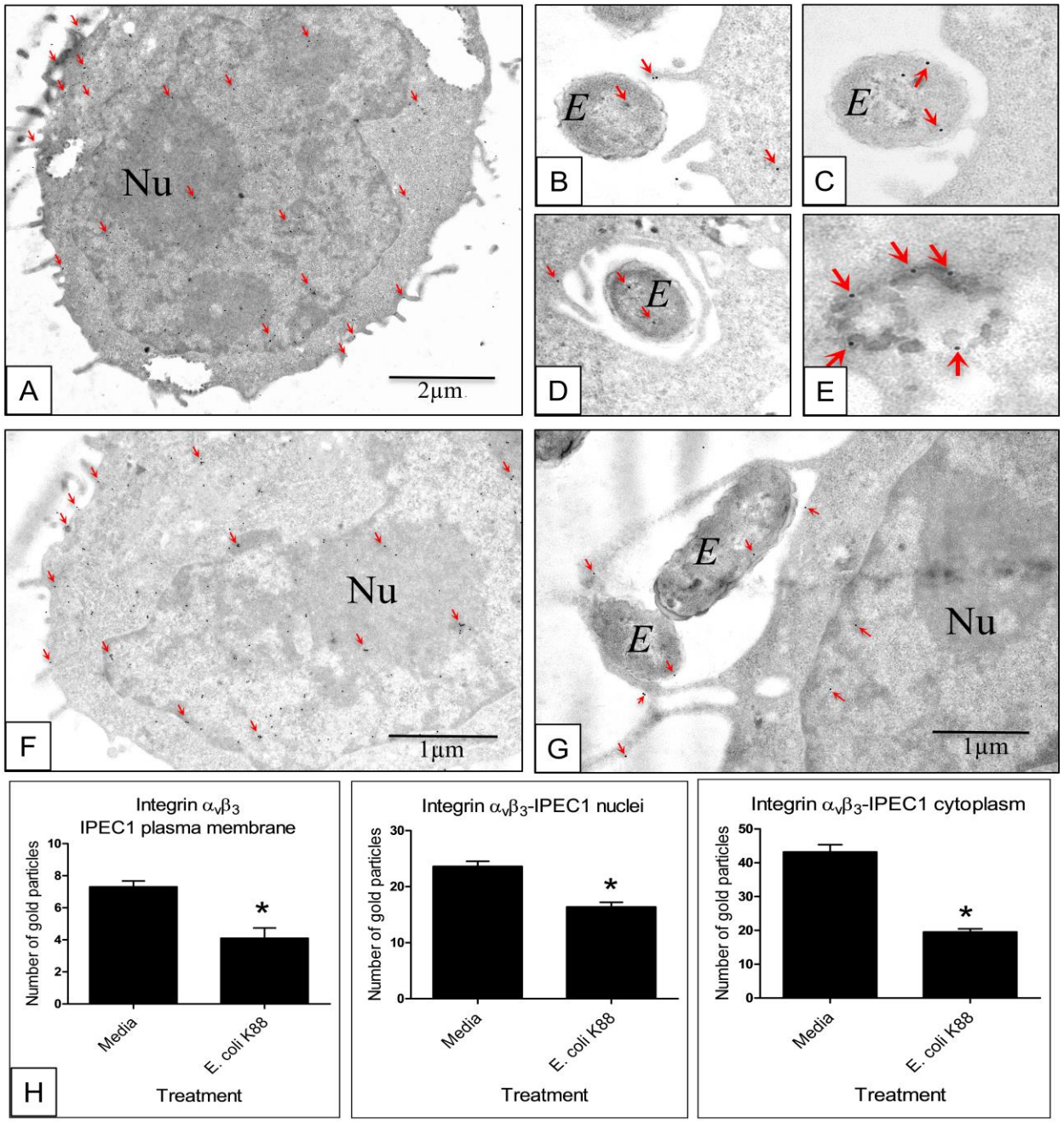

Figure 4.2. Immuno-gold electron micrograph of integrin αvβ3 in normal IPEC1and E. coli F4 infected IPEC1.

Transmission immuno-electron micrographs illustrated that integrin αvβ3 (arrows) is ubiquitously present in the nucleus (Nu), cytoplasm, and plasma membrane of medium-treated healthy control IPEC1 (A, F). The cross-sections of E. coli F4-challenged IPEC1 (B, C, D, E, and G) showed the

membrane ruffles at the site of contact with E. coli (C). The elongated microvilli of IPEC1 engulfed E. coli (G). Figure D showed an intracellular E. coli after one hour of challenge. Immuno-gold staining images illustrated the presence of integrin αvβ3 on E. coli and IPEC1, particularly on the binding site of E. coli and IPEC1 (B, C), internalized E. coli (D, G), vesicles (E), and nucleus (G). The statistical analysis of the number of gold particles (H) showed a decrease (=P<0.05; n=10 IPEC1) in all compartments (nucleus, cytoplasm, and plasma membrane) in E. coli F4 -treated compared to medium-treated IPEC1. Data were expressed as mean ± SEM. Error bars indicate SEM. Abbreviation: Nu: Nucleus, E: E. coli F4. Original magnification: 20,000×.*

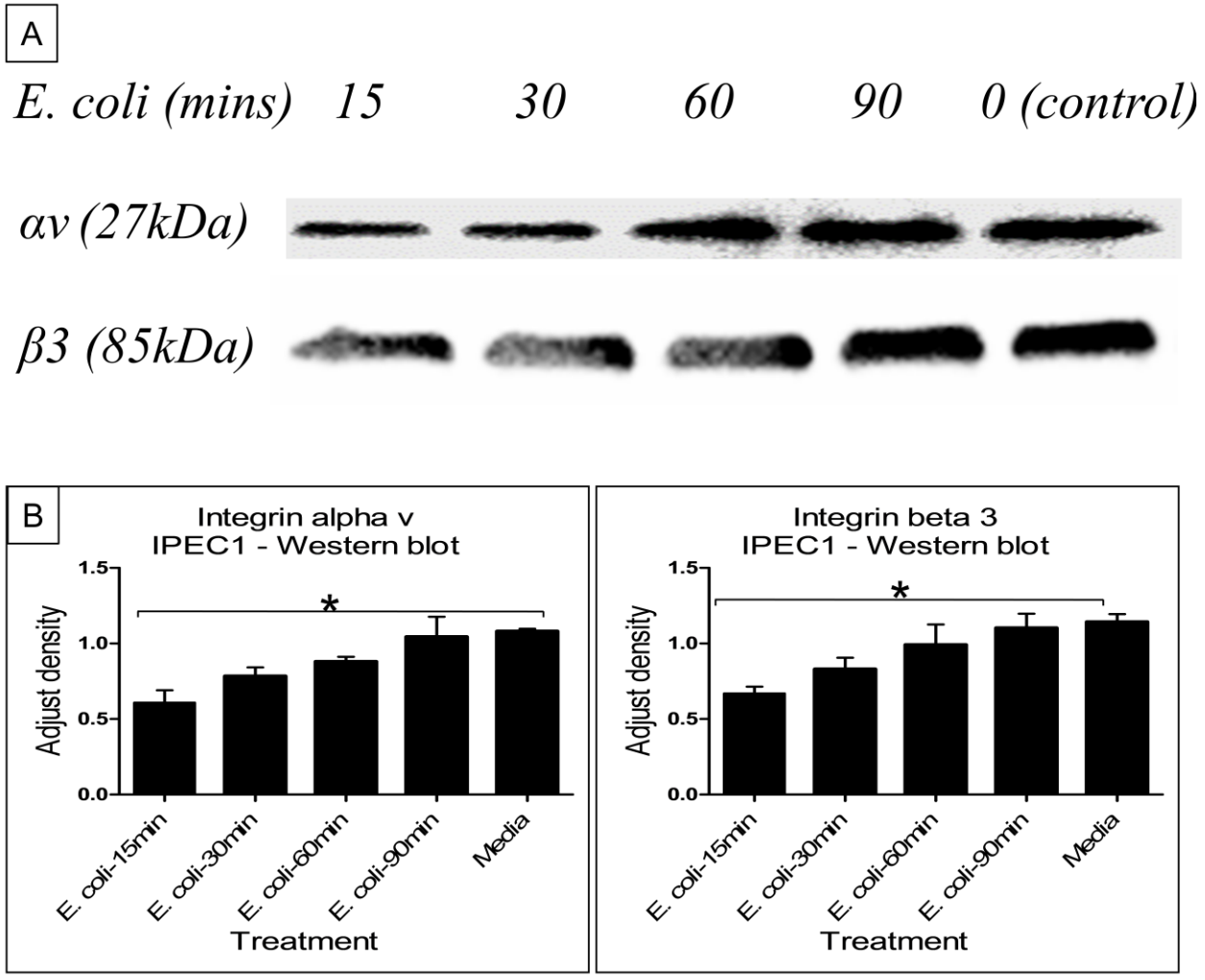

Figure 4.3. Immunoprecipitation for integrin αvβ3 following western blot for integrin αv and β3 subunits in normal control IPEC1 and E. coli F4 infected IPEC1

(A) Western blots performed on IPEC1 showed the light chain of integrin αv expressed at about 27 kDa, and integrin β3 at about 85 kDa. The densitometric analyses (B) showed decreased integrin αv and integrin β3 on IPEC1 at 15 minutes of E. coli F4 infection compared with normal control IPEC1. Data were expressed as mean ± SEM. Asterisk (*) indicates a significant difference from the normal media-treated IPEC1 control group ($P<0.05$, $n=4$).

4.4.2. Characterization of integrin αvβ3 in *E. coli*

The immunocytochemistry on the cytospin of *E. coli* showed that *E. coli* DH5α lab-strain (Figure 4.4C) had the weak staining of integrin αvβ3 while *E. coli* F4 (Figure 4.4D) had intense integrin αvβ3 staining. To have deeper understanding of the expression of integrin αvβ3 in *E. coli,* which can interact with RGD motif, we used immuno-gold electron microscopy. The results from immuno-gold staining showed *E. coli* F4 (K88) had more gold particle positive staining with anti-integrin αvβ3 antibody compared with *E. coli* DH5α (Figure 4.4.H). We also found that *E. coli* F4 (Figure 4.4.G) expressed integrin αvβ3 on the plasma membrane and cytoplasm of the bacteria. To semi-quantify the levels of integrin αvβ3, we performed immunoprecipitation to pull down integrin αvβ3 complex using anti-integrin αvβ3 antibody. Then, this immunoprecipitated protein was western blotted with integrin αv antibody and integrin β3 antibody (Figure 4.4. A). Densitom-etry quantification from western blot showed that *E. coli* F4 had more integrin αvβ3 than *E. coli* DH5α (Figure 4.4.B, E). We continued using immunoprecipitated protein from anti-integrin αvβ3 antibody on *E. coli* lysates for a mass-spectrometry analysis. The pilot study showed that although the protein from the band in gel was lacking stability and was not in high concentration, *E. coli* F4 had distinct/unique valid peptides same as in human integrin alpha v (SPSHSk, YDPnVYSIk, VSCFNVRFCLkADGk, QEREPVGtCFLQDGTKTVEYAPCR, LQEVGQVSVSL, qDKILACAPLYHWRTEMk, LEVSVDSDQKK matching with database accession number P06756) and distinct/unique valid peptides same as in human integrin beta 3 (IGDTVSFSIEAK-VRGCPQEK matching with database accession number P05106).

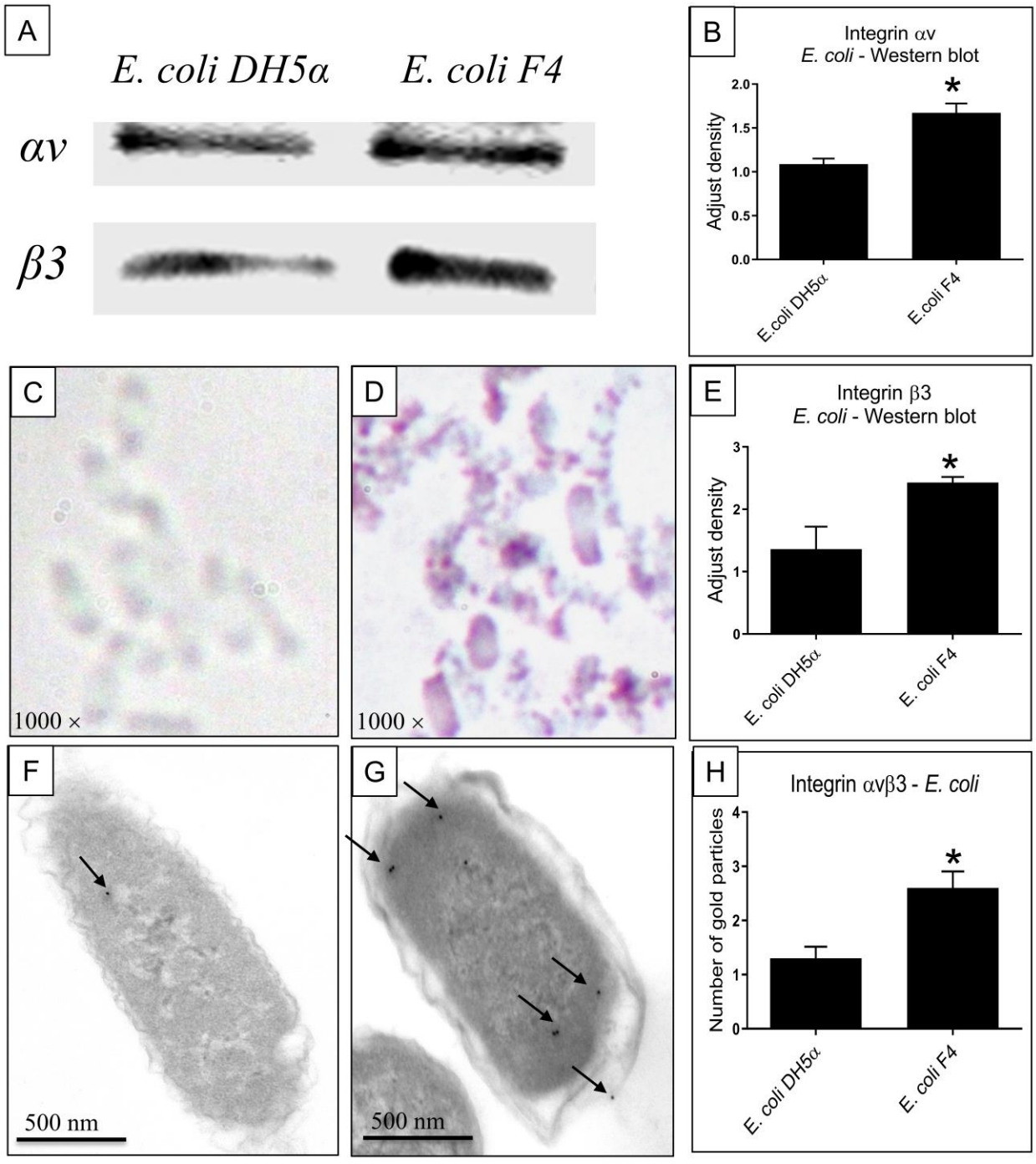

Figure 4.4. Integrin αvβ3-like protein in E. coli.

Immunoprecipitation for integrin αvβ3 following western blot for integrin αv and integrin β3 (A) on E. coli lysate show integrin αv band at about 27 kDa. (the light chain), and integrin β3 at about

85 kDa. The densitometric analyses (B, E) showed that E. coli F4 had more integrin αvβ3 than E. coli DH5α. Data were expressed as mean ± SEM. Asterisk (*) indicates a significant difference from E. coli DH5α (P<0.05, n=3). The immunocytochemistry (C, D, purple: integrin αvβ3, light green: methyl green-stained DNA), immuno-gold electron staining (E, F, arrow) and statistical analysis of quantity of integrin αvβ3 gold particles (H) showed E. coli F4 (D, G) had stronger positive staining with integrin αvβ3 than E. coli DH5α (C, F) (=P<0.05; n=10). Data were expressed as mean ± SEM. Error bars indicated SEM. Original immuno-gold electron micrograph magnification: 25,000×.*

To confirm that *E. coli* had an integrin αvβ3-like protein, we performed *in vitro* binding assays in 96-well high binding plates coated with anti-integrin αvβ3 antibody. The principle is that the measured fluorescence intensity depends on the number of *E. coli* bound to the integrin αvβ3 antibody-coated on wells, which is the representative of the presence of the integrin αvβ3-like protein on *E. coli*. Data showed that with the same dose of *E. coli, a* significantly higher number of *E. coli* binding to the anti-integrin αvβ3 antibody-coated wells comparing with uncoated ones ($P<0.05$) (Figure 4.5). These data suggested that *E. coli* had an epitope of integrin αvβ3 which can bind to anti-integrin αvβ3 antibody.

Here, we also found that the number of *E. coli* binding to the well plate depended on the different concentrations of the integrin αvβ3 antibody used for coating on the plate wells (Figure 4.6). It again suggests that *E. coli* has a protein domain like integrin αvβ3.

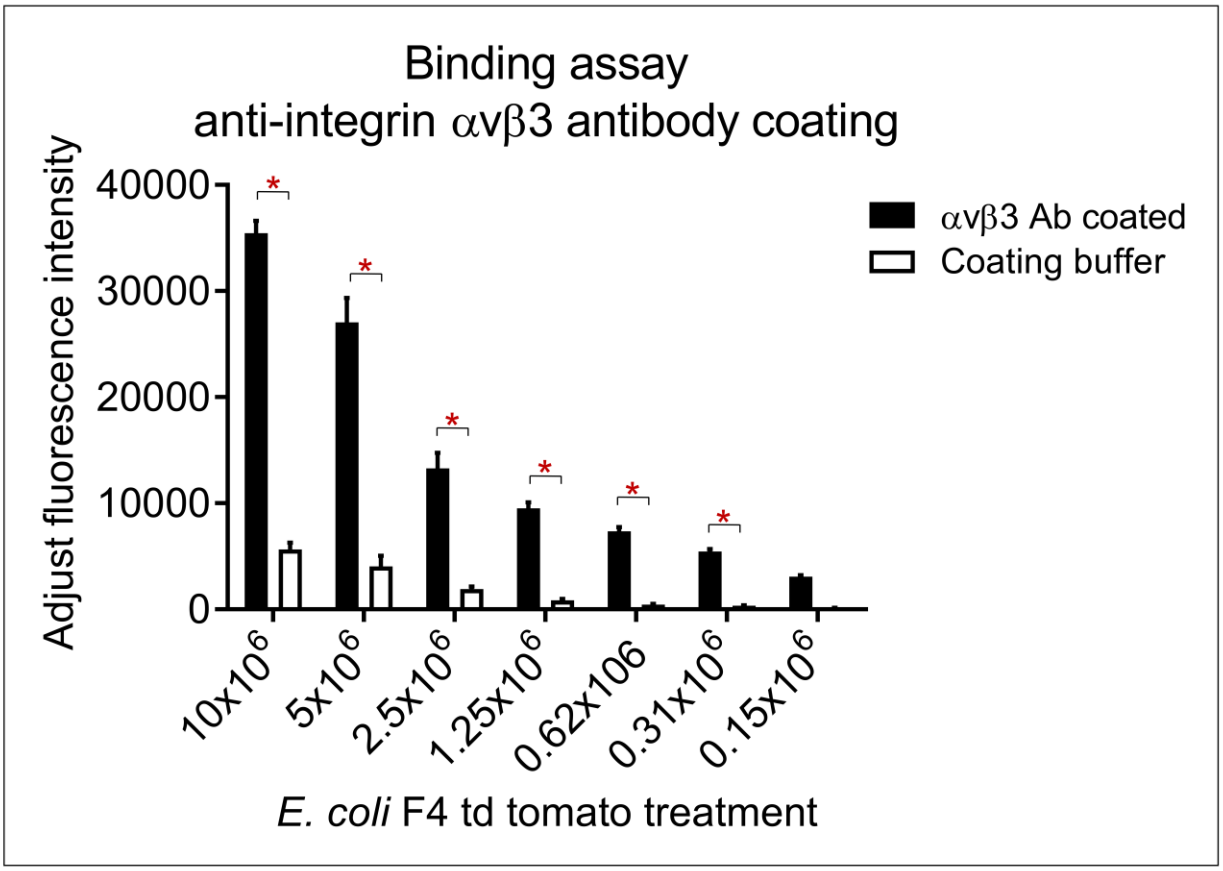

Figure 4.5. Binding assay on anti-integrin αvβ3 antibody-coated 96 well plates.

E. coli F4 pFPV::tdTomato at seven different concentrations was added to monoclonal integrin αvβ3 antibody-coated wells and uncoated wells of high binding plates. pFPV::tdTomato fluorescence from binding E. coli was measured at 530nm excitation /570nm emission in POLAR Start OPTIMA microplate fluorescence reader. Fluorescence intensity was adjusted with the background fluorescence of the wells without adding E. coli. Data were expressed as mean ± SEM. Error bars indicate SEM. Asterisk (*) indicates a significant difference from the uncoated well with the respective dose of E. coli ($P<0.05$, $n=4$).

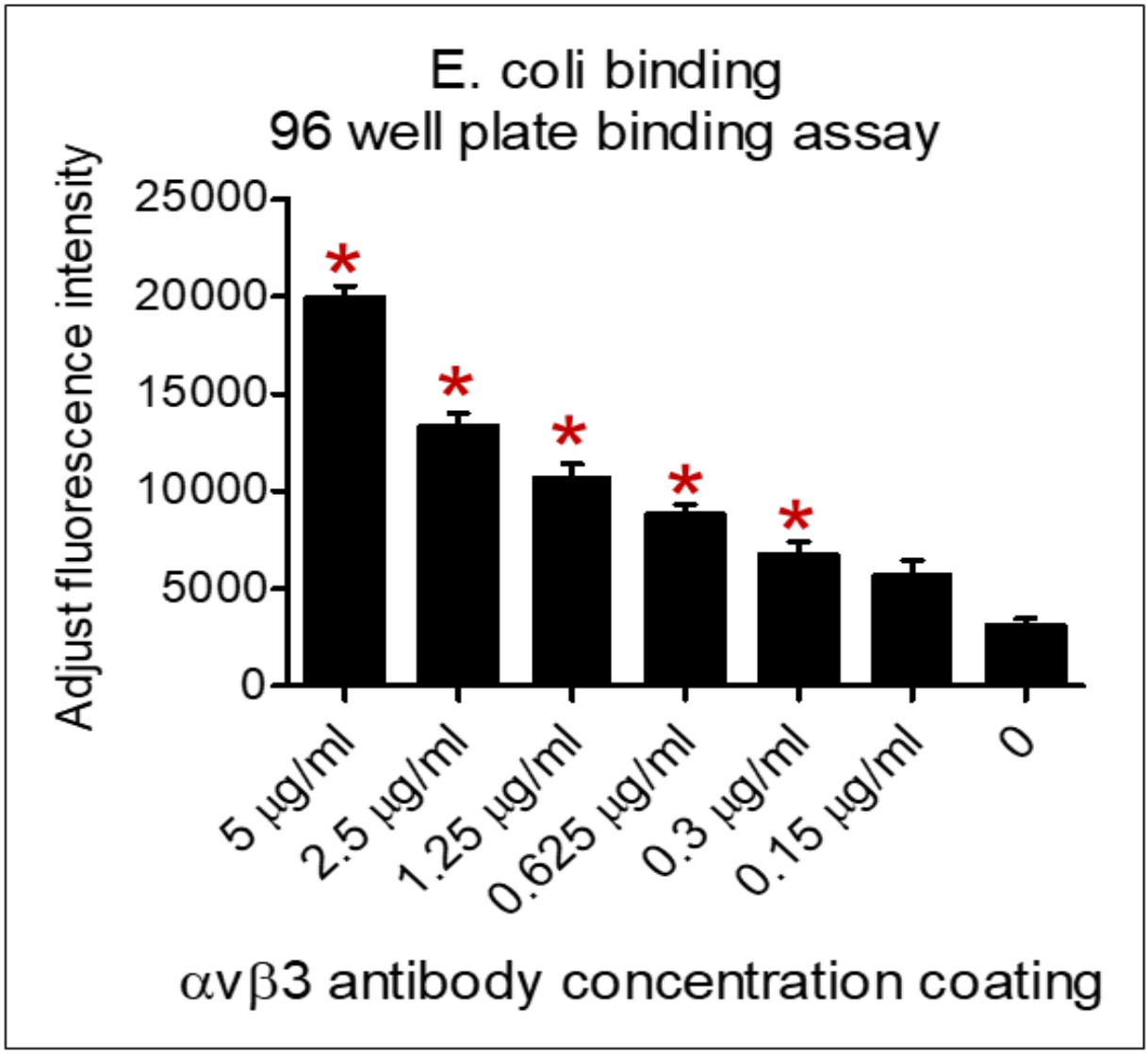

Figure 4.6. E. coli binding to anti-integrin αvβ3 antibody-coated well plates.

E. coli F4 pFPV::tdTomato was added to high binding plates, which were coated with six different concentrations of monoclonal antibody anti-integrin αvβ3. E. coli has an integrin αvβ3-like protein domain which can bind to anti-integrin αvβ3 antibody-coated well plates. Data were expressed as mean ± SEM. Asterisk (*) indicates a significant difference compared with an uncoated-well group (0) ($P<0.05$, $n=3$ each group).

4.5. DISCUSSION

There are no data on whether the epithelial integrin αvβ3 has an impact on the cellular attachment and uptake of *E. coli*. In this study, a series of experiments were conducted to demonstrate that the integrin αvβ3 has a role in the binding of *E. coli* bacteria to the cell surface.

Although integrin αvβ3 expression was not reported in prokaryotes in the past (203), Tchesnokova and colleagues recently revealed that *E. coli* K12 had an integrin-like allosteric site on FimH, an adhesive subunit of type 1 fimbriae of *E. coli* (232). Moreover, micronemal adhesin MIC2 of *Toxoplasma gondii* had integrin-like A domain to interact with LAMTOR1 and RNaseH2B proteins of the host cell during parasite invasion (253). In this study, we found integrin αvβ3-like protein in *E. coli* F4. These data were collected with many methods. The immunohistochemical expression of the integrin was further confirmed through Western blots and immunogold electron microscopy. Interestingly, there was a difference in the expression of integrin αvβ3 between two strains of *E. coli*, and reasons for these differences remain unknown. The identity of the protein being detected by the antibodies in microscopy and Western blot was confirmed with blotting of the immuno-precipitates with integrin αvβ3 antibody. Lastly, the pilot sequencing of the immunoprecipitated protein bands showed the homology with the human integrin αv and β3 sequences. Taken together, our data prove that *E. coli* expresses an integrin αvβ3-like protein domain.

Our data also show the novel role of integrin αvβ3 in the adherence of bacteria. The *in vitro* assay on plate wells coated with integrin αvβ3 antibody showed the binding of integrin αvβ3 antibody concentration-dependent binding of *E. coli*. It is possible that integrin αvβ3 is important in the uptake of *E. coli* by IPEC1 cells. Our *in vitro* experiment using IPEC1 cell line showed that *E. coli* infection decreased the expression of the integrin αvβ3 on the cell line. The data were

collected by western blot, immune-gold, and immunofluorescent staining. The implications of the downregulation of the integrin expression are not clear, but it may be a mechanism that *E. coli* uses it to prevent the activation of the cells or to down regulate the immune response. The integrin has previously been shown to be a receptor for pathogens such as virulent Foot-and-mouth disease virus type O1 (164) and *Staphylococcus aureus* binding to integrin αvβ3 on the endothelium leading to endothelial dysfunction (149). The attachment of *E. coli* and *Staphylococcus* to human endothelial cells was reduced by Cilengitide through inhibiting integrin αvβ3 (73, 149). As is well known, the integrin αvβ3 binds to RGD peptides, which are present in extracellular matrix molecules such as fibronectin, osteopontin, collagen, and vitronectin (196, 220). The integrin αvβ3 regulates cell functions such as activation, proliferation, and adherence through a variety of signals (196, 220). We confirmed that *E. coli* F4 efficiently binds to the IPEC1 cell line *in vitro* (126). Therefore, our data showed that the integrin might also be a receptor for *E. coli*, thus creating a possible route to interference with its adherence to the intestinal epithelium of pigs (106).

Overall, the results in this chapter indicate that integrin αvβ3 was expressed on IPEC1. We also found that *E. coli* has an integrin αvβ3-like functioned protein. The information on the expression of integrin αvβ3 on IPEC1 and *E. coli* upon infection is the initial essential understanding to develop a new approach to modulate intestinal diseases. The next chapter, therefore, should move on to discuss the function of integrin αvβ3 on intestinal epithelium.

ACKNOWLEDGMENTS

We thank the Saskatchewan Agriculture Development Fund (ADF), the Natural Science and Engineering Research Council (NSERC), the Graduate Student Scholarship program from the Integrated Training Program in Infectious Disease, Food Safety and Public Policy (ITraP), the Devolved Graduate Scholarship program from the Department of Veterinary Biomedical Sciences,

and the Graduate Student Scholarship program from the Western College of Veterinary Medicine at the University of Saskatchewan, Canada for supporting this research. We thank Dr. Abdul Lone, Siew Hon Ng, Champika Fernando, LaRhonda Sobchishin, and Eiko Kawamura for the technical support. We sincerely thank Dr. Douglas Call at the Washington State University, USA; Dr. Janet Hill, Dr. Francois Meurens, and Dr. Heather L. Wilson, VIDO-InterVac at the University of Saskatchewan for their generous gift materials.

GRANTS

The study was funded through the Saskatchewan Agriculture Development Fund (ADF) and the Discovery Grant from the Natural Sciences and Engineering Research Council of Canada (NSERC) to Dr. Baljit Singh.

CHAPTER 5. THE EFFECTS OF RGDSK-HRNs-FITC AND INTEGRIN αvβ3 INTERACTION ON INHIBITING *E. COLI* ADHERENCE TO IPEC1 *IN VITRO* AND PORCINE VILLI *EX VIVO*

To manage outbreaks of intestinal diseases and foodborne illness, numerous scientists have attempted to reduce the bacterial colonization in the intestines. Results from the previous chapter suggested that integrin αvβ3 was involved in *E. coli* F4 infection. Integrin αvβ3 recognizes and binds the RGD peptide. There are no data on whether the integrin αvβ3 in the jejunum has an impact on the cellular attachment of *E. coli* F4. Therefore, in this chapter, we used RGDSK-HRNs and further investigate its functions in blocking the attachment of *E. coli* to IPEC1 *in vitro* and porcine villi *ex vivo*.

5.1. ABSTRACT

Intestinal diseases and foodborne illness, particularly due to *E. coli* infection, cause many deaths and economic losses worldwide. One of the strategies to reduce the incidence of these disease outbreaks is to reduce bacterial colonization in the intestines. Integrin αvβ3 recognizes arginine-glycine-aspartic acid (RGD) sequences and has important functions in cell adhesion, signalling, and survival. However, the role of the integrin αvβ3 in the adhesion of *E. coli* F4 on the intestinal epithelium remains elusive. To study this gap of information, we performed a series of experiments using a novel RGDSK-HRNs-FITC, the intestinal porcine epithelial 1 cell line **(**IPEC1), porcine villi, and *E. coli* F4.

In this study, we found that RGDSK-FITC peptides and RGDSK-HRNs-FITC bound to integrin αvβ3 on both IPEC1 and *E. coli* F4. RGDS peptides blocked the attachment of *E. coli* F4

to IPEC1 ($P<0.05$) and reduced the survival of *E. coli* F4 ($P<0.05$). RGDSK-HRNs-FITC pretreatment at 1 μM concentration mediated a half of the attachment of *E. coli* F4 to IPEC1 ($P<0.05$). The data from binding assays on 96-well plates showed that the number of *E. coli* binding to the integrin αvβ3 coated wells was significantly higher than that binding to uncoated wells with the same dose of *E. coli* ($P<0.05$). We then performed *ex vivo* villus adhesion assays on scraped villi from porcine jejunum. The data showed that in F4 receptor-positive villi, RGDSK-HRNs-FITC significantly reduced the number of adhering *E. coli* for up to 12 hours compared with the *E. coli*-only challenged group ($P<0.05$). Both RGDSK-FITC peptide and monoclonal anti-integrin αvβ3 antibody were effective in inhibiting the *E. coli* binding to villi for up to 24 hours. Confocal microscopy confirmed the binding of RGDSK-HRNs-FITC to both villi and *E. coli* F4.

In conclusion, these are the first data showing the function of the integrin αvβ3 in the adherence of *E. coli* to the intestinal epithelium, and showing that novel RGDSK-HRNs-FITC intervention, maybe a potential alternative to antibiotics, can inhibit the attachment of *E. coli* to the epithelium.

Key Words: integrin αvβ3**,** nanotubes**,** porcine epithelium, *E. coli*

5.2. INTRODUCTION

E. coli is usually found in the environment, food, and the intestines of animals and humans (233). Although some *E. coli* strains are harmless and controllable (233), others infect the intestinal, urinary, and respiratory systems (115). The first step of infection is the adhesion of bacteria to the epithelium via their fimbrial binding or other mechanisms (124). Some specific adhesive receptors have been reported that are used as an alternate by *E.coli* to bind to the intestinal epithelium when any one of them is inhibited (F4, F41, F1, …) (70). Because of redundancy in

adhesive receptors, changes in biological characteristics, and many virulence factors, concerted global efforts to manage and control *E. coli* infections have been only partially successful (34, 35, 185, 247). Therefore, we need to identify other putative receptors for *E. coli* binding and exploit them to reduce intestinal colonization by these bacteria.

Integrin αvβ3, a heterodimeric glycoprotein, recognizes and binds arginine-glycine-aspartic acid (RGD) sequences (159, 220). Integrin αvβ3, known as a transmembrane receptor, plays a key role in bidirectional signalling across the membrane, and cell-matrix adhesion of cells (155, 159, 193, 220). Some bacteria and viruses likely use integrin αvβ3 on the surface of the epithelium as their receptors (58, 123, 149, 164). Our lab reported that integrin αvβ3 was abundantly expressed in the porcine gut epithelium in addition to those of calves and dogs (213). However, the role of integrin αvβ3 in the adhesion and colonization of *E. coli* to gut epithelium remains unknown.

Nanotechnology has ushered in a new area of material design, starting from the atomic scale (1, 142). There are novel nanomaterials with potential applications in bacterial infection treatment or cancer diagnostics (1, 142). One of the novel nanomaterials is the helical rosette nanotubes (HRNs), which are non-metallic, organic, bio-compatible, and water-soluble (63, 64, 134). The HRNs are synthesized through a novel system where guanine (G) - cytosine (C) bases, also known as a GΛC- motif, assemble themselves in a helical rosette shape. The HRNs present many sites for the attachment of various functional groups and their display on the surface (63, 64, 134).

Researchers have integrated RGD peptide sequences into nanomaterials to bio-functionalize them (83, 125, 155). The reason for functionalizing RGD sequences is because the same RGD amino acid sequence occurs in several extracellular matrices (ECM) proteins such as fibrinogen,

vitronectin, and fibronectin, which mediate cell adhesion to the ECM (155). Recently, the Fenniri laboratory has conjugated Arg-Gly-Asp-Ser-Lys (RGDSK) peptide to HRNs (RGDSK-HRNs) to functionalize the tubes to target integrins for specific medical and biological applications (39). Based on our finding of the expression of integrin αvβ3 on *E. coli*, we tested the hypothesis that RGDSK-HRNs would localize along the integrin αvβ3 expressing IPEC1 and block the attachment of *E. coli* to IPEC1 *in vitro*.

5.3. MATERIALS AND METHODS

5.3.1. Materials

Novel HRNs were designed by Dr. Fenniri and were supplied by his laboratory at the Department of Chemical Engineering, the College of Engineering, Northeastern University, Boston, USA. (39, 63, 64).

E. coli F4 strain EC52, serotype O101:K30+:K99-: F4+ and IPEC1 were generous gifts from Dr. Francois Meurens and Dr. Heather L. Wilson at the Vaccine and Infectious Disease Organization-International Vaccine Centre (VIDO-InterVac). IPEC1 cells were developed from the jejunum of unsuckled, mixed-bred piglets less than 12 hours old (85). IPEC1 cells were cultured in 75 cm^2 flask in Dulbecco's Modified Eagle Medium/Nutrient Mixture F-12 at 37ºC in a humidified 5% CO_2 incubator (84, 126).

Mouse monoclonal integrin αvβ3 antibody (clone LM609, Chemicon Inc., Temecula, USA), Alexa Fluor 633 conjugated secondary antibody polyclonal goat anti-mouse immunoglobulins (Thermo Fisher, Rockford, USA), RGDSK-FITC (American peptide company, Sunnyvale, CA., USA.), and CF^{TM}488A-Annexin V (AnV) and Propidium Iodide (PI) Apoptosis Kit (Biotium, Hayward, CA., USA.) were purchased commercially.

5.3.2. Preparing *E. coli*

E. coli strain EC52, serotype O101:K30+:K99-: F4+, having pFPV::tdTomato fluorescence protein, was cultured for 18 hours on Luria broth supplemented with ampicillin. The concentration of bacteria was determined by adjusting the optical density at 620nm (OD_{620}) to 1 to achieve $4x10^9$ CFU/ml as determined by prior CFU counting. *E. coli* was centrifuged at 16,200 xg for 5 minutes, followed by three washes in 0.1M PBS supplemented with ampicillin at pH=7.4. Serial dilution was done to reach the desired concentration of the bacteria for the assay later, according to previously cited procedure (126).

5.3.3. Preparing RGDSK-HRNs-FITC

TBL/TB- RGDSK is a twin GΛC – based rosette nanotubes (RNTs) functionalized with arginine-glycine-aspartic acid-serine-lysine (RGDSK) peptide sequence which can bind to integrin αvβ3. The TBL/TB-FITC is a fluorescein isothiocyanate (FITC) conjugated twin GΛC – based rosette nanotubes (RNTs). TBL/TB-FITC and TBL/TB-RGDSK in 1:10 molar ratio of FITC and RGDSK were mixed to yield the composite of RGDSK and FITC functionalized helical rosette nanotubes (RGDSK-HRNs-FITC). This more stable self-assembling HRNs expresses RGDSK, and is visualized by fluorescence microscope (39, 225). The suspension was sonicated for 5 minutes in a water bath following by 30-second vortex and one-minute heating. The mixture was placed at room temperature in the dark for 48 hours to allow for the synthesis of the RGDSK-HRNs-FITC. The RGDSK-HRNs-FITC stock was stored in 4^oC for future use in experiments. RGDSK-HRNs-FITC was diluted in an appropriate dilution buffer (0.1M PBS or DMEM/F12) at preferring molar concentration regarding the equivalent RGDSK on the surface of HRNs.

5.3.4. *In vitro* binding assay on 96-well high binding plates

To examine whether *E. coli* can bind integrin αvβ3, we performed an *in vitro* integrin αvβ3 binding assay, modified from previous protocols (27, 149). In brief, 96-well high binding plates were precoated overnight with 50µl of 5µg/ml human integrin αvβ3 protein (CC1018, EMD Chemicon Inc., Temecula, USA) in 100 mM HCO_3^-/CO_3^- coating buffer. Wells with coating buffer without integrin αvβ3 was used as a negative control. The wells were washed gently with 100µl of sterile 0.1%Tween-TBS then were incubated in 1% BSA to prevent non-specific binding. *E. coli* F4 having pFPV::tdTomato fluorescence protein was added at seven concentrations (50 µl of $10x10^6$, $5x10^6$, $2.5x10^6$, $1.25x10^6$, $0.62x10^6$, $0.31x10^6$, $0.15x10^6$ CFU per well). After a one-hour incubation, non-adhering *E. coli* was removed by rinsing with PBS ampicillin. The bound *E. coli* were fixed in 2% paraformaldehyde. pFPV::tdTomato fluorescence from binding *E. coli* was measured at 530nm excitation /570nm emission in POLAR Start OPTIMA microplate fluorescence reader. Fluorescence intensity was adjusted with background fluorescence from well without *E. coli*. The experiment was repeated four times.

5.3.5. Quantifying *E. coli* binding to RGDSK-HRNs treated IPEC1

For binding assay, $2x10^5$ IPEC1/well were seeded into 24-well plate, having cover slides at the bottom. After being confluent overnight, IPEC1 cells were washed using 1 ml of fresh DMEM/F12 without serum per well. Cells were exposed to RGDS peptide (0.1, 1, 10, 50 µM) as controls at three different time points (5, 10, 15 minutes) or RGDSK-HRNs (containing equivalent 0.1, 1, 5µM RGDSK) at three different time point (2, 5, 10 minutes) or media only for control. Cells then were treated with $1x10^7$ *E. coli* F4/ml into RGDS peptide groups or $1x10^8$ *E. coli* F4/ml into RGDSK-HRNs groups.

In evaluating the biological effects of RGDSK-HRNs on *E. coli*, the supernatants were collected. These supernatants were serial diluted and cultured on blood agar and Luria broth agar with ampicillin plates. The number of *E. coli* colonies on the agars as an indicator of viable *E. coli* in the supernatants were counted for statistical analysis.

The supernatants were centrifuged at 16,200 xg for 5 minutes. Then the supernatants were stored at -80^{o}C for future experiments. Pellets were washed three times in 1X PBS, resuspended in 1X PBS, and cytospin onto microscope slide at 1,000 rpm in 4 minutes. Samples were fixed in methyl alcohol and assessed Wright-Giemsa staining following manufacture insert (EMD, Millipore, Temecula, USA.). An average number of *E. coli* binding to each IPEC1 (n=10 IPEC1/group) on cytospin slides were objectively calculated. The experiments were repeated three times for statistical analysis.

5.3.6. Immunofluorescent staining integrin αvβ3

For immunofluorescent staining, 2x10^{5} cells/well were seeded into 24-well plates having cover slides at the bottom. After being confluent overnight, IPEC1 cells were washed with 1 ml of fresh DMEM/F12 without serum per well. Cells were exposed to 10 µM RGDSK-FITC peptide in 5 minutes or RGDSK-HRNs-FITC (containing equivalent 5µM RGDSK) in 2 minutes or media only for the control group. Then cells were challenged with 10^{7} *E. coli* F4/ml.

The samples were fixed in 4% paraformaldehyde. Non-specific binding was blocked by 10% BSA. Samples were incubated with monoclonal anti-integrin αvβ3 antibody (dilute 1:50, clone LM609, Chemicon Inc., Temecula, USA) then Alexa flour 633 conjugated goat anti-mouse IgG secondary antibody (dilute 1:100). Cells were incubated for 5 minutes in 0.33µg/ml DAPI for staining DNA of nuclei. Samples were observed by a confocal scanning laser microscope Leica TCS SP5 LSCM, with a 63× objective lens under oil immersion. Negative controls for the

specificity of primary, secondary antibody, and protocol include mouse IgG1 isotype control, the omission of primary antibody, or the omission of both a primary antibody as well as a secondary antibody conjugated Alexa flour 633.

5.3.7. *Ex vivo* villus adhesion assay

As already known, the uptake of *E. coli* F4 is related to F4 receptor (F4R) mediation (240). Therefore, we used both F4R positive and F4R negative pigs to explore the function of integrin αvβ3 in the adhesion of *E. coli* F4 through a villus adhesion assay method described previously (241). Briefly, a segment of jejunum was washed three times with 0.1M PBS to remove intestinal contents. That segment was then opened and washed in cold Krebs-Henseleit buffer (120mM NaCl, 14 mM KCl, 25mM $NaHCO_3$, one mM KH_2PO_4) with 1% formaldehyde. Subsequently, porcine jejunal villi were gently scraped with a slide and let to settle at the bottom of the tube in this buffer. The supernatant was then discarded, and replaced by the same buffer until it was clear. At the time of the assay, the villi were washed in Krebs buffer to remove formaldehyde and were resuspended in 0.1M PBS ampicillin. To test the function of integrin αvβ3 and RGDSK-HRNs-FITC on *E. coli* F4 binding, $5x10^8$ of *E. coli* F4 was treated with RGDSK-HRNs-FITC (equivalent 5µM RGDSK) in 15 minutes. Five µM RGDSK-FITC, 5µg/ml mouse monoclonal integrin αvβ3 antibody (clone LM609, Chemicon Inc., Temecula, USA), 5µM TBL-FITC (nanotube without RGDSK group), rabbit anti-F4 antibody serum, 0.1M PBS were used as controls. Then, the treated *E. coli* F4 was added to an average of 50 villi for each treatment. Bacteria and villi were incubated for 4, 8, 12, and 24 hours at 37°C. Supernatants were collected and cultured in LB agar ampicillin to evaluate biological effects of RGDSK-FITC peptide, RGDSK-HRNs-FITC, mouse monoclonal anti-integrin αvβ3 antibody, TBL-FITC (nanotube without RGDSK

group), rabbit anti-F4 antibody serum, 0.1M PBS on *E. coli* F4 adhesion. The number of *E. coli* F4 colonies representing *E. coli* F4 viability in the supernatant was counted for statistical analysis.

To remove the unbound *E. coli* F4, the cultures were washed in 0.1M PBS, and samples were fixed in 4% paraformaldehyde to stop further *E. coli* F4 adhesion. After that, the number of bacteria adhering to 250 μm of the brush border of villi was quantified under a phase-contrast microscope at 1000× magnification. Five different regions were counted, and data were presented as the average number of bacteria adhering to 250 μm of the brush border. The experiment was repeated three times.

5.3.8. Statistical analysis

We used the GraphPad Prism version 5.04 software (San Diego, CA, USA.) to analyse data. Quantitative results were expressed as mean ± SEM, and error bars represented standard error. The normal distribution of residuals was tested by histogram and Shapiro-Wilk test. Data were analyzed by Analysis Of Variance (ANOVA), followed by Bonferroni multiple comparison test. A significant difference was set when the critical value of α was below or equal to 0.05 as (two-tailed, $p<0.05$).

5.4. RESULTS

5.4.1. The binding ability of *E. coli* depends on integrin αvβ3 *in vitro*.

To examine whether *E. coli* can bind integrin αvβ3, we performed an *in vitro* binding assay on integrin αvβ3 coated 96-well high binding plates. Data showed that with the same dose of *E. coli,* a significantly higher number of *E. coli* bound to the integrin αvβ3 coated wells compared with the uncoated ones (Figure 5.1). It means that coating integrin αvβ3 significantly increased the binding of *E. coli* into the plate. With the same concentration of integrin αvβ3 protein

coated in each well, the fluorescence intensity as an indicator of numbers of bound *E. coli* into the plate increased with the increased concentration of the bacteria ($P<0.05$). We did not have control groups with substitute protein coated control and with different strains of *E. coli.* However, the binding of *E. coli* to integrin αvβ3 coated wells suggested the presence of an RGD-like ligand in *E. coli*.

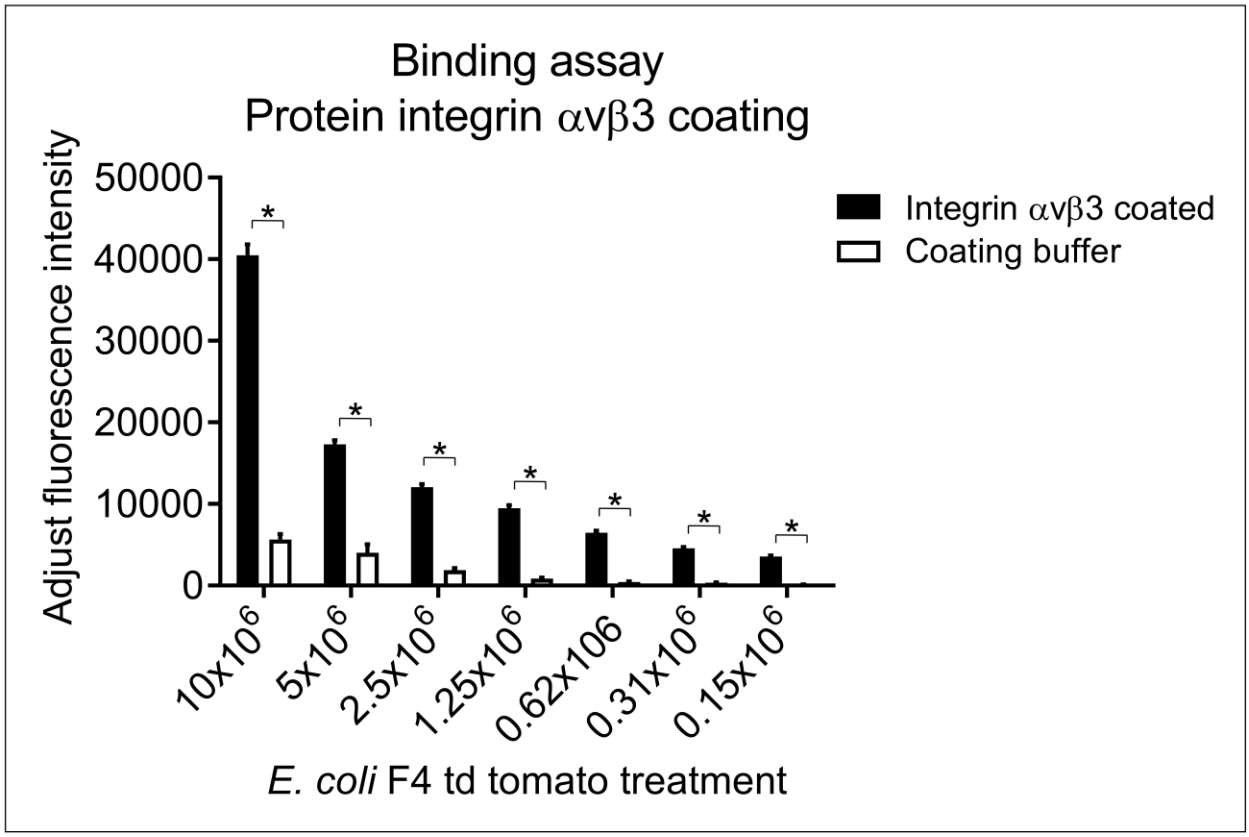

Figure 5.1. Integrin αvβ3 protein-coated 96-well plate binding assay.

E. coli F4 pFPV::tdTomato was added at seven concentrations to integrin αvβ3 coated high binding plates. pFPV::tdTomato fluorescence from binding E. coli was measured at 530nm excitation /570nm emission in POLAR Start OPTIMA microplate fluorescence reader. Fluorescence intensity was adjusted with background fluorescence from well without E. coli. Data were expressed as mean ± SEM. Error bars indicate SEM. An asterisk (*) indicates significant difference from the uncoated well with a respective dose of E. coli (n =4 each group, P<0.05).

5.4.2. RGDS peptide can block the attachment of *E. coli* to IPEC1 and affect *E. coli* survival *in vitro*.

We exposed IPEC1 to four different doses of RGDS (0.1, 1, 10, 50 μM) at three different time points (5, 10, 15 minutes), followed by a challenge with 10^7 *E. coli* F4/ml. To evaluate the effect of RGDS on the ability of *E. coli* to bind to IPEC1, we performed Wright-Giemsa staining the samples (Figure 5.2A), and calculated the number of *E. coli* binding to each IPEC1 cell. Our results show that the number of *E. coli* binding to each IPEC1 cell decreased significantly when IPEC1 was exposed to RGDS 5 minutes ($P<0.05$). However, there was no significant difference at a more extended time point beyond 15 minutes (Figure 5.2B). To test the biological effects of RGDS on *E. coli,* we determined *E. coli* viability in the supernatant by culturing it on blood agar and Luria broth agar with ampicillin. The number of colonies was calculated for statistical analysis. We found that RGDS peptide can affect *E. coli* survival, particularly when IPEC1 was exposed to 50μM RGDS in 10 minutes. However, there are no significant differences at longer time points after 15 minutes ($P<0.05$) (Figure 5.2C).

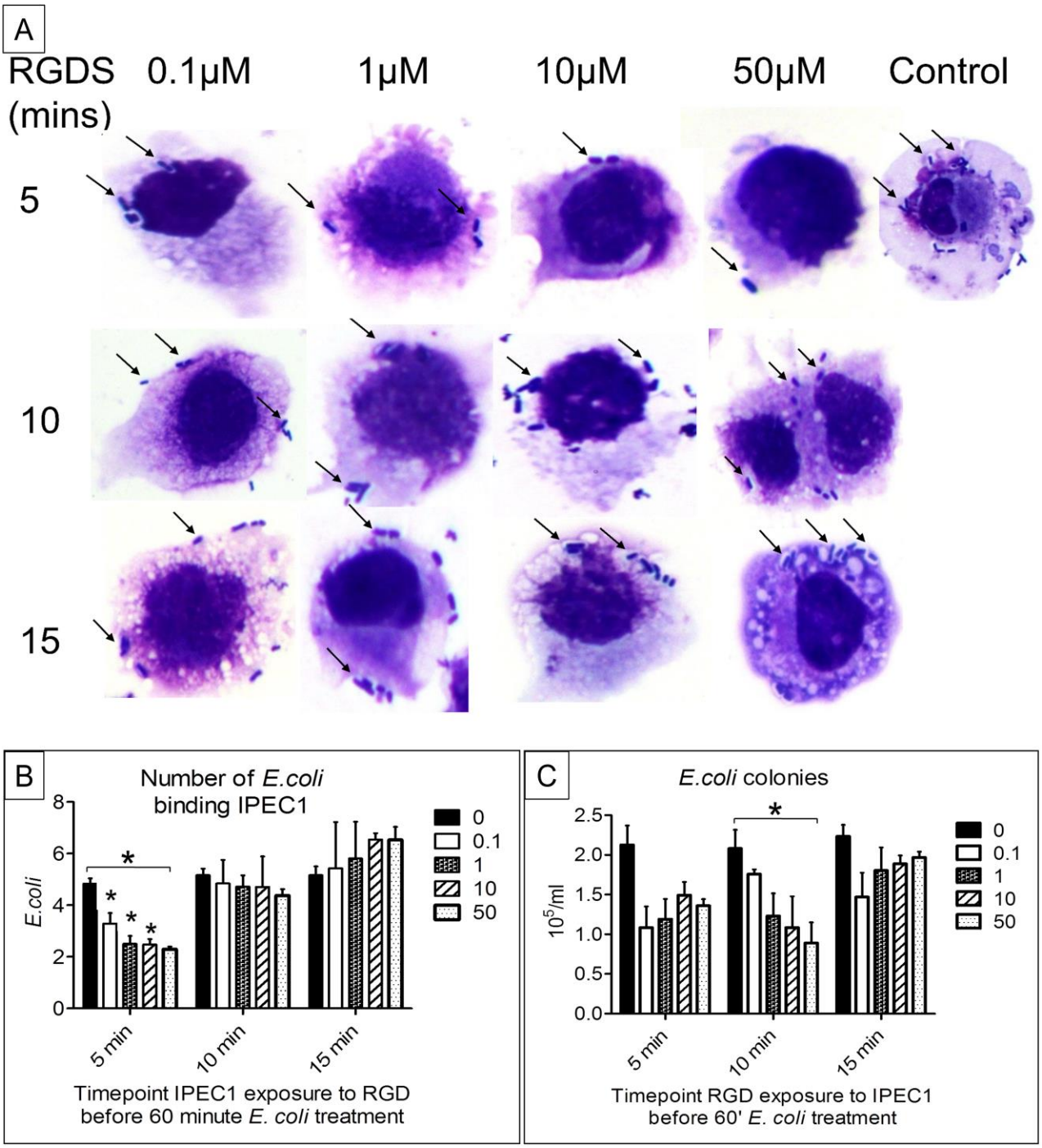

Figure 5.2. RGDS peptides can block the attachment of E. coli to IPEC1 and affect the survival of this bacteria.

To evaluate the effect of RGDS on the ability of E. coli in binding to IPEC1, we performed Wright-Giemsa staining (A), and calculated the number of E. coli binding to each IPEC1 (B). The number

*of E. coli binding to each IPEC1 decreased significantly in the group that IPEC1 was exposed to RGDS 5 minutes. However, there was no significant difference at longer timepoint. (C) To test the biological effects of RGDS on E. coli, we determined E. coli survival in the supernatant by culturing on Luria broth with ampicillin. The number of colonies was calculated for statistical analysis. We also found that RGDS peptide could reduce E. coli colonies in the supernatant, particularly in the group that IPEC1 was exposed to 50μM RGDS in 10 minutes. However, there were no significant differences at a longer timepoint after 15 minutes. (A) Representative Wright-Giemsa staining pictures of E. coli binding to IPEC1, challenging with different doses of RGDS at different time points. Data were expressed as mean ± SEM. Error bars indicated SEM. An asterisk (*) indicates a significant difference from the control no RGDS (n=3 each group, * P<0.05).*

5.4.3. Effect of RGDSK-HRNs on the attachment of *E. coli* to IPEC1 and *E. coli* death

We exposed IPEC1 to 3 different doses of RGDSK-HRNs (equivalent 0.1, 1, 5 µM RGDSK) at three different time points (2, 5, 10 minutes) before challenging these cells to 10^8 *E. coli* F4/ml. To evaluate the effect of RGDSK-HRNs on the ability of *E. coli* to bind to IPEC1, we performed Wright-Giemsa staining the samples (Figure 5.3.A), and calculated the number of *E. coli* binding to each IPEC1 cell. We found that compared with the group without HRNs-RGDSK, the number of *E. coli* binding to each IPEC1 decreased significantly in the group where IPEC1 was exposed to 5µM HRNs-RGDSK for 10 minutes before challenging with *E. coli* F4 (Figure 5.3.B). We also found that compared with the media treatment group (0), the number of viable *E. coli* in the supernatant was significantly higher in the group that IPEC1 was exposed to 5µM HRNs-RGDSK in 10 minutes before being challenged to *E. coli* F4 (Figure 5.3.C). These findings suggested that RGDSK-HRNs blocked integrin αvβ3 of *E. coli* and IPEC1, thus preventing these bacteria from interacting with IPEC1; consequently, more *E. coli* F4 left in the supernatant. The higher number of survival *E. coli* left in supernatant also proved that RGDSK-HRNs did not kill *E. coli* F4, expecting nontoxic to the cell. Other groups with different strains of *E. coli* or another substitute protein should be considered next time.

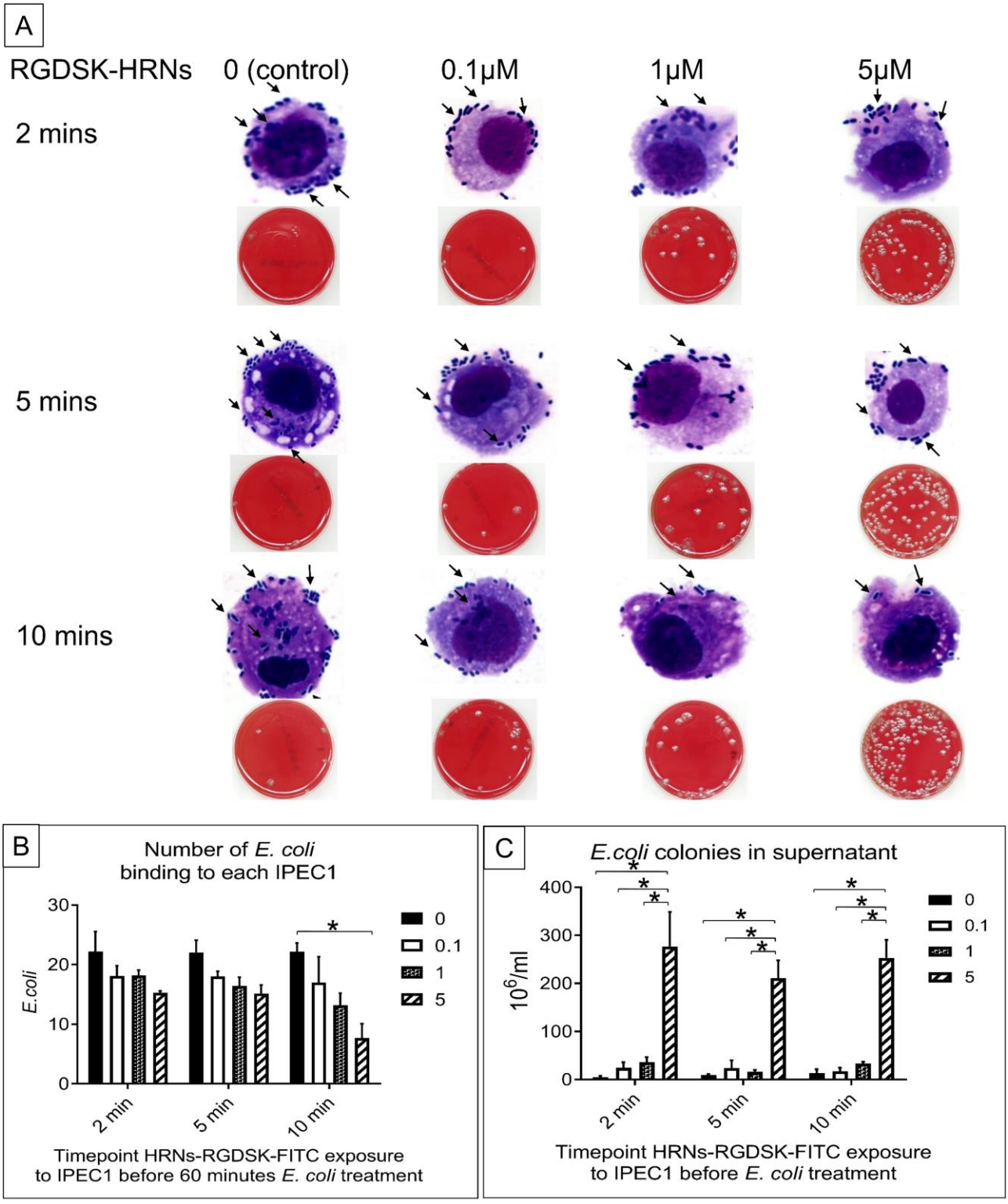

Figure 5.3. RGDSK-HRNs can block the attachment of E. coli to IPEC1 in vitro.

To evaluate the effect of RGDSK-HRNs on the ability of E. coli in binding to IPEC1, we performed Wright-Giemsa staining (A) and calculated the number of E. coli binding to each IPEC1 (B). To test the biological effects of RGDSK-HRNs on E. coli, E. coli viability in the supernatant was determined by cultured on blood agar with ampicillin (C). The number of colonies was calculated for statistical analysis. (A) This is representative pictures of the Wright-Giemsa staining of IPEC1, challenging with E. coli F4 as well as different doses of RGDSK-HRNs at different time points and E. coli colony left in the supernatant. Data were expressed as mean ± SEM. Error bars indicated SEM. The experiment was repeated four times. An asterisk (*) indicates a significant difference from the control without RGDSK-HRNs ($P<0.05$).*

5.4.4. RGDSK-HRNs-FITC and RGDSK-FITC can bind integrin αvβ3 in IPEC1 and an integrin αvβ3-like protein on *E. coli* F4

We performed immunofluorescent staining for integrin αvβ3 to observe interactions between RGDSK-HRNs-FITC and integrin αvβ3 on epithelial cell line upon *E. coli* infection (Figure 5.4A). Confocal images confirmed that integrin αvβ3 was strongly expressed in IPEC1 (Figure 5.4, row 4, column 1). The intensity of integrin αvβ3 staining on IPEC1 decreased upon a one-hour *E. coli* infection (Figure 5.4, row 4, column 2). RGDSK-HRNs-FITC bound to integrin αvβ3 in IPEC1 and an integrin αvβ3-like protein on *E. coli* F4 (Figure 5.4, row 2, column 3). We also found that RGDSK peptide at 50μM concentration blocked an integrin αvβ3-like protein in *E. coli* F4 *(*Figure 5.4*B,* row 1 column 4, and row 2 column 4) and integrin αvβ3 in all compartments of the IPEC1 cells *(*Figure 5.4*B,* row 3). The binding of RGDSK-HRNs-FITC or RGDSK-FITC, along with *E. coli* infection, decreased the intense positive staining of integrin αvβ3 on *E. coli* F4 *(*Figure 5.4*B,* row 1, and 2) and IPEC1 (Figure 5.4A, row 4, column 3).

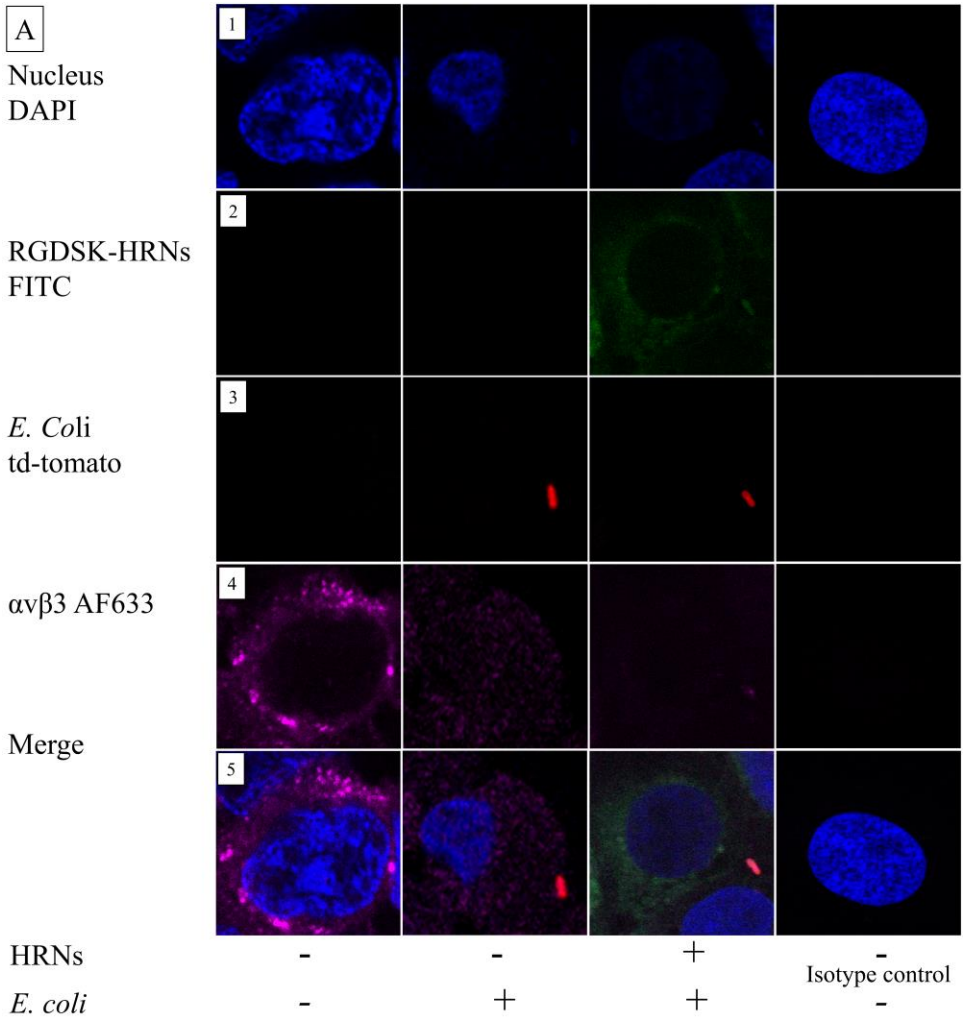
A
Nucleus
DAPI
RGDSK-HRNs
FITC
E. Coli
td-tomato
αvβ3 AF633
Merge
1
2
3
4
5
HRNs
E. coli
-
-
-
+
+
-
-
Isotype control

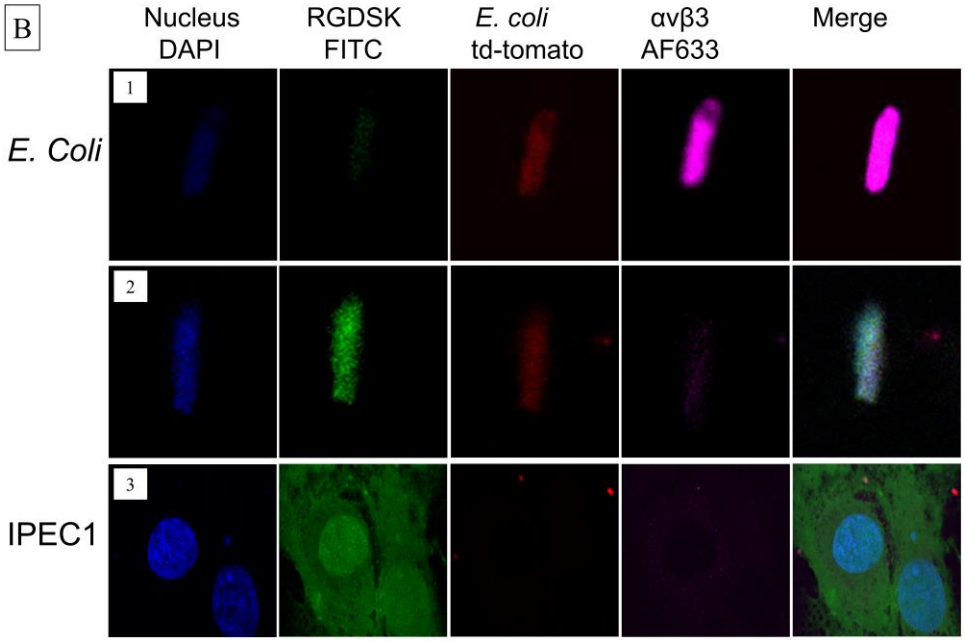
B
Nucleus
DAPI
RGDSK
FITC
E. coli
td-tomato
αvβ3
AF633
Merge
E. Coli
IPEC1
1
2
3

Figure 5.4. Representative images from immunofluorescent staining integrin αvβ3 under a confocal microscope.

(A) The interaction of RGDSK-HRNs-FITC with integrin αvβ3 on epithelial cell line upon E. coli infection: IPEC1 cells were pre-treated with 5μM RGDSK-HRNs-FITC for 10 minutes before being challenged with E. coli F4 for one hour. The final concentrations of treatments were 1μM of RGDSK-HRNs-FITC and 10^7 E. coli F4 in 1ml media. The concentration of RGDSK-HRNs-FITC means the equivalent concentration of RGDSK. (B) The interaction between RGDSK-FITC, E. coli and integrin αvβ3 on IPEC1: IPEC1 cells were pre-treated with 0.1μM RGDSK (row 1) or 50 μM RGDSK (row 2, 3) in 10 minutes before being challenged with E. coli F4 for one hour. The final concentrations of treatments were 0.01μM of RGDSK (row 1) or five μM RGDSK (row 2, 3) and 10^7 E. coli F4 in 1ml media. Both RGDSK-HRNs-FITC and RGDSK-FITC peptide can bind integrin αvβ3. Magenta: integrin αvβ3; Red: pFPV::td tomato E. coli F4; Green: RGDSK-HRNs-FITC; Blue: DAPI

5.4.5. RGDSK-HRNs-FITC could prevent *E. coli* adhering to porcine jejunal villi through interaction with integrin αvβ3 in an *ex vivo* villus adhesion assay

We performed *ex vivo* villus adhesion assay on scraped villi from porcine jejuna, as described above. To explore the function of integrin αvβ3-like protein on *E. coli* and the role of integrin αvβ3 on the epithelium of villi on *E. coli* binding, we pre-treated *E. coli* with RGDSK-HRNs-FITC for 15 minutes. Control treatments included RGDSK-FITC, TBL-FITC, monoclonal antibody anti-integrin αvβ3, anti-F4 antibody serum, and PBS. After that, porcine villi were added and incubated for 4, 8, 12, and 24 hours. We used both F4R positive and F4R negative pigs to explore the function of integrin αvβ3 because much of the uptake of *E. coli* is F4 receptor-mediated. Data showed that in F4 receptor-positive villi, RGDSK-HRNs-FITC significantly reduced the number of adhering *E. coli* compared with the *E. coli* challenged group until 12 hours ($P<0.05$), but not significant in longer timepoint (24 hours) (Figure 5.5A, Figure 5.6).

Similarly, in F4R negative villi groups, the number of adhering *E. coli* in the RGDSK-HRNs-FITC pretreated group was significantly lower than *E. coli* only challenge group at 4 hours timepoint, but not for longer incubation ($P<0.05$) (Figure 5.5B). These data suggested that RGDSK-HRNs-FITC prevented *E. coli* adhering to porcine jejunum villi but not over a more prolonged duration of exposure. Maybe long-time exposure gave a chance to the RGDSK peptide on the surface of nanotubes to bind both the integrin αvβ-like protein on *E. coli* and the villus integrin αvβ3; consequently, RGDSK-HRNs-FITC became a bridge between the bacteria and the epithelium. Other groups with diffenrent strains of *E. coli* or another substitute protein should be considered next time.

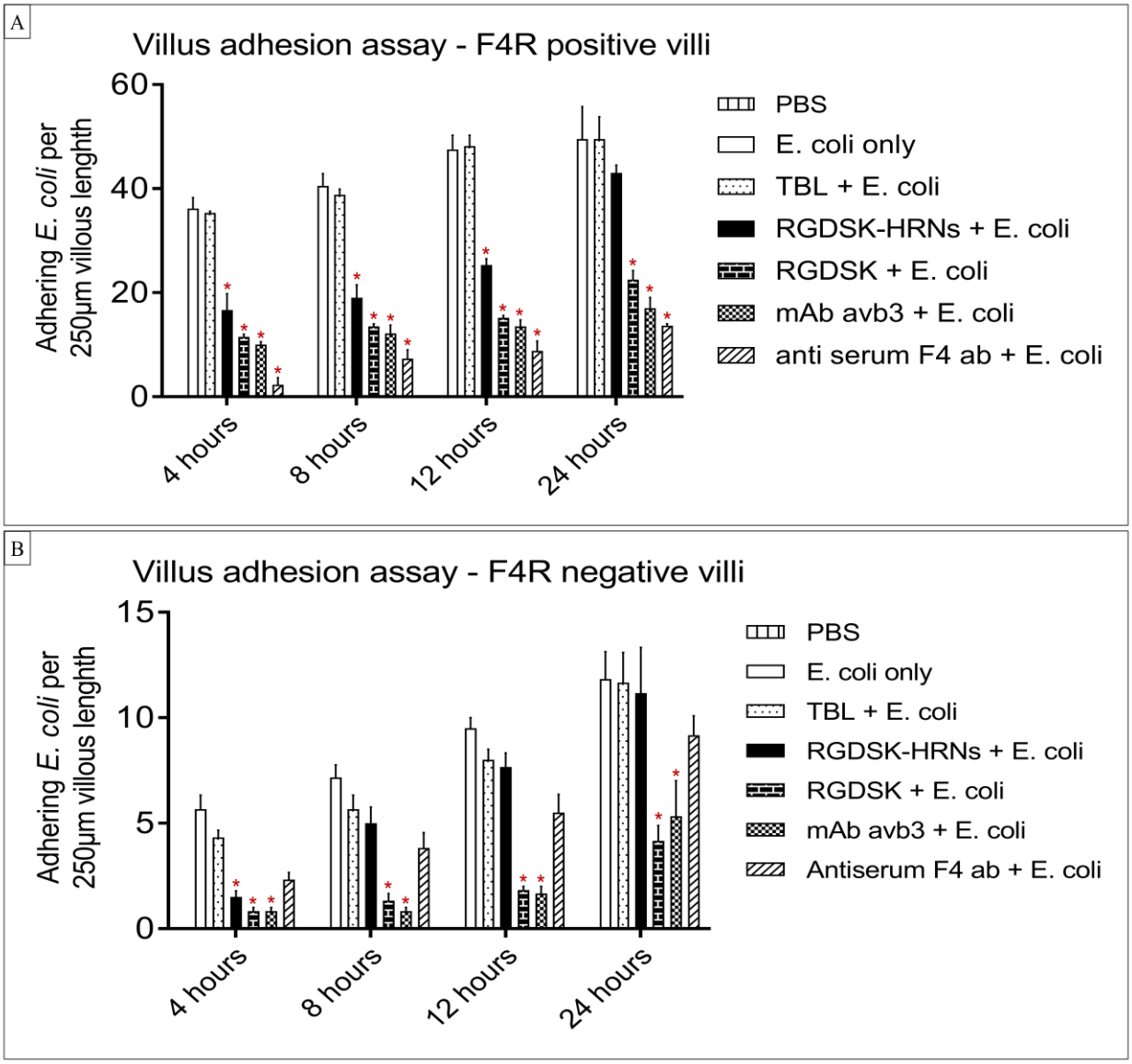

Figure 5.5. Ex vivo villus adhesion assay on scraped villi from porcine jejunum.

The number of adhering E. coli per 250 µm villus length were counted using a phase-contrast microscope. The number of adhering E. coli of the RGDSK-HRNs-FITC treatment group was significantly fewer than that of the E. coli infection group until 12 hours in F4 positive receptor villi (A). In F4 receptor negative villi, compared with E. coli only challenged group, RGDSK-HRNs-FITC significantly reduced the number of adhering E. coli at 4 hours timepoint but not for more prolonged incubation (B). Data were expressed as mean ± SEM. Error bars indicated SEM. An

asterisk (*) indicated a significant difference compared with E. coli treatment only group (P<0.05). The experiments were repeated three times.*

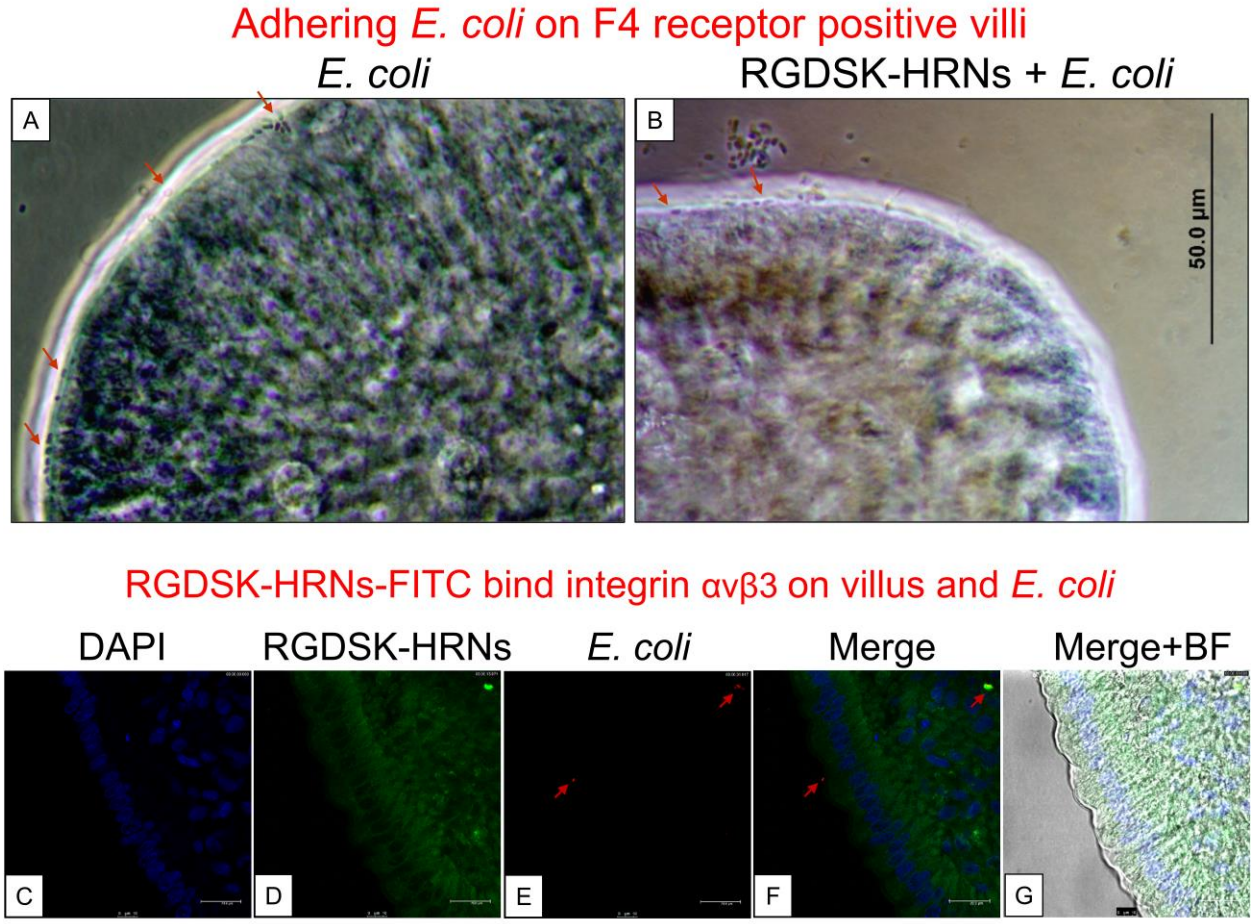

Figure 5.6. Representative pictures of villus adhesion assay

Images from phase-contrast microscope illustrate the number of adhering E. coli on F4 receptor-positive villi (A) was significantly higher than that in the RGDSK-HRNs-FITC pretreated group (B) after four-hour E. coli F4 incubation. Confocal images illustrate that RGDSK-HRNs-FITC bind to integrin in porcine villus and E. coli F4 (C, D, E, F, G). Red: pFPV::td tomato E. coli F4; Green: RGDSK-HRNs-FITC; Blue: DAPI

5.4.6. RGDSK-FITC, but not RGDSK-HRNs-FITC, affects the survival of *E. coli* significantly

Supernatants from *ex vivo* villus adhesion assay were collected and cultured in LB agar ampicillin to evaluate the biological effects of RGDSK-FITC peptide, RGDSK-HRNs-FITC, mouse monoclonal anti-integrin αvβ3 antibody, TBL-FITC (nanotube without RGDSK group), rabbit anti-F4 antibody serum, and 0.1M PBS on *E. coli* F4. The number of *E. coli* F4 colonies representing viable *E. coli* F4 in the supernatant was counted for statistical analysis. Results showed that *E. coli* F4 exposed to RGDSK-FITC before being incubated with the villi had significantly lower numbers of viable bacteria in the supernatant at 12 hours than that in the media treatment group ($P<0.05$). The results from 24 hours exposure time point showed that RGDSK-FITC or anti-F4 antibody serum had a fewer number of *E. coli* colonies in supernatant compared with *E. coli* control group ($P<0.05$). (Figure 5.7).

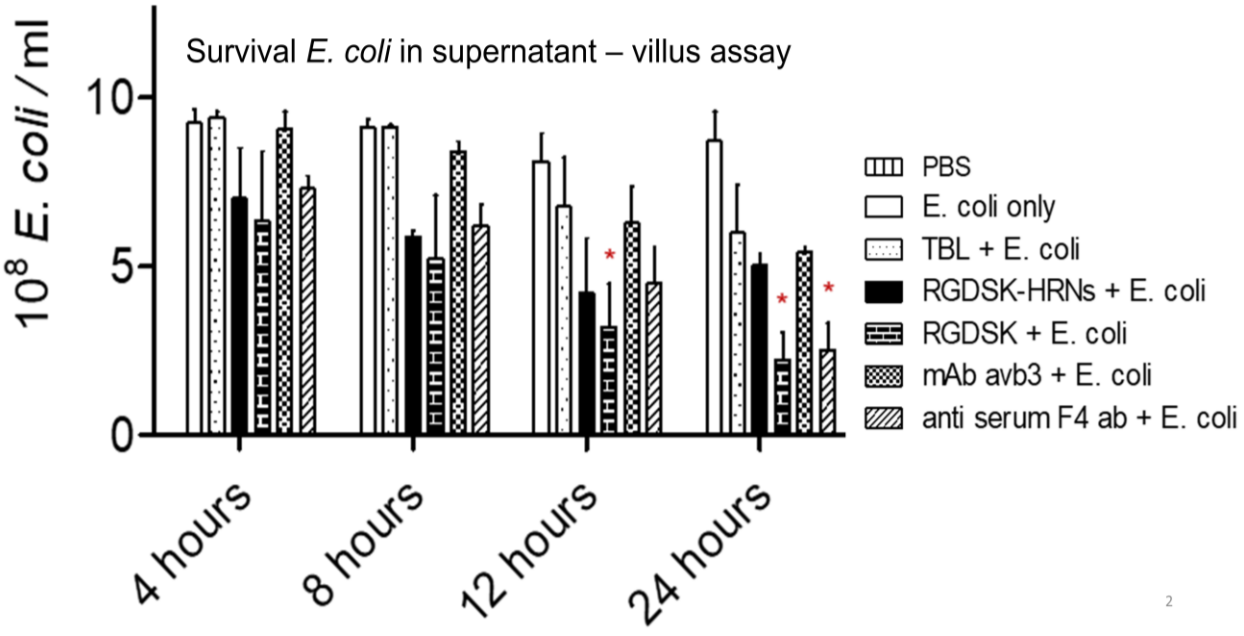

Figure 5.7. The number of survival E. coli left in the supernatant in the villus adhesion assay

The number of survival E. coli left in the supernatant was counted in LB agar ampicillin culture plates. At the 24-hours time point, compared with the E. coli group, the number of E. coli left in the supernatant was significantly reduced in RGDSK-FITC peptide control and anti-F4 antibody serum treatment group ($P<0.05$), but not in RGDSK-HRNs-FITC treatment group. Data were expressed as mean ± SEM. Error bars indicated SEM. An asterisk (*) indicated a significant difference compared with E. coli treatment only group. ($n = 3$ each group, $P<0.05$).

5.5. DISCUSSION

Intestinal diseases and foodborne illnesses due to *E. coli* infection are responsible for numerous deaths and many economic losses worldwide (34, 35, 185). To manage these disease outbreaks, one of the proposed approaches is to reduce bacterial colonization or virus entry into the intestine. Most of the data has focused on the identification of molecular adhesion receptor for the entry of the bacteria or virus into non-phagocytic cells. For example, replication of porcine epidemic diarrhea virus (PEDV) on African green monkey Vero E6 cells was reduced by RGD peptide, polyclonal antibodies anti-integrin αv, and polyclonal antibodies anti-integrin β3 treatments via its interaction with integrin αvβ3 (138). Moreover, Isberg and co-workers reported that the immobilized invasin of *Yersinia pseudotuberculosis* enteric bacterium could bind integrin $\alpha 3\beta 1$, $\alpha 4\beta 1$, $\alpha 5\beta 1$, and $\alpha 6\beta 1$ (104). Another example is *Shigella flexneri*, which releases Ipa proteins, forming a high molecular matrix structure, and interacting with integrin α5β1 on the epithelium. This interaction activates the rearrangement of actin cytoskeletons, which allows the bacteria to invade the host epithelium (254). In this study, we discovered that *E. coli* could bind integrin αvβ3 for its colonization *in vitro*.

Prior studies have found that many ligands of *E. coli* adhered to specific receptors of the host. For example, Hemolysin (HlyA) toxin from uropathogenic *E. coli* was mediated by β2 integrins in U-937 human monocytic cell line, demonstrating the involvement of β2 integrins in the sensitivity of the host cell to toxins from uropathogenic *E. coli* (191). It was also reported that *eae* gene in enterohemorrhagic *E. coli* enables the pathogen to attach to and desquamates colonic epithelial cells, recruiting inflammatory cells and causing edema as well as microvilli loss (56). Another well-known example of *E. coli* ligands is the F4 antigen, also known as F4, which binds to the F4 receptor of the host (70, 197). This ligand was described as thin, and flexible threads, having

a fimbria like structure with a 2.1 nm diameter, covered with filamentous-appearance material (70, 197). Despite the existing knowledge on *E. coli* receptors, we built our experiments on the identification of integrin αvβ3 on intestinal epithelium, and the presence of an integrin αvβ3-like protein on *E. coli* to examine the potential role of the integrin in bacterial adhesion.

Surprisingly, our results from a binding assay on 96-well plates indicated that the number of *E. coli* binding to integrin αvβ3 coated wells increased significantly compared with that of uncoated wells. These data suggested that the binding of *E. coli* F4 depended on integrin αvβ3. The second major finding of this *E. coli* O101 F4+ using PCR method is that this *E. coli* strain is negative for AIDA-1, *eae*, LT, STa, STb, and Stx2e toxins. We continued using this *E. coli* O101 F4+ strain in our experiments to focus on studying the adherence stage of the bacteria in the pathogenesis of the disease. Our results supported previous findings that although some *E. coli* O101 strains lacked some virulence factors, such as ST, LT, hemolysin, *eaeA*, they possessed a Shiga-like toxin, causing hemorrhagic colitis and hemolytic-uremic syndrome in human (66) and diarrhea in calves (219). Dangerously, the pigs show no symptoms of disease yet are infected by the bacteria, a result with serious implications: if this strain uses the pigs as its reservoir, the bacterium can be transferred to humans from contaminated porcine products (30, 66). In the same way, the literature has shown that other *E. coli* strains without *eaeA* still adhere to the intestinal mucosa, causing edema disease (such as O139) (18) and colitis (such as O18, O91, O113, O117, O145) (143). These data create the possibility that proteins other than the already known receptors may be playing a role in the attachment of *E. coli* with the epithelium.

One possible implication of our result is that *E. coli* can use integrin αvβ3 to support its binding in the absence of other receptors. Although we do not know for certain if *E. coli* contains an RGD peptide sequence, one theory is that integrin αvβ3 possibly binds to motifs that extend

beyond RGD-containing protein. Another possible explanation for this binding is that *E. coli* has a structure with the same characteristic and properties as found in RGD-containing ligands. This RGD-like peptide structure of *E. coli*, likely functioning as RGD, can bind to the identical site on the integrin αvβ3 of the jejunal epithelium, enabling *E. coli* to attach to and penetrate the intestinal epithelium.

From the nanoscale bio-mimetic features of nanotubes, the novel RGDSK-HRNs provide RGDSK surface chemistry and a cell-favorable environment. Because little is known either about the molecular interaction between *E. coli*, RGDSK, RGDSK-HRNs, and integrin αvβ3 or the distribution of RGDSK-HRNs on the gut epithelial cell, we used FITC-conjugated RGDSK-HRNs, and FITC-conjugated RGDSK to visualize them in a cell culture model. Immunofluorescent staining showed that RGDSK-FITC and RGDSK-HRNs-FITC could bind integrin αvβ3 in IPEC1 and integrin αvβ3-like protein in *E. coli* F4. This study supports evidence from the previous observations about the expression of integrin αvβ3 in IPEC1 and integrin αvβ3-like protein in *E. coli* F4 in the previous chapter.

E. coli F4 efficiently binds to the IPEC1 cell line *in vitro* (126). To modify *E. coli*-induced diarrhea in pigs, a suggested novel intervention could be the obstruction of the receptor adhesion sites to inhibit *E. coli* attachment to the epithelium (106). A group of researchers reported that the RGDSK-HRNs, targeting integrin αvβ3, can enhance osteoblast adhesion and proliferation due to an increase of fibronectin (268). In our study, we discovered that RGDSK-HRNs mediated the attachment of *E. coli* to IPEC1 efficiently. It suggests that the delivery of HRNs has an impact on RGDSK activity.

To further study the effect of RGDSK-HRNs-FITC, we then performed an *ex vivo* villus adhesion assay on scraped villi from porcine jejunum. We found that RGDSK-HRNs-FITC

prevented *E. coli* F4 from adhering to porcine jejunum villi. However, one unanticipated finding was that RGDSK-HRNs-FITC were less efficient than RGDSK-FITC peptide and monoclonal antibody anti-integrin αvβ3 on preventing *E. coli* F4 binding to villi until 24 hours. The implication of this result is the possibility that some RGDSK-HRNs-FITC have some RGDSK bound to integrin αvβ3 on the epithelium and some RGDSK bound to the integrin αvβ3-like protein on *E. coli*, leading to the observation that *E. coli* F4 is likely adhering to the epithelium as seen at 24 hours RGDSK-HRNs-FITC incubation treatment. The *E. coli* F4 clumps in binding to the RGDSK-HRNs-FITC imply the next step about adding another type of functionalized group, such as an anti-F4 antibody or anti-integrin αvβ3 antibody, or antibiotic, on the surface of the tube in the future. This potential treatment can increase the efficiency of the antibiotic in targeting bacteria, reducing the emergence of bacterial resistance.

Another exciting aspect of the data from our villus adhesion assay is the effect of RGDSK-FITC peptides and the monoclonal antibody anti-integrin αvβ3 treatment groups. There was clear evidence that the RGDSK-FITC peptides and the monoclonal anti-integrin αvβ3 antibody remained effective in significantly inhibiting the *E. coli* binding to villi up to 24 hours, whether the F4 receptor was present or not. These findings contributed to our understanding of the involvement of integrin αvβ3 in the attachment of *E. coli* to villi and to account for situations where F4 may not have accounted for all of the bindings of *E. coli*.

Our *ex vivo* villus adhesion assay data showed that RGDSK-HRNs could block *E. coli* adhesion to F4R-positive porcine jejunum villi. Interestingly, results showed that after 12 hours, the number of viable *E. coli* exposed to RGDSK was significantly lower than that in the media treated *E. coli* group ($P<0.05$). After 24 hours, either RGDSK or serum anti-F4 antibody significantly reduced the *E. coli* colonies in the supernatant, compared with *E. coli* control group

($P<0.05$). The higher number of survival *E. coli* left in the supernatant in this experiment suggests that RGDSK-HRNs do not affect the growth of *E. coli* in LB agar as RGDSK peptide or serum anti-F4 antibody, expected low toxic and not to increase the endotoxin from dead *E. coli*. In 2017, Coddens and colleagues reported that cranberry extract inhibited F4ac$^+$*E. coli* adhering to porcine jejunal villi (43). A separate incubation cranberry extract with *E. coli* showed that the cranberry extract did not influence the viability of *E. coli* (43). However, these authors did not mention the *E. coli* left in the supernatant in the villus adhesion assay (43).

In conclusion, the purpose of our current study was to investigate the functions of the RGDSK sequence and the vehicle of HRNs in blocking the attachment of *E. coli* F4 to the intestinal epithelium *in vitro*. We found that integrin αvβ3 can be a receptor for *E. coli* F4 to adhere to the porcine intestinal epithelium. Secondly, the data showed that blocking integrin αvβ3 by RGDSK peptide-functionalized HRNs can inhibit *E. coli* F4 adherence to the epithelium. This report has provided a more in-depth insight into the mechanism of bacterial colonization. Further work is required to establish the therapeutic efficiency of RGDSK-HRNs-FITC and the role of integrin αvβ3 with other complicated factors, such as vitronectin and F4 receptor *in vivo*, for developing new interventions for intestinal diseases.

ACKNOWLEDGMENTS

We sincerely thank the Saskatchewan Agriculture Development Fund (ADF), the Natural Science and Engineering Research Council (NSERC), the Graduate Student Scholarship program from the Integrated Training Program in Infectious Disease, Food Safety and Public Policy (ITraP), the Devolved Graduate Scholarship program from the Department of Veterinary Biomedical Sciences, and the Graduate Student Scholarship program from the Western College of Veterinary Medicine, the University of Saskatchewan, Canada for supporting this research. We

thank Siew Hon Ng, Champika Fernando, and Eiko Kawamura for the technical support. We sincerely thank Dr. Douglas Call at the Washington State University, USA; Dr. Janet Hill, Dr. Francois Meurens, and Dr. Heather L. Wilson, Prairie Diagnostic Services and VIDO-InterVac at the University of Saskatchewan for their generous gift materials.

GRANTS

The study was funded through the Saskatchewan Agriculture Development Fund (ADF) and the Discovery Grant from the Natural Sciences and Engineering Research Council of Canada (NSERC) to Dr. Baljit Singh.

CHAPTER 6. THE EFFECT OF RGDSK-HRNs-FITC EXPOSURE ON THE APOPTOSIS AND SURVIVAL OF IPEC1 UPON *E. COLI* INFECTION

Scientists have found that blocking integrin αvβ3 by a peptide or an antibody antagonist can up-regulate endothelium apoptosis, preventing angiogenesis. In the previous chapter, we found that RGDSK-HRNs declined the attachment of *E. coli* F4 to IPEC1 and porcine jejunal villi but did not decrease *E. coli* K88 growth in LB agar. Therefore, in this chapter, we continued exploring the effect of RGDSK-HRNs exposure on apoptosis and survival of IPEC1 upon *E. coli* F4 infection.

6.1. ABSTRACT

In this report, we provide data on the investigation of the effect of RGDSK-HRNs exposure on the apoptosis and survival of the intestinal epithelium cell line (IPEC1) upon *E. coli* infection. We challenged IPEC1 with RGDSK-HRNs or other control treatments before exposure with *E. coli*. Then we performed western bot and flow cytometry analysis. Flow cytometry data showed that the Staurosporine-treated control but not those treated with RGDSK-HRNs increased dead cells significantly. Interestingly, RGDSK-HRNs improved IPEC1 cell survival upon *E. coli* infection compared with *E. coli* infection alone group ($P<0.05$). Western blot results showed that RGDSK-HRNs-FITC treatment significantly decreased the level of p-p53 compared with monoclonal anti-integrin αvβ3 antibody treatment in *E. coli* infection, and the level of p-p38MAPK compared with RGDSK-FITC group in *E. coli* infection ($P<0.05$). In conclusion, these are the first data reported that RGDSK-HRNs reduced the apoptosis of IPEC1 upon *E. coli* infection to maintain their survival.

Key Words: integrin αvβ3, nanotubes, porcine epithelium, *E. coli*

6.2. INTRODUCTION

Integrin αvβ3 is involved in the processes of angiogenesis, osteoporosis, migration, survival, differentiation, and proliferation of the cell (155, 159, 193, 220). These vital functions are related to normal cellular physiology and mechanisms of disease (155, 193). Besides that, antagonists of integrin αvβ3, such as RGD peptide sequence induced apoptosis while agonists reduced cell death.

For example, in 1994, Brooks and colleagues highlighted that the blockage of integrin αvβ3 by an RGD peptide or an antibody upregulated endothelial apoptosis and inhibited angiogenesis (28). Conversely, in 2003, Morozevich and colleagues mentioned that activated integrin αvβ3 expression up-regulated anoikis, known as extracellular matrix-dependent apoptosis (159). Vice versa, inhibition of integrin αvβ3 prevented this type of apoptosis (159). These scientists also reported that antisense oligonucleotide down-regulated the apoptosis rate of human intestinal carcinoma Caco-2 cells compared with untreated controls (159). These findings imply that the integrins-related apoptosis mechanism depends on cell type, nature of apoptosis-inducing signals, and other molecular mechanisms (152).

Currently, there are no data on the role of integrin αvβ3 in the porcine intestinal apoptosis and survival. Considering the implication of apoptosis, the maintenance of the integrity of intestinal epithelium in bacterial infections, we tested the hypothesis that RGDSK-HRNs enhanced the apoptosis of intestinal epithelium upon *E. coli* F4 infection.

6.3. MATERIALS AND METHODS

6.3.1. Materials

Novel HRNs, which were designed and provided by the lab of Professor Hicham Fenniri at the Department of Chemical Engineering, the College of Engineering, Northeastern University, Boston, USA (39, 63, 64). *E. coli* F4 strain EC52, serotype O101:K30+:K99-: F4+ and IPEC1 were gifts from Dr. Francois Meurens and Dr. Heather L. Wilson at the Vaccine and Infectious Disease Organization-International Vaccine Centre (VIDO-InterVac). IPEC1 cells were developed from the jejunum of unsuckled, mixed-bred piglets less than 12 hours old (85). IPEC1 cells were cultured in 75 cm^2 flask in Dulbecco's Modified Eagle Medium/Nutrient Mixture F-12 at 37ºC in a humidified 5% CO_2 incubator (84, 126). RGDSK-FITC (American peptide company, Sunnyvale, CA., USA.), and CF^{TM}488A-Annexin V (AnV) and Propidium Iodide (PI) Apoptosis Kit (Biotium, Hayward, CA., USA.) were purchased commercially.

6.3.2. Preparing *E. coli*

E. coli strain EC52, serotype O101:K30+:K99-: F4+, having pFPV::tdTomato fluorescence protein, was cultured for 18 hours on Luria broth supplemented with ampicillin. The concentration of bacteria was determined by adjusting the optical density at 620nm (OD_{620}) to 1 to achieve $4x10^9$ CFU/ml as determined by prior CFU counting. *E. coli* was centrifuged at 16,200 xg for 5 minutes, followed by three washes in 0.1M PBS supplemented with ampicillin at pH=7.4. Serial dilution was done to reach the desired concentration of the bacteria for the assay later according to previously cited procedure (126).

6.3.3. Preparing RGDSK-HRNs-FITC

TBL/TB- RGDSK is a twin GΛC – based rosette nanotubes (RNTs) functionalized with arginine-glycine-aspartic acid-serine-lysine (RGDSK) peptide sequence which can bind integrin αvβ3. Another TBL/TB-FITC is a fluorescein isothiocyanate (FITC) conjugated twin GΛC – based rosette nanotubes (RNTs). TBL/TB-FITC and TBL/TB-RGDSK in 1:10 molar ratio of FITC and RGDSK were mixed to yield the composite of RGDSK and FITC functionalized helical rosette nanotubes (RGDSK-HRNs-FITC). This nanomaterial is a more stable self-assemble HRNs expressing RGDSK and is visualized by fluorescence microscopy (39, 225). The suspension was sonicated for 5 minutes in sonicating water bath following by 30-second vortex and one-minute heating. The mixture was placed at room temperature in the dark for 48 hours to allow for the synthesis of the RGDSK-HRNs-FITC. The RGDSK-HRNs-FITC stock was stored at 4^{o}C for future treatment. RGDSK-HRNs-FITC were diluted in an appropriate dilution buffer (0.1M PBS or DMEM/F12) at preferring molar concentration regarding the equivalent RGDSK on the surface of HRNs.

6.3.4. Apoptosis analysis by flow cytometry

Apoptosis was confirmed using CF^{TM}488A-Annexin V (AnV) and Propidium Iodide (PI) Apoptosis Kit (Biotium, Hayward, CA., USA.) according to the manufacturer's instructions. Briefly, for examining the effect of RGDSK-HRNs on the apoptosis of IPEC1, 1x10^{6} IPEC1 cells were exposed to RGDSK-HRNs (containing equivalent 5µM RGDSK) in 5 hours, 12 hours, and 24 hours. Positive and negative controls for apoptosis were 5µM TBL making HRNs without peptide conjugation, or 5µM RGDS peptide, or 0.5 µM Staurosporine. IPEC1 cells were harvested by trypsin EDTA, then were washed in 0.1M PBS, followed in working buffer.

For examining the effect of RGDSK-HRNs in association with *E. coli* infection on the apoptosis of IPEC1, $1x10^6$ IPEC1 cells were exposed to RGDSK-HRNs (containing equivalent 5µM RGDSK) in 15 minutes. Positive and negative controls for apoptosis were 5µM TBL making HRNs without peptide conjugation, or 5µM RGDS peptide, or monoclonal integrin αvβ3 antibody (25 µg/ml). Then cells were challenged with $1x10^7$ *E. coli* CFU/ml at 37ºC in a humidified 5% CO_2 incubator in 1 hour, 5 hours, and 24 hours. Staurosporine (0.5 µM) was used as a positive control for apoptosis. IPEC1 cells were harvested by trypsin EDTA then were washed in 1X PBS, followed by a working buffer from the kit.

After that, all cells were stained with five µl CF^{TM}488A-Annexin V (AnV) and two µl propidium iodide (PI) in 15 minutes in the dark. Untreated cells stained with CF^{TM}488A-Annexin V or PI dye alone are single stained compensation controls. Flow cytometry data were analyzed using CyFlow®Space flow cytometer (Partec, Swedesboro, NJ, USA) with commercial FlowMax Software © version 2.6 (Quantum Analysis GmbH, Münster, Germany). The gated population was determined with unstained cells based on size (forward scatter) and granularity (side scatter). Data were acquired on at least 10,000 gated counts.

6.3.5. Apoptosis analysis by western blot p-akt1, p-p38MAPK, and p-p53

IPEC1 at $1x10^6$ cells concentration were seeded into 25 cm^2 flask. After being confluent overnight, cells were challenged at 24 hours with seven treatments at final concentration as following: (1) DMEM/F12 medium without serum, (2) 1 x 10^8 *E. coli* F4, (3) 1 µM TBL and 1 x 10^8 *E. coli* F4, (4) RGDSK-HRNs-FITC (equivalent 1 µM RGDSK) and 1 x 10^8 *E. coli* F4, (5) 1 µM RGDSK-FITC and 1 x 10^8 *E. coli* F4, (6) 5 µg/ml monoclonal anti-integrin αvβ3 antibody and 10^8 *E. coli* F4, and (7) 0.5 µM Staurosporine. The supernatant in this experiment was collected and stored at -80ºC for future use. Cell lysis procedures were followed as per manufacturer protocols

(Bio-rad, Mississauga, ON, Canada). Briefly, the treatment reaction was stopped by adding ice-cold wash buffer to the cells. Samples were homogenized by adding lysing solution. The protein concentrations of samples were measured by using detergent compatible Bradford protein assay kit (Bio-rad, Mississauga, ON, Canada). The samples were diluted to have the same protein concentration to have the same amount of total protein for western blot.

The western blot procedure was appropriately modified from a previous protocol (105). We first probed for mouse monoclonal antibody anti-p-p53 (1:200) and polyclonal goat anti-mouse immunoglobulins (1:20,000, Dako) (n = 3 each group). Incubation without primary antibody served as a negative control. The detection blots were performed with Amersham ECL western blotting detection reagents kit (GE Healthcare, Freiburg, Germany). Finally, the membranes were scanned using Bio-rad ChemiDoc MP Imaging system scanner and Imagelab 5.2.1 software (Bio-rad, Mississauga, ON, Canada). For detecting p-akt1, p-p38MAPK, beta-actin, the probed membranes were stripped with blot restore membrane rejuvenation kit (Millipore, Billerica, MA, USA) before being re-probed with another primary and appropriate secondary antibody. Densitometric quantification was performed using Imagelab 5.2.1 software (Bio-rad, Mississauga, ON, Canada) to evaluate the relative density of p-p53, p-akt1, and p-p38MAPK adjusted to beta-actin in all groups compared with loading control.

6.3.6. Statistical analysis

We used the GraphPad Prism version 5.04 software (San Diego, CA, USA.) to analyse data. Quantitative results were expressed as mean ± SEM, and error bars represented standard error. The normal distribution of residuals was tested by histogram and Shapiro-Wilk test. Data were analyzed by Analysis Of Variance (ANOVA), followed by Bonferroni multiple comparison

test. A significant difference was set when the critical value of α was below or equal to 0.05 as (two-tailed, $p<0.05$).

6.4. RESULTS

6.4.1. RGDSK-HRNs did not induce IPEC1 apoptosis significantly but enhanced the survival of IPEC1 upon *E. coli* infection

To examine the cytotoxicity of RGDSK-HRNs to the intestinal cell, we challenged IPEC1 with RGDSK-HRNs. Treatment controls included RGDS peptide only, TBL nanotube without RGDSK functional groups, Staurosporine positive control for apoptosis. After 5, 12, and 24 hours, we stained the IPEC1 with AnV and PI. Flow cytometry data showed that Staurosporine exposure for 5 hours significantly increased both early and late apoptosis of IPEC1, thus confirming the validity of the control (Figure 6.1A, and 6.1B, respectively). TBL, which is nanotubes without conjugate RGDSK functional groups, did not affect cell survival compared with untreated controls. RGDS peptide and RGDSK-HRNs modestly increased cell apoptosis compared to the untreated group at respective time points (Figure 6.1A, B). These results highlighted the role of the RGDSK peptide functional group associated with the nanotubes vehicle in early apoptosis and cell death.

We then examined the effect of RGDSK-HRNs exposure on the survival of IPEC1 upon *E. coli* F4 infection. We pre-challenged IPEC1 with RGDSK-HRNs, RGDS, TBL 15 minutes before exposing IPEC1 with *E. coli* F4 for 1 or 5 hours. Staurosporine was used again as a positive treatment control for apoptosis. Then, we stained the intestinal cell with AnV and PI. Flow cytometry results showed that compared with *E. coli* F4 infection group, RGDSK-HRNs improved *E. coli* F4 infected IPEC1 cell survival (Figure 6.1C). Five – hour staurosporine exposure

significantly increased cell death. TBL control group for nanotubes without conjugate RGDSK peptide did not affect cell survival (Figure 6.1C).

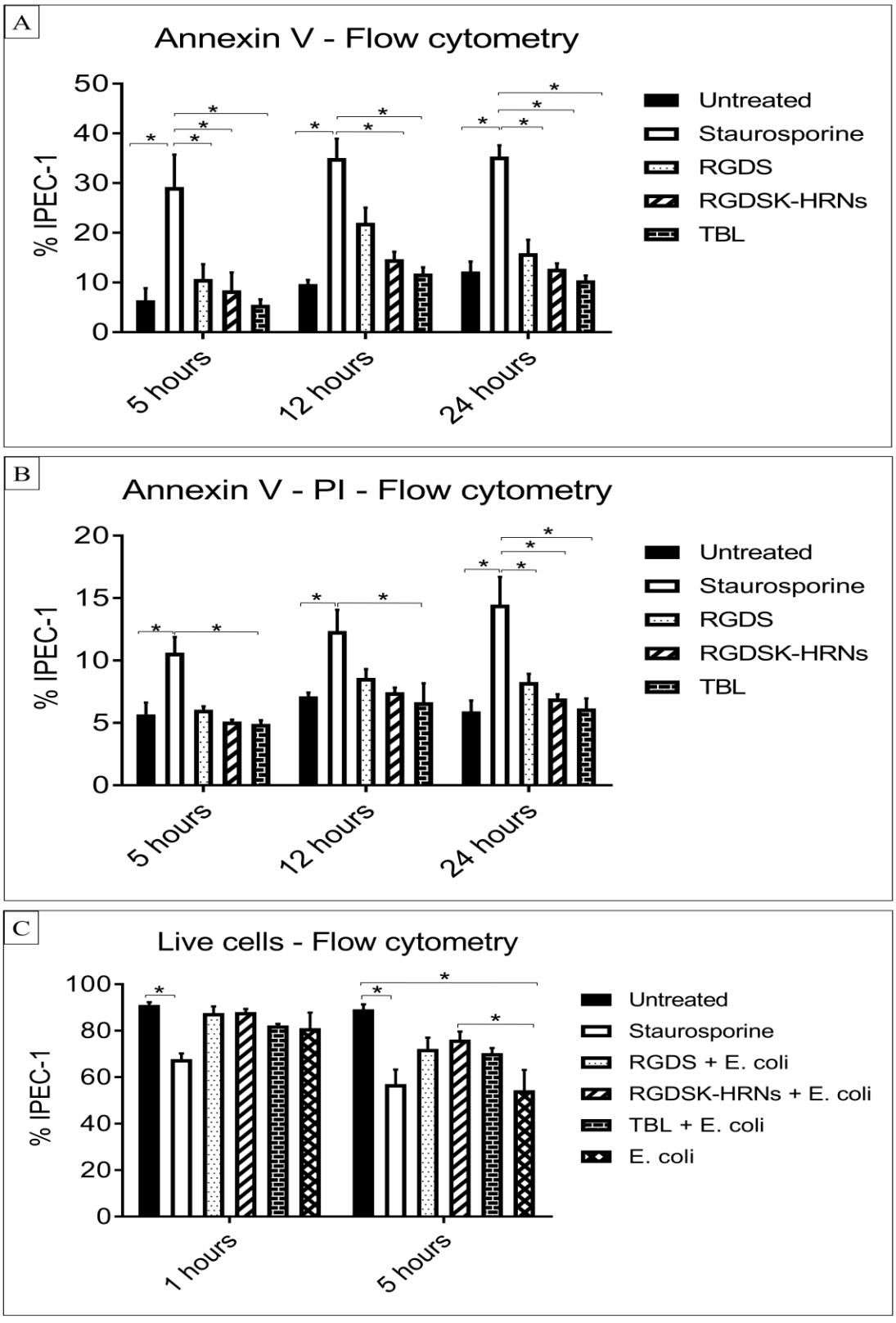
A
Annexin V - Flow cytometry
% IPEC-1
50
40
30
20
10
0
5 hours
12 hours
24 hours
Untreated
Staurosporine
RGDS
RGDSK-HRNs
TBL
B
Annexin V - PI - Flow cytometry
% IPEC-1
20
15
10
5
0
5 hours
12 hours
24 hours
Untreated
Staurosporine
RGDS
RGDSK-HRNs
TBL
C
Live cells - Flow cytometry
% IPEC-1
100
80
60
40
20
0
1 hours
5 hours
Untreated
Staurosporine
RGDS + E. coli
RGDSK-HRNs + E. coli
TBL + E. coli
E. coli

Figure 6.1. RGDSK-HRNs slightly induced IPEC1 apoptosis but enhanced the survival of IPEC1 upon E. coli infection using flow cytometry analysis.

*Comparing to untreated IPEC1 at the respective time point, RGDSK-HRNs and RGDS peptide did not induce early (A) and late (B) apoptosis significantly. (C) Comparing to E. coli F4 treated group, RGDSK-HRNs improved the survival of IPEC1 upon E. coli F4 infection. Data were expressed as mean ± SEM. Error bars indicated SEM. An asterisk (*) indicated a significant difference (n=3 each group, * $P<0.05$).*

6.4.2. RGDSK-HRNs-FITC could decrease the apoptotic process of *E. coli* F4 infected IPEC1

Our results showed that at the 24-hour timepoint, the level of p-akt1 was significantly lower in cells treated with *E. coli* F4, TBL+*E. coli* F4, integrin αvβ3 antibody + *E. coli* F4, and staurosporine compared to the medium alone control ($P<0.05$). Integrin αvβ3 antibody + *E. coli* F4 group had the highest level of p-p53, and significantly higher than that of RGDSK-HRNs-FITC + *E. coli* F4 ($P<0.05$). RGDSK-FITC peptide + *E. coli* F4 had the highest level of p- p38MAPK, and significantly higher than RGDSK-HRNs-FITC + *E. coli* F4 ($P<0.05$). There was no significant difference between RGDSK-HRNs-FITC + *E. coli* F4 and medium control group regarding the level of p-akt1, p-p53, p-p38MAPK (Figure 6.2).

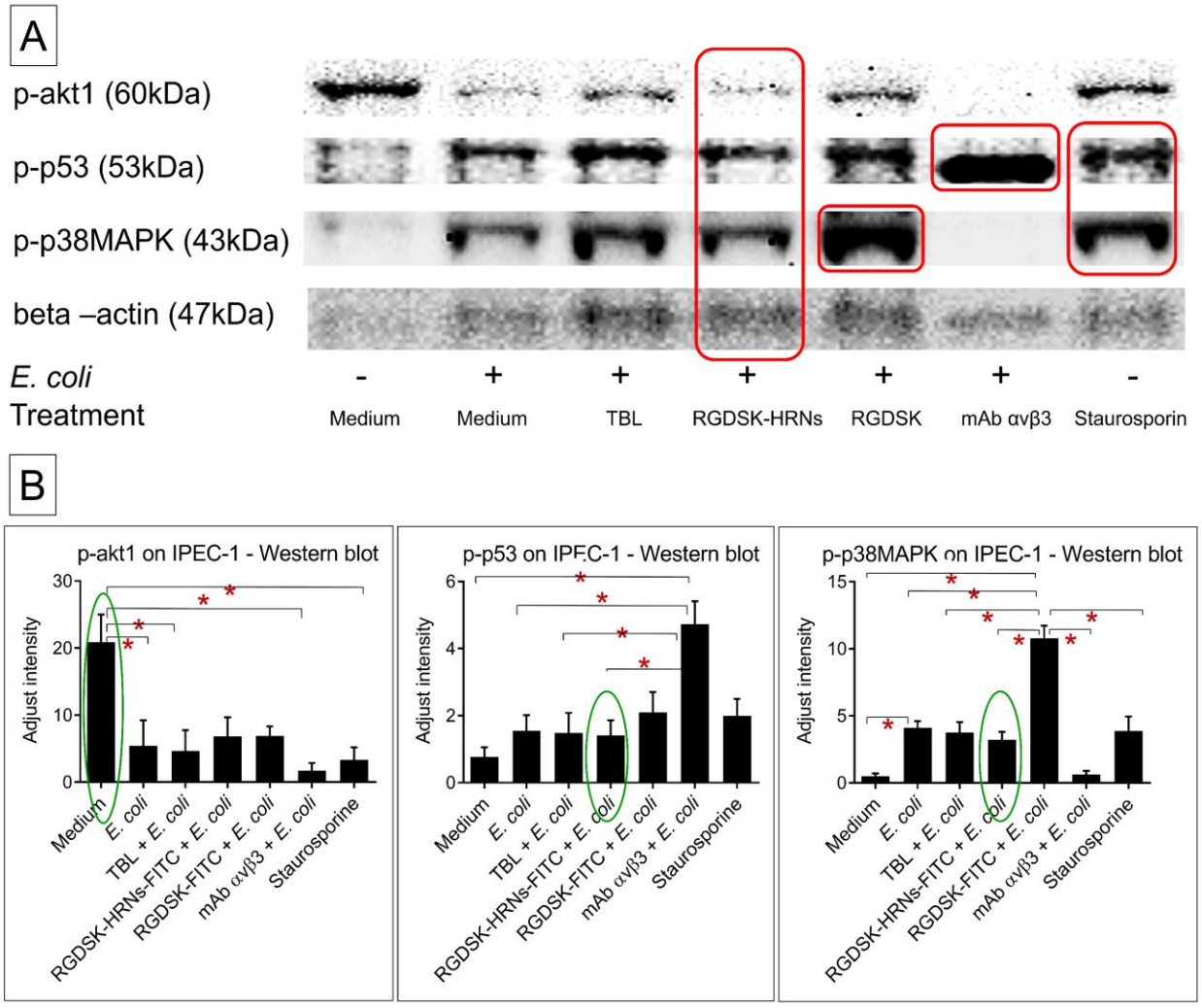

Figure 6.2. Western blots for IPEC1 apoptosis

(A) Western blots for p-akt1 (60 kDa), p-p53 (53 kDa), p-p38MAPK (43 kDa), and beta–actin (47 kDa, a housekeeping gene protein) were performed on IPEC1 upon six treatments and medium control after 24 hours. (B) The densitometric analyses showed the adjust intensity to beta-actin. Normal IPEC1 cell line in medium had highest level of p-akt1. E. coli infection inhibited p-akt1, and increased the level of p-p38MAPK compared with normal IPEC1 cell control (P<0.05). RGDSK-FITC peptide + E. coli F4 group had higher level of p- p38MAPK than RGDSK-HRNs-FITC + E. coli (P<0.05). There was no significant difference between RGDSK-HRNs-FITC + E.

coli groups and medium control groups regarding the level of p-akt1, p-p53, p-p38MAPK. Data were expressed as mean ± SEM. Asterisk (*) indicates a significant difference between groups (P<0.05, n=3 each group).

6.5. DISCUSSION

It is known that the mechanism of integrins-related apoptosis is involved in cell type-specific, and apoptosis-inducing signals (152, 159). For example, antagonism of integrin αvβ3 by a peptide or an antibody can up-regulate endothelial apoptosis and prevent angiogenesis (28). In reviewing the literature, no data was found on the association between RGDSK-HRNs-FITC and the apoptosis of intestinal epithelium through integrin αvβ3. Hence, this is the first study on the cytotoxicity of RGDSK-HRNs-FITC on the intestinal epithelium by exploring the effect of RGDSK-HRNs-FITC exposure on the apoptosis and survival of IPEC1 upon *E. coli* F4 infection.

We found that RGDSK-HRNs-FITC enhanced the survival of *E. coli* F4 infected IPEC1 compared with *E. coli* F4 challenged group. The flow cytometry analysis results from Annexin V and PI staining on IPEC1 in this chapter were consistent with the previous data of the survival *E. coli* F4 left in the supernatant. The higher number of surviving *E. coli* F4 left in the supernatant suggested that RGDSK-HRNs-FITC has low toxicity to the *E. coli*, and therefore do not increase the levels of endotoxin released from the dead *E. coli* F4. These data again support that RGDSK-HRNs-FITC are biocompatible to the cells (39, 223).

Several reports have noted that integrins stimulate survival signals via phosphoinositide (PI) 3 kinase or mitogen-activated protein kinase (MAPK) pathway. The absence of integrin can activate p53 or jun N- terminal kinase (JNK) death signals, and downregulates Bcl-2 expression and function of the endothelium (152). Akt, named as PKB, or Rac, supports cell growth and prevents the apoptosis (67, 272). Therefore, in this study, we examined IPEC1 apoptosis pathway through the phosphorylation of p53, p38MAPK, and akt1. We performed Western blot followed by densitometry quantification for the level of their phosphorylation in IPEC1 cell lysate. Our results showed that at the 24-hour timepoint, *E. coli* F4 infection increased the apoptosis of

intestinal porcine epithelium cell line 1 through phosphorylating both p53 and p38MAPK and inhibiting p-akt1. Similarly, staurosporine, an apoptosis inducer, inhibited p-akt1 and activated p-p53 and p-p38MAPK. Interestingly, blocking integrin αvβ3 by anti-integrin αvβ3 antibody inhibited the phosphorylation of p-38MAPK and akt1. This inhibition led to the apoptosis of intestinal epithelium through activating p53 phosphorylation. Compared with RGDSK-FITC peptide, and staurosporine, RGDSK-HRNs-FITC decreased the apoptotic process of the intestinal porcine epithelium in *E. coli* F4 infection. Other scientists also reported that K/RGDSK-RNTs inhibited the phosphorylation of ERK1/2 and p38 MAPK, consequently reducing the migration of bovine neutrophils (134). However, K^{10}/$RGDSK^{1}$-HRNs induce inflammation and apoptosis in human bronchial epithelial adenocarcinoma cells by enhancing cell death genes, p38 mitogen-activated protein kinase (MAPK) phosphorylation, caspase-3 activity, and DNA fragmentation (226). It suggests that the effect of the RGDSK peptide functional group on HRNs may depend on the cell type and in combination with other functional groups.

In summary, in our study, RGDSK-HRNs-FITC slightly induced IPEC1 apoptosis compared to a normal control without treatment but enhanced the survival of IPEC1 upon *E. coli* F4 infection compared to *E. coli* infected group. This result highlighted that the HRNs conjugated to RGDSK peptide functional group were not toxic to the intestinal cells. An *in vivo* study is required to continue investigating the molecular pathway of the effects of RGDSK-HRNs in the intestinal immune response to *E. coli*.

ACKNOWLEDGMENTS

We sincerely thank the Saskatchewan Agriculture Development Fund (ADF), the Natural Science and Engineering Research Council (NSERC), the Graduate Student Scholarship program from the Integrated Training Program in Infectious Disease, Food Safety and Public Policy

(ITraP), the Devolved Graduate Scholarship program from the Department of Veterinary Biomedical Sciences, and the Graduate Student Scholarship program from the Western College of Veterinary Medicine at the University of Saskatchewan, Canada for supporting this research. We sincerely thank VIDO-InterVac, at the University of Saskatchewan for their generous gift materials.

GRANTS

The study was funded through the Saskatchewan Agriculture Development Fund (ADF) and the Discovery Grant from the Natural Sciences and Engineering Research Council of Canada (NSERC) to Dr. Baljit Singh.

CHAPTER 7. THE EFFECT OF RGDSK-HRNs ON *E. COLI* F4 INFECTION IN A PORCINE GUT LOOP MODEL

In vitro experiments in previous chapters suggested that integrin αvβ3 played a role in *E. coli* binding to the jejunal epithelium and RGDSK-HRNs could reduce the binding. In this chapter, we performed an *in vivo* porcine gut loop model, developed in Dr. Volker Gerdts's laboratory in VIDO, to have a deeper understanding of the effects of RGDSK-HRNs on *E. coli* infection,

7.1. ABSTRACT

Intestinal diseases and foodborne illness, particularly due to *E. coli* infection, cause many deaths and economic losses worldwide. Integrin αvβ3 protein has important functions in cell adhesion, signalling, and survival. Integrin αvβ3 acts as an adhesion and entry receptor for some of the bacteria and viruses. However, the expression and role of integrin αvβ3 in the adhesion of *E. coli* to the porcine jejunum epithelium is not known, and also unknown is the effect on the generation of the immune response in the gut epithelium. We used an *in vivo* porcine gut loop model to study the role of integrin αvβ3 in interactions of *E. coli* F4 with the gut epithelium.

Immunohistochemistry showed normal porcine jejuna strongly expressed integrin αvβ3 in the nucleus and the apical surface of epithelia as well as crypts. The expression of integrin αvβ3 decreased in the epithelium but increased in the vascular endothelium of the jejunum infected with *E. coli* or *E. coli* associated with *Salmonella* ($P<0.05$). In the *in vivo* porcine gut loop model, the number of *E. coli* F4 binding to villi were significantly decreased in the *E. coli* F4 treated with RGDSK-HRNs-FITC group compared with *E. coli* F4 treatment group ($P<0.05$). The number of live *E. coli* F4 significantly decreased in RGDSK-FITC peptide treatment group ($P<0.05$), but not RGDSK-HRNs-FITC treatment group. TUNEL assay showed no significant difference in DNA fragmentation in the RGDSK-HRNs-FITC treatment group compared to

normal control group. Immunogold electron microscope confirmed the presence of the gold particle positive staining with integrin αvβ3 on the porcine jejunal epithelium and *E. coli* F4.

In conclusion, these are the first data to show the expression of integrin αvβ3 on the intestinal epithelium infected with *E. coli* F4, and that novel RGDSK-HRNs-FITC intervention can inhibit the attachment of *E. coli* F4 to the porcine villi without affecting the viability of the epithelial cells.

Key Words: integrin αvβ3, nanotubes, porcine villi, *E. coli*

7.2. INTRODUCTION

E. coli infection outbreaks, mainly associated with food poisoning, edema, and persistent diarrhea with a high mortality rate, have occurred both in developing and industrialized countries (34, 35, 185). *E. coli* F4 causes neonatal and post-weaning diarrhea (69). Prevention of the disease caused by *E. coli* F4 is challenging due to its multiple virulence factors (271). One of the strategies being pursued is to reduce the colonization of the intestine by *E. coli* F4 (34, 35, 185, 247).

Integrin αvβ3 belongs to the integrins family of adhesion and signalling receptors. This heterodimeric glycoprotein, comprising of α and β subunits, recognizes and binds arginine-glycine-aspartic acid (RGD) sequences (159, 220). It was initially identified as the protein that drives angiogenesis in melanoma, and over the years, a much broader array of functions has been attributed to this integrin. The integrin αvβ3 is blocked by RGD peptide resulting in the inhibition of angiogenesis and an increase in apoptosis as a potential cancer treatment (152, 228). However, the detailed mechanisms have not been elucidated.

Some studies show potential applications for nanotechnology in textiles, electronics, food, medicine, and environmental remediation (44, 142, 207, 235). The novel water-soluble helical rosette nanotubes (HRNs), invented by Dr. Fenniri, have no adverse effects on the respiratory system in an *in vivo* murine model, and are not toxic to cells *in vitro* (112). Recent *in vivo* study illustrated that HRNs conjugated RGDSK peptide on its surface played an important role in acute lung inflammation (225). K^{90}/$RGDSK^{10}$-HRNs enhances an excessive immune response through up-regulating p38MAPK cascade in an endotoxin lipopolysaccharide (LPS) induced lung injury murine model (225). Interestingly, RGDSK-HRNs inhibited bovine neutrophil migration *in vitro* (134).

This study was focused on understanding whether RGDSK-HRNs-FITC can be a new molecular intervention to reduce the colocalization of intestinal epithelium by *E. coli* F4 and to reduce intestinal disease. In addition to *in vitro* experiments above, we continued studying such *in vivo* using the superior and innovative porcine intestinal loop model, which can be applied for humans (153). The porcine loop model has fundamentally changed the way we can study gut immune responses. In this model, the porcine gut is surgically divided into multiple loops that still have blood supply. Therefore, multiple treatments can be done within the same animal, thereby reducing the response variation due to inter-animal variation (51, 78, 153). I hypothesize that RGDSK-HRNs inhibit *E. coli* attachment to the mucosal membrane *in vivo*.

7.3. **MATERIALS AND METHODS**

7.3.1. **Materials**

Jejunum paraffin blocks from healthy, or *E. coli,* or *E. coli* - *Salmonella* infected pigs (n=3 each) were kindly provided from professor John Harding's lab and Prairie Diagnostic

Services Inc. (PDS), respectively, at the Western College of Veterinary Medicine, the University of Saskatchewan.

Novel HRNs, which was designed as a previous procedure, was kindly provided by the laboratory of Professor Hicham Fenniri at the Department of Chemical Engineering, the College of Engineering, Northeastern University, Boston, USA (39, 63, 64). *E. coli* F4 strain EC52 sero-type O101:K30+:K99-: F4+ was a gift from Dr. Francois Meurens and Dr. Heather L. Wilson at the Vaccine and Infectious Disease Organization-International Vaccine Centre (VIDO-InterVac). Mouse monoclonal anti-F4 antibody (IMM01) was a generous gift from Dr. Eric Cox (Laboratory of Immunology, Faculty of Veterinary Medicine, Gent University, Belgium). Mouse monoclonal anti-integrin αvβ3 antibody (clone LM609, Chemicon Inc., Temecula, USA), RGDSK-FITC (American peptide company, Sunnyvale, CA 94086, USA), in-situ cell death detection kit-Alka-line-phosphatase (AP) version 11.0 (Roche, Mannheim, Germany), proteinase K (Sigma-Aldrich, Ontario, Canada), Vector® VIP peroxidase substrate kit for peroxidase (Vector Laboratories, Burlingame, CA, USA), were purchased commercially.

7.3.2. **Immunohistochemical staining integrin αvβ3 for porcine jejuna.**

Paraffin blocks were sectioned at 5μm thickness for immunohistochemical staining following a previous protocol (213). Briefly, sections were deparaffinized, followed by quenching the endogenous peroxidase activity and treatment with pepsin. Following two hours blocking with 1% BSA, the sections were incubated with monoclonal anti-integrin αvβ3 antibody (clone LM609, Chemicon Inc., Temecula, USA) and appropriate polyclonal anti-mouse immunoglobulins/HRP secondary antibody. Vector® VIP peroxidase substrate kit was used to develop the positive color reaction. Sections stained with the anti-endothelial marker vWF served as a positive control.

Sections stained with isotype antibody matching control (mouse IgG1) instead of primary antibody or the omission of the primary antibody served as negative controls.

7.3.3. **Immuno-gold electron microscopy for integrin αvβ3**

Porcine jejuna in LR white resin were sectioned at 100nm thickness on nickel grids. The non-specific bindings were blocked by BSA 1% in Tris-buffered saline before one-hour incubation in the integrin αvβ3 antibody (50µg/ml). Section stained without primary antibody served as a negative control.

After three washes in Tris-buffered saline, the sections were incubated for one hour in a 15 nm gold-conjugated anti-mouse secondary antibody (1:100). Aqueous uranyl acetate served as an indicator of negative staining. Besides, we used Reynold's lead citrate to enhance the electron-scattering properties of biological components inside the cells. The electron micrographs were imaged using a transmission electron microscope (Hitachi HT7700 - XFlash 6T160, Germany) operated at 80KV.

7.3.4. **Preparing *E. coli***

E. coli strain EC52, serotype O101:K30+:K99-: F4+, having pFPV::tdTomato fluorescence protein, was cultured for 18 hours on Luria broth supplemented with ampicillin. The concentration of bacteria was determined by adjusting the optical density at 620nm (OD_{620}) to 1 to achieve $4x10^9$ CFU/ml as determined by prior CFU counting. *E. coli* was centrifuged at 16,200 xg for 5 minutes, followed by three washes in 0.1M PBS supplemented with ampicillin at pH=7.4. Serial dilution was done to reach the desired concentration of the bacteria for the assay later according to the previously cited procedure (126).

7.3.5. **Preparing RGDSK-HRNs-FITC**

TBL/TB- RGDSK is a twin GΛC – based rosette nanotubes (RNTs) functionalized with arginine-glycine-aspartic acid-serine-lysine (RGDSK) peptide sequence which can bind integrin αvβ3. The TBL/TB-FITC is a fluorescein isothiocyanate (FITC) conjugated twin GΛC – based rosette nanotubes (RNTs). TBL/TB-FITC and TBL/TB-RGDSK in 1:5 molar ratio of FITC and RGDSK were mixed to yield the composite of RGDSK and FITC functionalized helical rosette nanotubes (RGDSK-HRNs-FITC). This nanomaterial is a more stable self-assembly HRNs expressing RGDSK on the surface and being visualized by fluorescence (39, 225). The suspension was sonicated for 5 minutes in sonicating water bath following by 30-second vortex and one-minute heating. The mixture was placed at room temperature in the dark for 48 hours to allow for the synthesis of the RGDSK-HRNs-FITC. The RGDSK-HRNs-FITC stock was stored in 4^{o}C for future treatment. RGDSK-HRNs-FITC was diluted in an appropriate dilution buffer (0.1M PBS or DMEM/F12) at preferring molar concentration regarding the equivalent RGDSK on the surface of HRNs.

7.3.6. ***In vitro*** **integrin αvβ3 antibody binding assay**

In vitro integrin αvβ3 antibody binding assay was again modified from previous protocols (27, 149) to examine whether *E. coli* has the integrin αvβ3-like protein domain. In brief, 96-well high binding plates were precoated overnight with 50µl of 5µg/ml mouse monoclonal integrin αvβ3 antibody (clone LM609, EMD Chemicon Inc., Temecula, USA.) in 100 mM HCO_3^-/CO_3^{2-} coating buffer. To examine the function of the integrin αvβ3-like protein domain on *E. coli*, before adding to the monoclonal integrin αvβ3 antibody-coated wells, *E. coli* ($5x10^7$/ml) was treated with 6 different treatments (1) PBS control, (2) 1 µM TBL, (3) RGDSK-

HRNs-FITC (equivalent 1 µM RGDSK), (4) 1 µM RGDSK-FITC, (5) 5 µg/ml monoclonal integrin αvβ3 antibody, (6) RGDSK-HRNs-FITC (equivalent 1 µM RGDSK) and 5 µg/ml monoclonal antibody anti-F4. After a one-hour incubation, non-adhered *E. coli* was removed by rinsing with 0.1M PBS ampicillin. Bound *E. coli* on the bottom of the 96-well plate was fixed in 2% paraformaldehyde. pFPV::tdTomato fluorescence from bound *E. coli* was measured at 530nm excitation /570nm emission in POLAR Start OPTIMA microplate fluorescence reader. Fluorescence intensity was adjusted with the background fluorescence of the wells without adding *E. coli* F4. The experiment was repeated four times.

7.3.7. Porcine gut loop model surgery

All experiments were approved by the University of Saskatchewan's Animal Research Ethics Board & adhered to the Canadian Council on Animal Care guidelines for animal use in research. To explore the function of integrin αvβ3 in *E. coli* F4 binding in addition to the F4 receptor (F4R), we used F4 receptor-positive (F4R+) piglets. Five of three to four-week-old F4R(+) piglets were housed at VIDO-InterVac animal facility and were allowed to acclimatize one week before treatment. All pigs were injected ketamine (20 mg/kg) and xylazine (2 mg/kg) intramuscularly (im.) to induce anesthesia. Isoflurane was used for maintaining anesthesia for the duration of surgery.

In brief, multiple intestinal loops providing identical, and independent sites for at least four weeks for analyzing a variety of antigen uptake and mucosal immune responses were created as described before (78, 153). A jejunal segment was isolated and subdivided into 14-16 loops (5 cm/loop), and each separated by an interspace to prevent inter loop contamination (Figure 7.1). The number of loops in each animal depends on the individual pig's gastrointestinal conformation. All loops were identical and were assigned to 1ml of seven different treatment groups.

Experimental maps were designed to identify treatment and control loops. The experimental design for each pig is listed below (Sample size n = 10 loops /group).

- Loop 1 (group 1 for normal control loop): inject 1 ml of 0.1M phosphate-buffered saline (PBS) with 15 mg ampicillin.
- Loop 2 (group 2 for *E. coli* infected loop): inject 1ml of $5x10^7$ *E. coli* F4 in 0.1M PBS 15 mg ampicillin.
- Loop 3 (group 3): inject 1 ml of 5μM TBL-FITC and $5x10^7$ *E. coli* F4 in 0.1M PBS 15 mg ampicillin. Note: this group has the same nanotubes but unconjugated RGDSK peptide.
- Loop 4 (group 4): inject 1 ml of the mixture of RGDSK-HRNs-FITC (equivalent 5μM RGDSK) and 2 μg antibody anti F4, $5x10^7$ *E. coli* F4 in 0.1M PBS 15 mg ampicillin.
- Loop 5 (group 5 for testing F4 receptor control): inject 1 ml of the mixture of 2 μg antibody anti F4 and $5x10^7$ *E. coli* F4 in 0.1M PBS 15 mg ampicillin.
- Loop 6 (group 6 for testing the function of RGDSK-FITC peptide): inject 1 ml of 5μM RGDSK-FITC peptide and $5x10^7$ *E. coli* F4 in 0.1M PBS 15 mg ampicillin.
- Loop 7 (group 7 for testing function of RGDSK-HRNs-FITC): inject 1 ml of RGDSK-HRNs-FITC (equivalent 5μM RGDSK) and $5x10^7$ *E. coli* F4 in 0.1M PBS 15 mg ampicillin to inhibit bacterial overgrowth by existing intestinal flora. Note: FITC is a biologically inactive fluorescent tag.

Experiments were in duplicate for each treatment group on the remaining loops in each piglet. Continuity of the intestinal system is re-established by end-to-end anastomosis. The intestine was returned to the abdominal cavity, which was then closed in three layers. All pigs were administered flunixin meglumine post-surgically. After four hours, the piglets were euthanized.

Each loop was injected 1ml of 0.1M PBS ampicillin to remove *E. coli* F4 not bound to the villi and to collect the content inside the loop. All pigs were clinically examined before and after surgery. Plasma and serum were also collected before surgery and before euthanasia to confirm the normal status of the animal and no cross-contamination from blood circulation later. Blood in EDTA was analysed for total and differential leukocyte count. The segment of loops and their contents, the associated mesenteric lymph node, and lungs were collected. Each jejunal loop was subdivided into four parts:

- The first segment (1cm) was opened and transferred to cold Krebs-Henseleit buffer (120mM NaCl, 14 mM KCl, 25mM $NaHCO_3$, 1 mM KH_2PO_4) with 1% formaldehyde to stop *E. coli* binding.
- The second one (1cm) was fixed in 4% paraformaldehyde and processed for paraffin embedding.
- The third one was fixed in 4% paraformaldehyde, and processed for OCT embedding.
- The fourth one was fixed in 2% paraformaldehyde 0.1% glutaraldehyde in 0.1M sodium cacodylate buffer for immune-gold staining later
- The last one was stored in -80ºC freezer for western blot, PCR and ELISA later

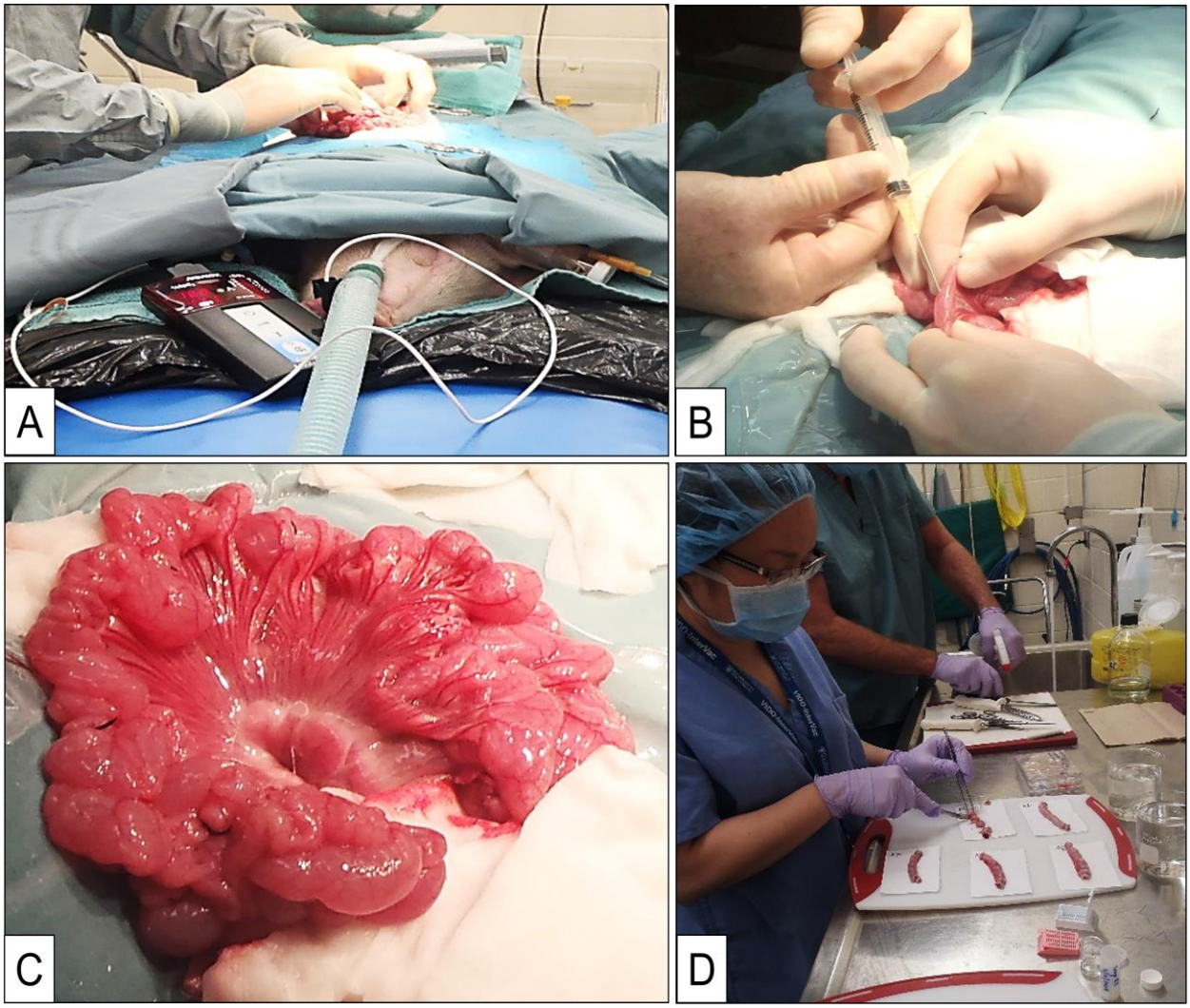

Figure 7.1. Porcine gut loop model

Multiple intestinal loops providing identical and independent sites were created (A). We treated E. coli F4 with six different treatments and injected them into the jejunal loops as described below (B, C). After four hours, the piglets were euthanized to collect samples (D). Each loop was injected 1ml of 0.1M PBS ampicillin to remove E. coli not bound to the villi gently and to collect the content inside the loop (D).

7.3.8. Enumerating the number of *E. coli* binding to jejunal villi

Subsequently, villi from the first segment were gently scraped with a slide and allowed to settle at the bottom of the tube. After that, the number of bacteria adhering to 250 μm of the brush border of villi was quantified under a phase-contrast microscope at 1000× magnification. Five different regions were counted, and data were presented as the average number of bacteria adhering to 250 μm of the brush border. Statistical analysis was done to evaluate the invasion of *E. coli* F4 to jejunal loop after different treatments.

The second segment from each jejunal loop embedded in paraffin was sectioned at 5 μm thickness. All sections were placed on poly-l-lysine coated glass slides and stained with hematoxylin and eosin for histopathological examination.

7.3.9. Counting the number of survival *E. coli* F4 left in the jejunal content

To investigate whether the RGDSK-HRNs-FITC control *E. coli* F4 viability, each loop was injected 1ml of 0.1M PBS ampicillin to wash unbound *E. coli* F4 from the villi gently and to collect the content inside the loop. The content (100μl) was serially diluted from 1-10 times before being incubated in LB-ampicillin agar plates for 24 hours at 37ºC. The number of *E. coli* F4 colonies were counted for statistical analysis. The rest of the content was centrifuged to collect the supernatant and the pellet, which was preserved at -80ºC for later microbial analysis

7.3.10. Terminal deoxynucleotidyl transferase dUTP nick end labeling assay

The second segment from each jejunal loop in the paraffin block was sectioned at 5 μm thickness. To observe the extend of apoptosis in the jejunal epithelium upon *E. coli* challenging and RGDSK-HRNs-FITC treatment, we performed Terminal deoxynucleotidyl transferase dUTP nick end labeling (TUNEL) assay on the tissue sections using a commercial *in situ* cell death

detection kit-Alkaline-phosphatase following per manufacturer's instruction. Briefly, tissues were de-paraffinized with xylene, re-hydrated with ethanol, then permeabilized with proteinase K. After that, the TUNEL reaction mixture, including enzyme terminal transferase solution and label solution, was added. The fluorescent signal was converted to a color signal by incubation in Converter-AP, followed in a substrate solution of the kit. Finally, DNA fragmentation morphology in the tissue was examined under a light microscope. The tissue which was stained without enzyme solution served as a negative control.

7.3.11. **Statistical analysis**

The GraphPad Prism version 5.04 software (San Diego, CA, USA.) was used to analyse data. Quantitative results were expressed as mean ± SEM, and error bars represented standard error. The normal distribution of residuals was tested by histogram and Shapiro-Wilk test. Data were analyzed by Analysis Of Variance (ANOVA), followed by Bonferroni multiple comparison test. A significant difference was set when the critical value of α was below or equal to 0.05 as (two-tailed, $p<0.05$).

7.4. **RESULTS**

7.4.1. **The level of integrin αvβ3 expression changed on *E. coli, Salmonella* infected porcine jejunum**

The immunohistochemistry showed intense staining for the integrin αvβ3 on cryptal cells and villar epithelium with especially intense reaction on the nucleus and apical surface of the cells in healthy porcine jejunum. The level of integrin αvβ3 expression decreased in the epithelium but increased in the vascular endothelium of jejuna infected with *E. coli* alone or in combination with *Salmonella*. Integrin αvβ3 was also expressed in some inflammatory cells, probably plasma cells,

and macrophages in the infected jejuna. Interestingly, the bacteria, likely *E. coli* showed staining with integrin αvβ3 antibody (Figure 7.2). Negative control showed only methyl green color (Figure 7.3)

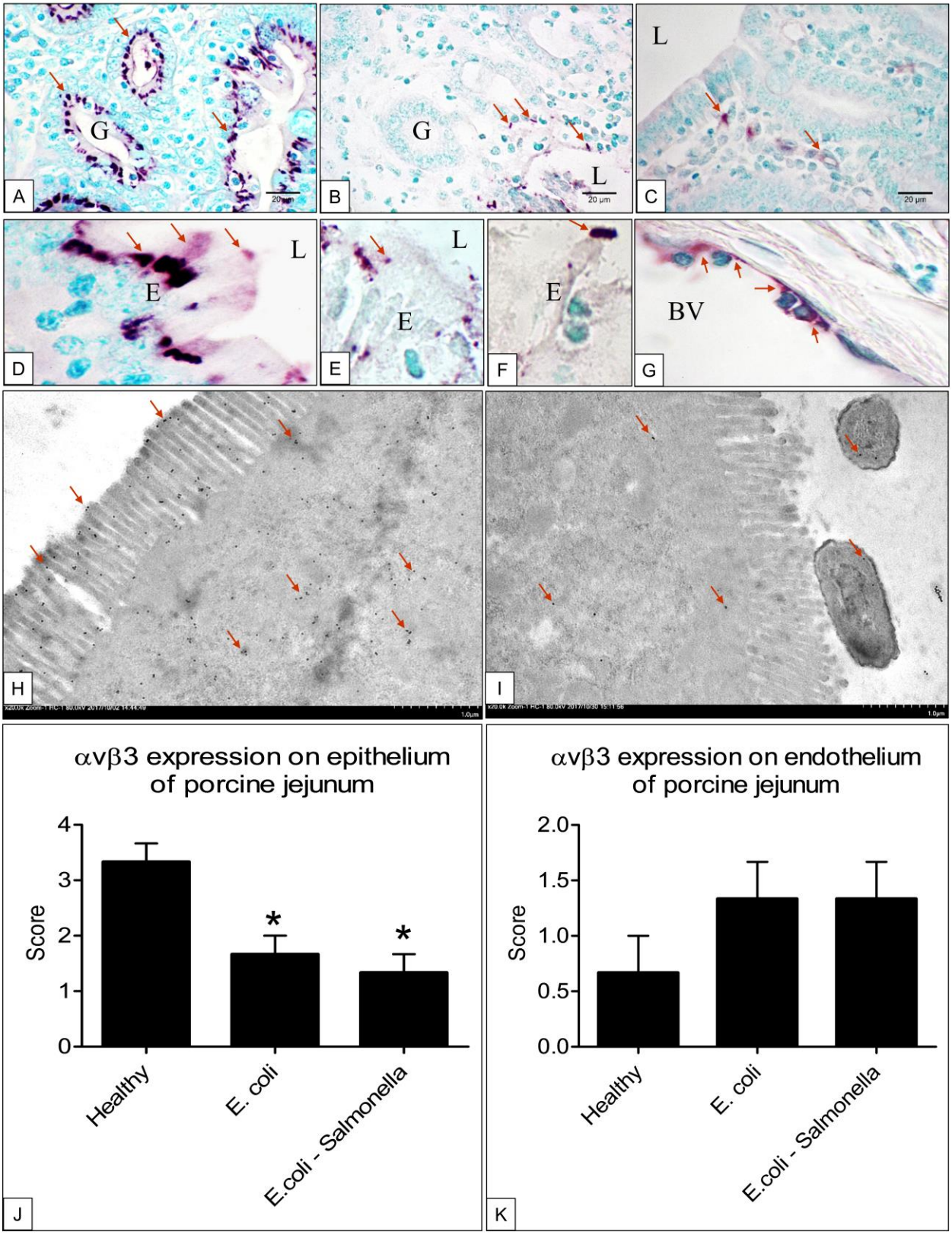

Figure 7.2. Porcine jejunal immunohistochemistry and immune-gold for integrin αvβ3.

The pictures from immunohistochemistry showed that in the jejunum section from the healthy normal pig (A, D), integrin αvβ3 positive staining (purple-pink color, arrows) is observed abundantly in the nucleus, cytoplasm and apical surface of the epithelium of villi (D) and crypts (A). In E. coli infected jejunum (B, E, F), the intensity of positive staining on epithelium decreased. Interestingly, maybe bacteria binding to epithelium has positive staining with integrin αvβ3 (F). In E. coli associated Salmonella infected jejunum (C, G), integrin αvβ3 was found not very strong staining on the epithelium. Integrin αvβ3 is expressed on the immune cells and the endothelium of blood vessels. Both figures H and I are the transmission immune-gold electron micrographs for integrin αvβ3 expression in porcine jejunum. On the epithelium of normal healthy porcine jejunum, integrin αvβ3 was expressed in the nucleus, cytoplasm, and apical surface of epithelium, especially the microvilli (H). The level of integrin αvβ3 on the epithelium decreased upon E. coli infection (I). Abbreviation: G: Gland (crypts), L: Lumen, E: Epithelium, BV: Blood vessel. Statistical analysis of semi-quantitative integrin αvβ3 expression from immunohistochemistry scoring of the porcine jejunal epithelium (J) and endothelium (K). We classified the intensity of staining that: 0, no staining; 1+, light staining; 2+, moderate staining; 3+, strong staining; and 4+, very strong staining. Asterisk (*) indicates significant difference from healthy jejunum ($P<0.05$, $n=3$).

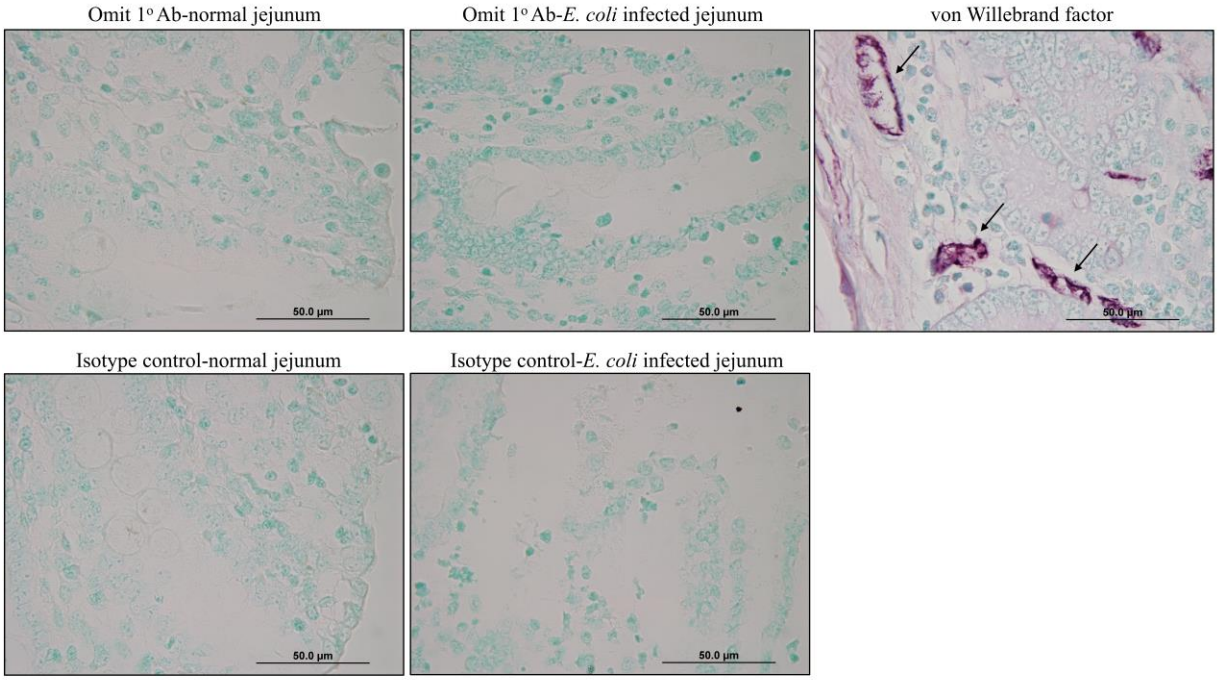

Figure 7.3. Integrin αvβ3 immunohistochemical staining controls of porcine jejunum

The porcine jejunal section, stained with bovine serum albumin and omitted integrin αvβ3 primary antibody, showed only the green-blue color of methyl green counterstaining. The porcine jejunal section, stained with IgG1 rabbit isotype control instead of integrin αvβ3 primary antibody, also served as negative control and did not show any positive reaction. The porcine jejunal section, stained with anti- von Willebrand factor (vWF) antibody, and served as a positive control for the protocol, reacted only with vascular endothelium (pink-violet, arrows). Magnification: 1000×.

7.4.2. *E. coli* has a protein domain functioning as integrin αvβ3

Previous data from 96-well plate binding assay showed *E. coli* binding was dependent on integrin αvβ3 and the number of *E. coli* F4 binding to the plate depended on the concentration of *E. coli* F4 added and the concentration of monoclonal anti-integrin αvβ3 antibody. We then performed another experiment with pretreated *E. coli* with six different treatments. We found that the number of *E. coli* F4 binding to the well plate coated with monoclonal integrin αvβ3 antibody decreased if *E. coli* F4 was treated with either RGDSK-HRNs-FITC, RGDSK-FITC, monoclonal anti-integrin αvβ3 antibody, anti-F4 antibody (Figure 7.4). It can be explained that RGDSK-HRNs-FITC, RGDSK-FITC, and monoclonal anti-integrin αvβ3 antibody block the integrin αvβ3-like protein domain on *E. coli* F4. The anti-F4 antibody blocked the binding site of F4 antigen of *E. coli* F4 to F4 receptor of the host cells (242), which maybe inactivate or opsonize the bacteria and can reduce their proliferation or survival. This possibility was explained by the number of *E. coli* colonies in the supernatant on the above objective 3.

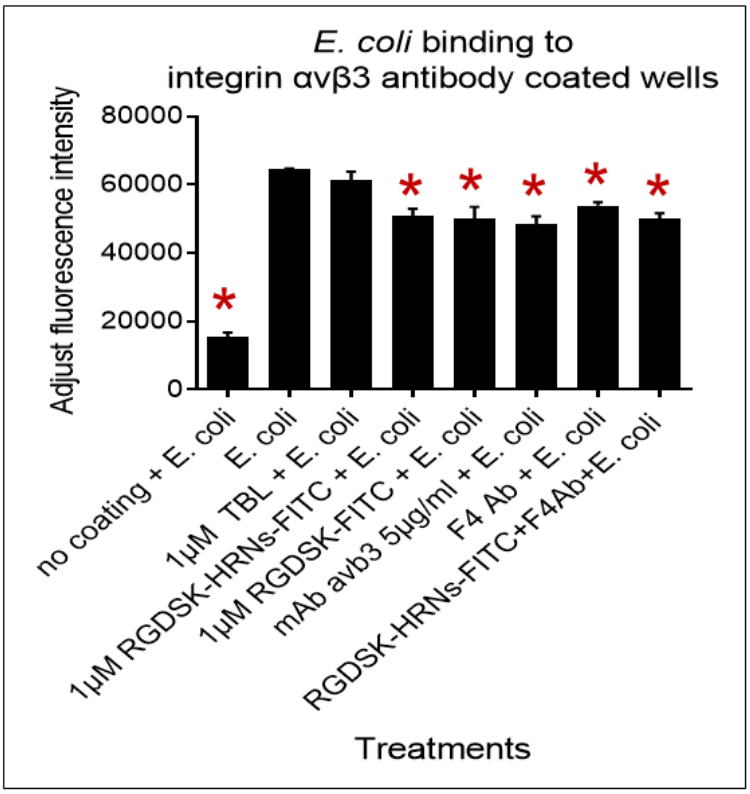

Figure 7.4. Binding assay on monoclonal integrin αvβ3 antibody-coated 96 well plates on pre-treated E. coli.

RGDSK-HRNs mediate E. coli adhering through interaction with the integrin αvβ3-like protein on E. coli. Data were expressed as mean ± SEM. Asterisk (*) indicates a significant difference compared with the E. coli group (P<0.05, n=3 each group).

7.4.3. Evaluating *E. coli* F4 binding to the villi in the porcine gut loop model

We scraped the villi from all loops and counted the number of *E. coli* F4 binding to villi. We found that the number of *E. coli* F4 binding to villi were significantly decreased in the *E. coli* treated with RGDSK-HRNs-FITC, RGDSK-FITC, or anti-F4 antibody compared with the group of *E. coli* F4 only without any treatment ($P<0.05$) (Figure 7.5). The *E. coli* F4 binding to villi was observed again in hematoxylin and eosin-stained tissues (Figure 7.6). We also observed DNA fragmentation of all groups by TUNEL assay staining on jejunal loops (Figure 7.8). However, we did not perform rating and statistical analysis on TUNEL assay staining as well as on hematoxylin and eosin. Compared with *E. coli* F4 treatment control, there was a significant decrease ($P<0.05$) in the number of viable *E. coli* F4 left in the content of the porcine jejunal lumen in RGDSK-FITC peptide, but not RGDSK-HRNs-FITC treatment. (Figure 7.7).

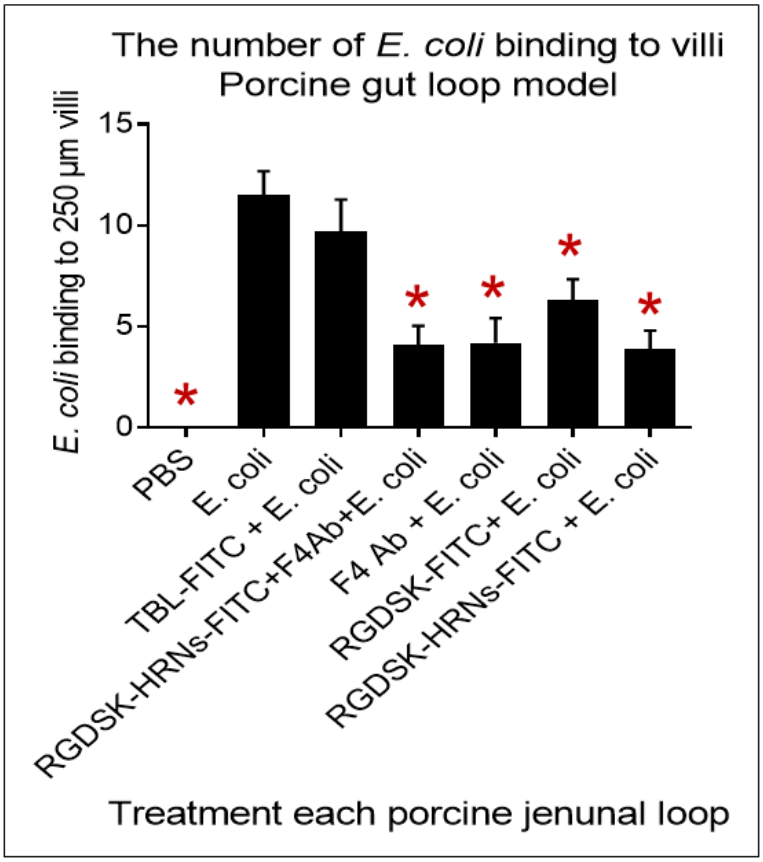

Figure 7.5. The number of E. coli F4 binding to 250 µm length of villi in the porcine jejunal loop model.

RGDSK-HRNs-FITC prevented E. coli binding to porcine jejunal villi. Data were expressed as mean ± SEM. Asterisk (*) indicates a significant difference compared with the E. coli group (P<0.05, n=10 loops each group).

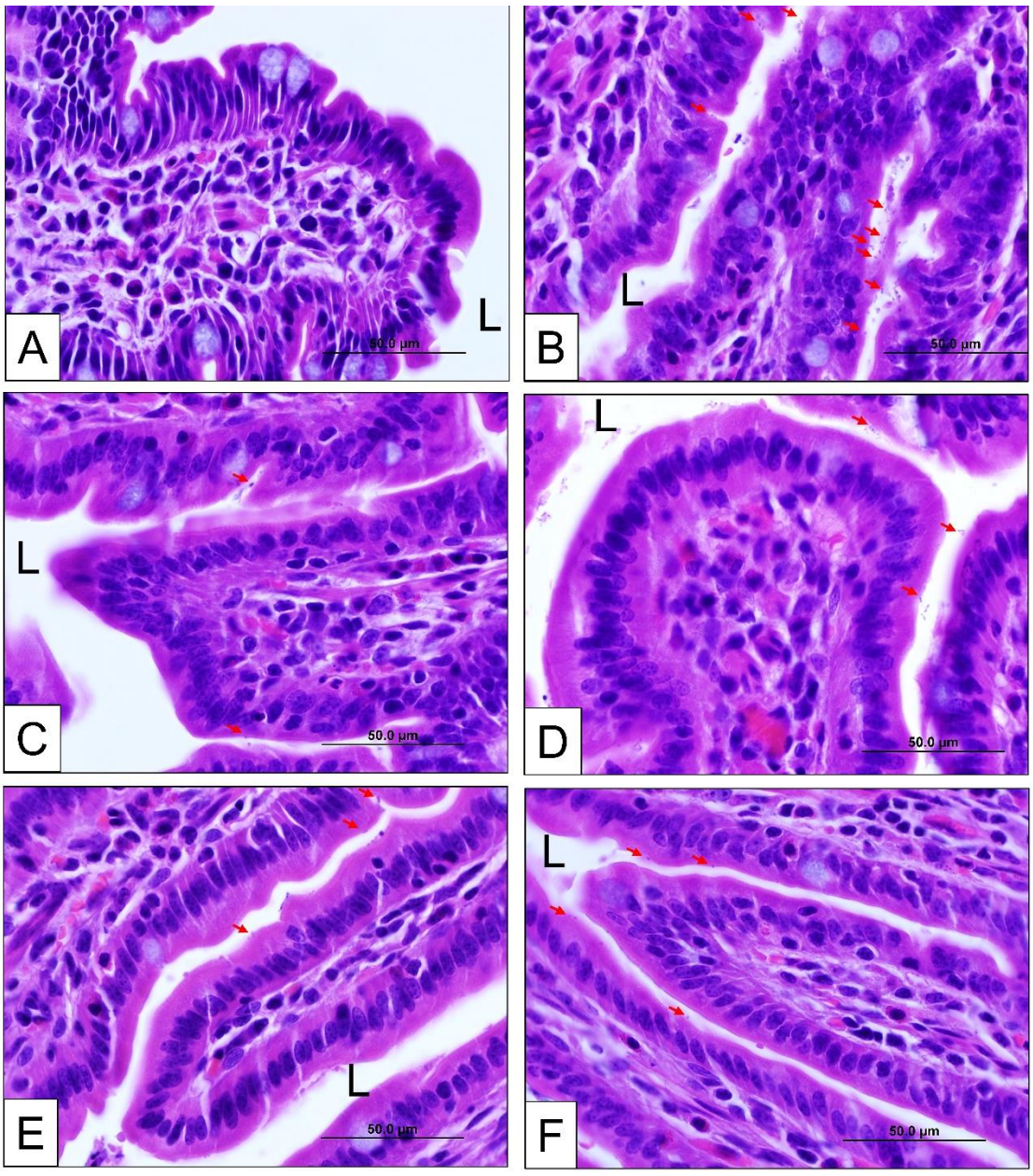

Figure 7.6. Histopathological observation of porcine jejunum with hematoxylin and eosin staining.

Jejunal loops with different treatments from (A) normal control, (B) E. coli F4, (C) RGDSK-HRNs-FITC + F4 Ab + E. coli F4, (D) F4 Ab + E. coli F4, (E) RGDSK-HRNs-FITC + E. coli F4, (F) RGDSK-FITC + E. coli F4 groups. Arrows indicate E. coli. Abbreviations: L: lumen. Magnification: 1000×..

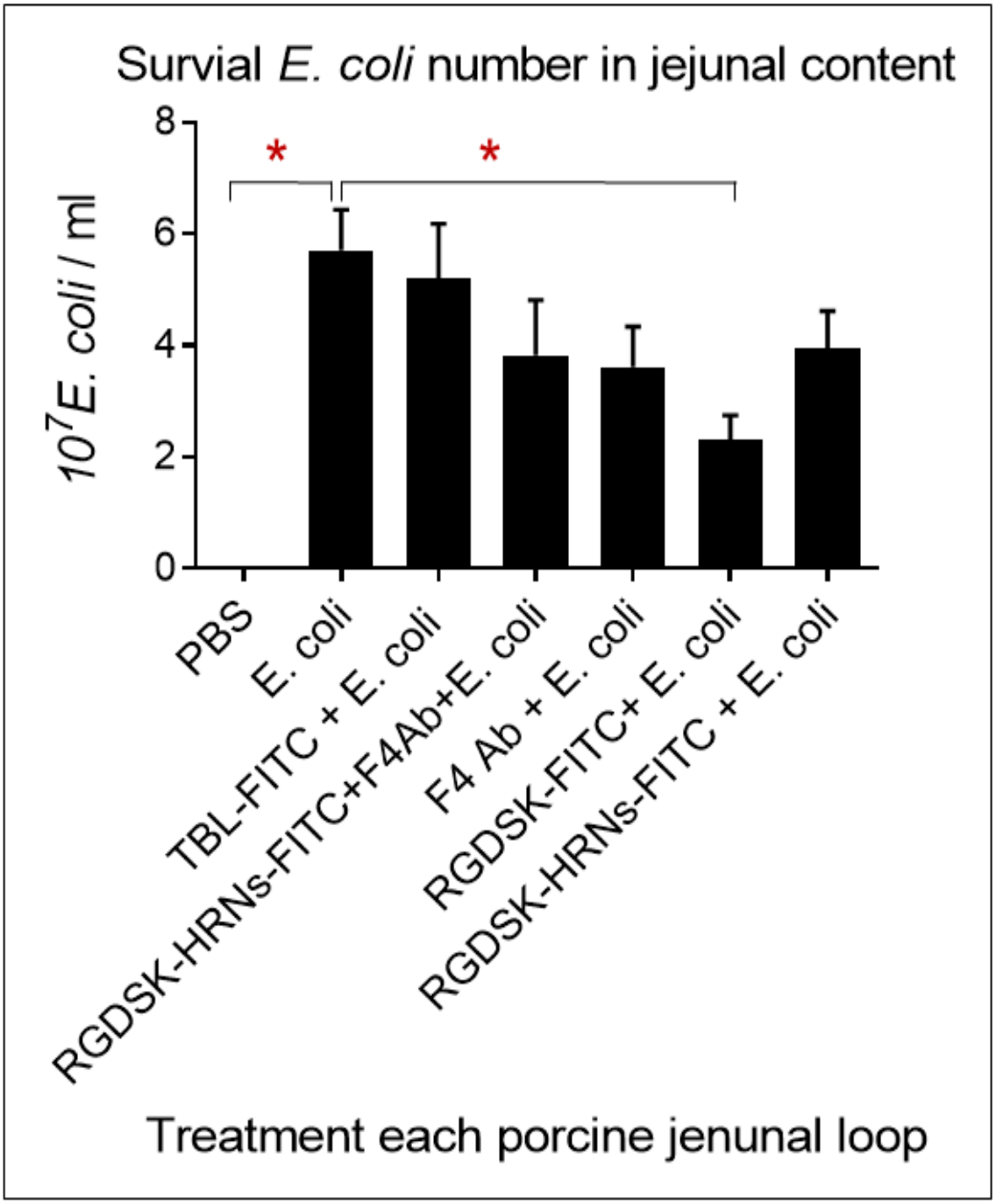

Figure 7.7. RGDSK-HRNs-FITC did not affect the proliferation of E. coli F4 significantly.

Data were expressed as mean ± SEM. Asterisk (*) indicates a significant difference compared with E. coli F4 group ($P<0.05$, $n=10$ each group).

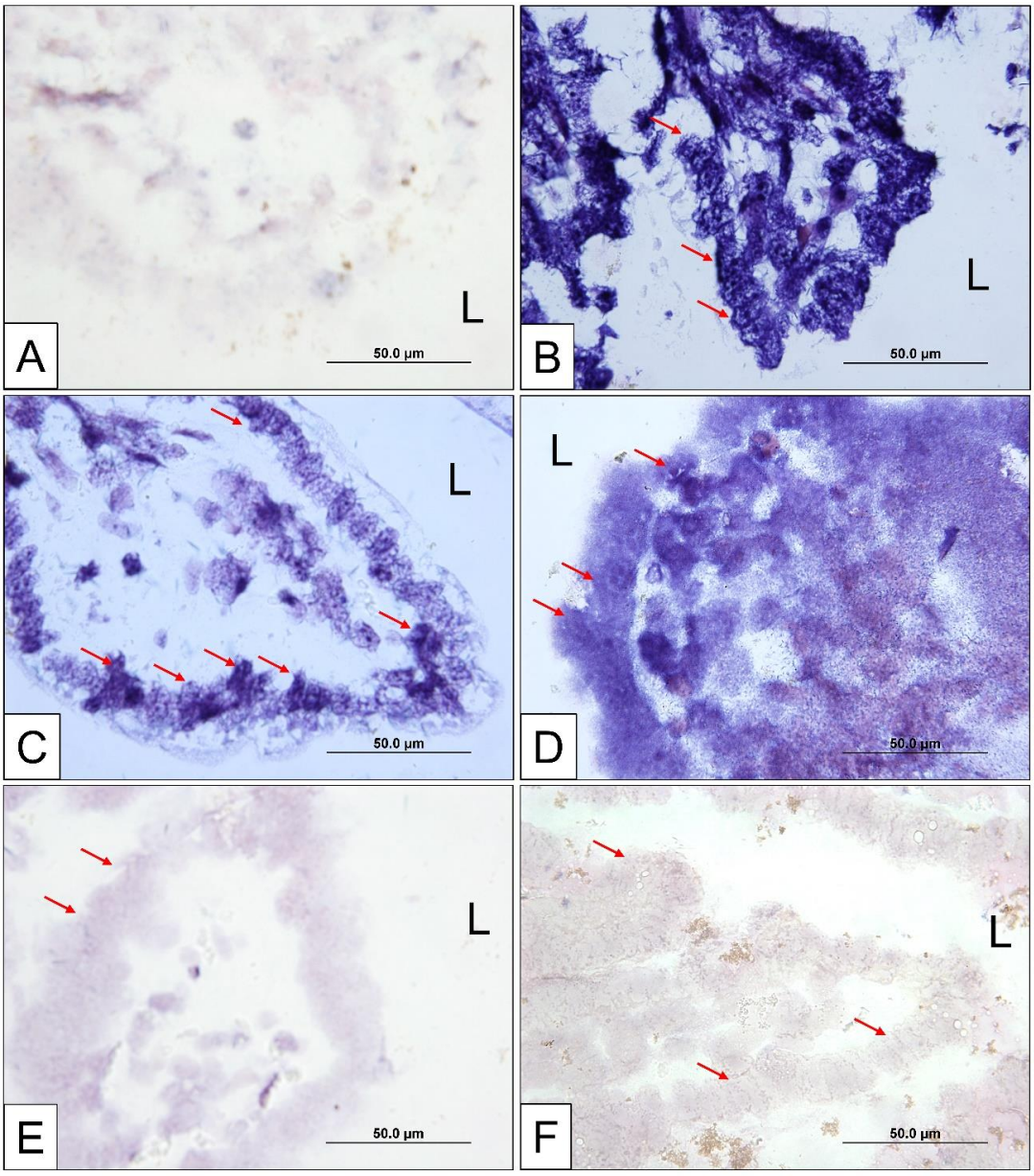

Figure 7.8. TUNEL assay on jejunal loops.

Jejunal loops with different treatments from (A) normal control, (B) E. coli F4, (C) RGDSK-HRNs-FITC + F4 Ab + E. coli F4, (D) F4 Ab + E. coli F4, (E) RGDSK-HRNs-FITC + E. coli F4, (F) RGDSK-FITC + E. coli F4 groups. Arrows indicate positive staining. Abbreviations: L: lumen. Magnification: 1000×.

7.5. DISCUSSION

Our laboratory has previously provided evidence on the expression of integrin αvβ3 on the normal porcine gastrointestinal tract (213). In this present study, we continued exploring the specific and detailed expression of integrin αvβ3 on the porcine jejunum upon infection. We found integrin αvβ3 was present on the apical surface and abundant in the nucleus of the epithelium of healthy porcine jejunum. The integrin αvβ3 expression level was decreased in *E. coli* or *E. coli* – *Salmonella* infected pigs. Taken together, our results suggest that there is an association between the integrin αvβ3 and the bacteria upon infection. Recently, Zhang and colleagues reported that integrin αL of the host was related to sensibility to *Salmonella* Typhimurium infection in a mouse model (267). Moreover, in 2017, Garciarena and colleagues mentioned that cilengitide treatment targeted integrin αvβ3 on the human endothelial cell line and prevented *E. coli* adherence to the cell (73).

Enterotoxigenic *Escherichia coli* (ETEC), which has a high economic impact on swine production and a threat to the safety of pork products, is one of the dangerous pathogens of diarrheal diseases worldwide in humans and animals (204, 249, 261). In this chapter, we continue to use the novel RGDSK-HRNs-FITC to investigate its function on preventing *E. coli* F4 binding to jejunum *in vivo*. The focus of our project was to evaluate the interactions of integrin αvβ3 with *E. coli* F4 and the RGDSK-HRNs-FITC using the innovative porcine gut-loop model and to find ways to exploit the interaction of the integrin and RGDSK-HRNs-FITC to manage bacterial colonization of gut epithelium. The results from this study prove the hypothesis is true that RGDSK-HRNs-FITC can inhibit bacterial colonization on the gut epithelium through blocking integrin αvβ3, thus preventing the epithelium-bacteria component attachment.

Recently, scientists reported that *E. coli* F4 infection-induced apoptosis on the jejunum of piglets (265) by activating caspase 3 as well as caspase 8, and increasing DNA fragmentation (264). However, to our knowledge, the effects of RGDSK-HRNs-FITC on the apoptosis of gut epithelium upon *E. coli* infection via blocking integrin αvβ3 have not been investigated. Our TUNEL staining showed that RGDSK-HRNs-FITC did not significantly increase the severity of DNA fragmentation compared to normal healthy control group. The most obvious implication for emerging from this study with previous *in vitro* study on IPEC1 cell line is that RGDSK-HRNs-FITC can be a potential drug delivery vehicle and is biocompatible to the host.

In conclusion, it is critical to understand the expression of integrin αvβ3. In this study, we detected integrin αvβ3 in the jejunum of pigs. Future studies are required to elucidate this signalling molecule function and the involvement of pathogenesis of intestinal diseases in the pig and human.

ACKNOWLEDGMENTS

We sincerely thank the Saskatchewan Agriculture Development Fund (ADF), the Natural Science and Engineering Research Council (NSERC), the Graduate Student Scholarship program from the Integrated Training Program in Infectious Disease, Food Safety and Public Policy (ITraP), the Devolved Graduate Scholarship program from the Department of Veterinary Biomedical Sciences, and the Graduate Student Scholarship program from the Western College of Veterinary Medicine, the University of Saskatchewan, Canada for supporting this research. We thank LaRhonda Sobchishin for the technical support in immune-gold staining. We sincerely thank VIDO-InterVac staff members at the University of Saskatchewan for supporting the gut loop model surgery. We sincerely thank Dr. John Harding, VIDO-InterVac, and PDS at the University of Saskatchewan for their generous gift materials.

GRANTS

The study was funded through the Saskatchewan Agriculture Development Fund (ADF) and the Discovery Grant from the Natural Sciences and Engineering Research Council of Canada (NSERC) to Dr. Baljit Singh.

CHAPTER 8. GENERAL DISCUSSION AND CONCLUSION

Enterotoxigenic *Escherichia coli*, which has a high economic impact on swine production and poses a threat to pork meat products, is one of the common causes of diarrheal diseases and public health concerns. To manage this outbreak, many scientists have attempted to reduce *E. coli* colonization in the intestine (34, 35, 185, 247). The intestinal epithelium is the earliest responders contacting pathogens in the gastro-intestinal tract in innate immune responses. The initial adhesion of *E. coli* to the gut epithelium is the first stage in the pathogenesis of this enteric disease (124).

Our data collected through an *in vitro* experiment by western blot, immune-gold, and immunofluorescent staining using the IPEC1 cell line showed *E. coli* F4 infection decreased the expression of the integrin αvβ3 in the cell line. Moreover, considering the change of integrin αvβ3 expression in the epithelium of porcine jejunal tissues in normal and *E. coli* or *E. coli* associated with *Salmonella* infected jejuna in our study, there is a clear need to fine-tune the function of integrin αvβ3 in the *E. coli* infected jejunums. The implications of the downregulation of the integrin expression are not clear, but it may be a mechanism that *E. coli* uses it to prevent the activation of the cells or to down regulate the immune response. In 2004, Janardhan and colleagues mentioned that the crosstalk between integrins is a possible reason for the decrease of integrin αv and integrin β3 subunits levels in *E. coli* infected rat lungs compared to control and *S. pneumoniae* infected groups (105). Although whether *E. coli* F4 containing an RGD peptide sequence is unclear, in this case, integrin αvβ3 of the host might bind to the RGD-containing peptide of *E. coli* F4. Another possible explanation is that *E. coli* F4 possesses the structure having the same characteristic and properties, as is found in RGD-containing ligands. This RGD-like structure or peptide can bind to the same site on the integrin αvβ3, promoting *E. coli* F4 attachment to and

penetration into intestinal epithelium. Similarly, a recent study reported that *Staphylococcus aureus* bound to integrin αvβ3 on the endothelium, leading to endothelial dysfunction (149). This binding was reduced by Cilengitide through inhibiting integrin αvβ3 (149).

Moreover, scientists reported that *eae* gene (encoding Intimin adhesion protein) in enterohemorrhagic *E. coli* enabled the pathogen to attach to and desquamate colonic epithelial cells, recruiting inflammatory cells and causing microvilli loss and edema (56). Here, we used the *eae* negative *E. coli* F4 strain and focused on the early adherence stage of *E. coli*. Another interesting observation in our study was the presence of an integrin αvβ3-like protein domain in *E. coli* F4, confirmed by western blot, immunohistochemical staining, 96-wells high binding assay, and a pilot mass spectrometry analysis. The role of the integrin αvβ3-like protein on the surface of *E. coli* is unknown, but may have implications for the adherence to and invasion of the bacteria.

Many scientists have provided a substantial amount of evidence about the bacteria-extracellular matrix interaction (257). In this study, we found that *E. coli* F4 had an RGD-like binding site with integrin αvβ3 in the jejunal epithelium, and *E. coli* had an integrin αvβ3-like protein domain. Therefore, integrin αvβ3 maybe one of the possible receptor molecules of *E. coli*. Our findings provide insights into the function of integrin αvβ3 in intestinal physiology, *E. coli* infection, and pathology. We believe this provides a direct link to the first stage of *E. coli* pathobiology as we have quantified *E. coli* binding.

Peptides are the alternatives of antibiotics to prevent bacteria and avoid antibiotic resistance and antibiotic-residues in animal products (158). Generally, antimicrobial peptides have a broader spectrum and electrostatic interaction with the membrane lipid components to disrupt bacterial membrane (40). Integrin αvβ3 is a heterodimeric transmembrane receptor that recognizes and binds arginine-glycine-aspartic acid (RGD) containing peptides. In this study, we used

biocompatible RGDSK-HRNs-FITC to target integrin αvβ3 protein presenting on the gut cells to prevent the bacterial attachment to the gut to protect the host from infections. The project aims were to develop a proof of concept for nanomedicine, a potential alternative to antibiotics, to ameliorate this important public health concern.

Here, we wanted to verify whether RGDSK-HRNs-FITC were able to mediate the integrins-dependent receptor in *E. coli* infection *in vitro* and *in vivo*. In an *in vitro* experiment, we found that RGDSK-HRNs-FITC could prevent the attachment of *E. coli* to IPEC1. *Ex vivo* villus adhesion assay showed that the best results were observed in RGDSK peptide treatment in maintaining inhibiting *E. coli* binding to the jejunal epithelium. RGDSK-HRNs-FITC treatment is efficient in a short-time period. It is difficult to interpret the findings from RGDSK-HRNs-FITC treatment because of the complexity of the interaction of multiple RGDSK on the nanotube surface with integrin αvβ3 on the jejunal epithelium and the integrin αvβ3-like function protein on *E. coli* in long-time period treatment.

To have deeper understanding of the effect of RGDSK-HRNs-FITC in humans and animals, an *in vivo* experiment should be performed. However, the oral bacterial challenging experiment is expensive and impractical due to the number of animals required, treatment variables and individual animal characteristics. Moreover, non-sentient animals would not provide the complete biological readouts necessary to evaluate the efficacy of RGDSK-HRNs-FITC to *E. coli* infection. Moreover, because the intestinal immune system of pigs is considered similar to that of humans, and both are the most common target mammalian species at high risk of *E. coli* infection (79, 154, 165, 195), we used the adherence porcine gut loop model to determine efficacy of RGDSK-HRNs-FITC in preventing the *E. coli* F4 colonization in diarrhea.

In this study, we found that RGDSK-HRNs-FITC reduced the number of *E. coli* F4 binding to villi compared with *E. coli* F4 treatment group. Moreover, RGDSK-FITC peptide but not RGDSK-HRNs-FITC treatment decreased the number of live *E. coli* F4 left in the jejunal lumen. Besides the ability in targeting integrin αvβ3 in the jejunal epithelium and integrin αvβ3-like protein in *E. coli* F4, RGDSK peptide itself likely effects the survival of *E. coli* F4. Our results highlighted the role of the RGDSK peptide functional group associated with the nanotubes vehicle down-regulated the toxicity of RGDSK peptide to the jejunal cells and *E. coli* F4. These data imply that the nanotubes vehicle mostly maintained the function of RGDSK and even reduced the adverse effect of RGDSK on cell death.

Integrin αvβ3 binds to RGD peptides, which are present in extracellular matrix molecules such as fibronectin, osteopontin, collagen, and vitronectin (196, 220). The integrin αvβ3 regulates cell functions such as activation, proliferation, and adherence through a variety of signals (196, 220). This study added to our understanding that integrin αvβ3 was known as a receptor for bacteria (149). We confirmed that *E. coli* F4 efficiently binds to the IPEC1 cell line *in vitro* (126). Our findings support the previous statement that obstructing the receptor adhesion sites to inhibit *E. coli* attachment to the intestines, particularly epithelia, can result in a novel intervention to modify this enterotoxigenic pathogen-induced diarrhea in pigs (106).

The literature review showed that LM609 monoclonal integrin αvβ3 antibody was used in many previous papers as its specific recognition of integrin αvβ3 (14, 167, 210). Some researchers mentioned that LM609 antibody blocked integrin αvβ3 via allosteric sites which reducing the activity of integrin αvβ3 such as a conformation change involving protein dynamics (14). In our study, RGDSK-HRNs-FITC interact with integrin αvβ3 mainly via the RGD binding site. This reason may explain the little difference in the effects of these two treatments in cell survival and

in preventing *E. coli* F4 binding to villi. RGDSK-HRNs-FITC had almost the same blocking function as LM609 monoclonal anti-integrin αvβ3 antibody treatment in preventing the *E. coli* F4 binding to jejunal epithelium at short time point. This suggests that integrin αvβ3 plays a role in the binding of *E. coli* F4 to the jejunal epithelium in an early stage of adherence.

We also tested whether any advantages of combining RGDSK-HRNs-FITC and F4 antibody treatment. We did not observe significant additional efficacy of using both treatments at the same time in inhibiting *E. coli* F4 binding to porcine villi, implying that these F4 and integrins targets likely to be arranged in sequence or at the same binding site with integrin αvβ3. Integrin αvβ3 is possibly a coreceptor with the F4 receptor for *E. coli* F4 adhesion and colonization. Perhaps either integrin αvβ3 or F4 receptor is in the initial attachment step, and the other is in the subsequent post attachment step of the multistep process involving the *E. coli*-jejunal epithelium adherence. Another explanation is that both integrin αvβ3 and F4 receptor are required as co-targets of the *E. coli* to attack the host cell at the same time.

Taken together, this study added the information on the biology of integrin αvβ3 in the jejunum and the biocompatibility of helical rosette nanotubes and their potential use in inflammatory diseases (Figure 8.1). This novel RGDSK-HRNs-FITC can target and interface with integrins conferring great promise as a potential drug-delivery system for intestinal inflammation, particularly due to *E. coli* F4 in this study. The aim is to develop a proof of concept for nanotubes-based molecular interventions to reduce *E. coli* colonization of the gut. The investigation will contribute to offering new strategies in the prevention and management of these costly diseases, expecting ameliorating diarrheal situation.

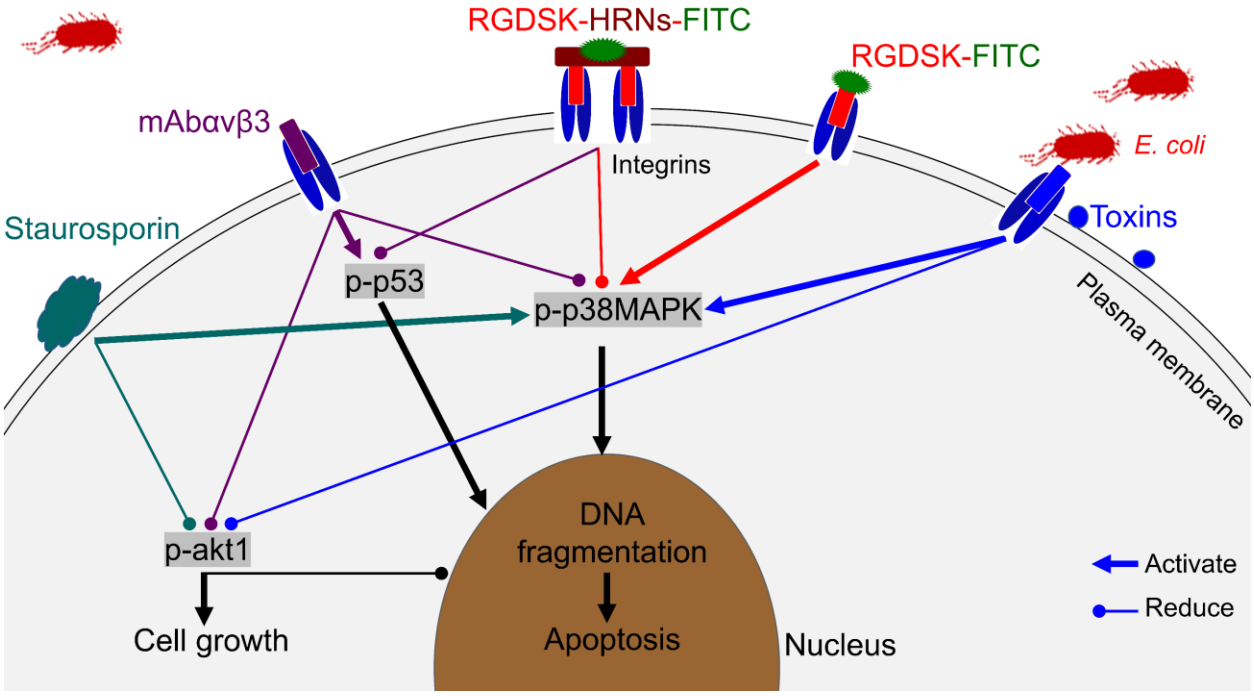

Figure 8.1. The schematic diagram illustrates the effect of RGDSK-HRNs-FITC and other treatments on the porcine jejunal epithelium.

This diagram shows that E. coli infection induces p-p38MAPK and inhibits p-akt1. The RGDSK-HRNs-FITC prevent E. coli binding to the intestinal epithelium, reduced the level of p-p53 and p-p38MAPK compared with monoclonal anti-integrin αvβ3 antibody and RGDSK peptide, respectively, in E. coli infection, lessened the DNA fragmentation, and slowed down the apoptosis process. It leads to improve the survival of epithelium. Thinner arrows indicate inhibition, and thicker arrows indicate a stimulation.

CHAPTER 9. SUPPLEMENTAL RESULTS

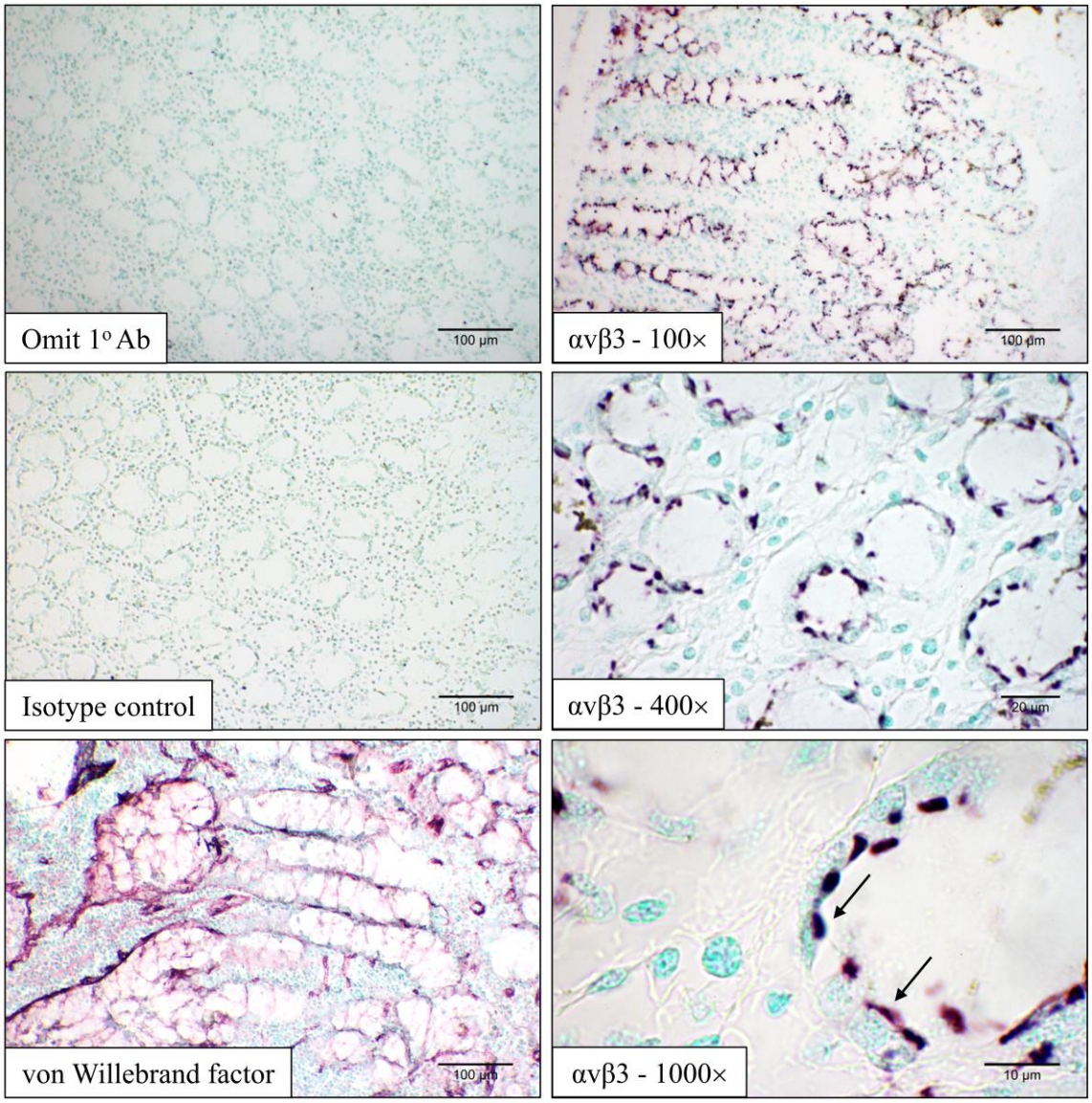

Figure 9.1. Expression of integrin αvβ3 in the porcine gastrointestinal tract

Immunohistochemical staining normal porcine gastrointestinal tract was performed with monoclonal anti-integrin αvβ3 antibody (clone LM609, Chemicon Inc., Temecula, USA). Integrin αvβ3 is expressed in the epithelium, especially in the apical surface of the cells (dark purple). Negative controls for the specificity of primary, secondary antibody and protocol included mouse IgG1 isotype control, omission of primary antibody or both primary antibody and secondary antibody

conjugated HRP. All negative controls show the only green-blue color of methyl green counter-staining, no positive staining reaction. The controls staining with the anti-endothelial marker von Willebrand factor (vWF, dark purple) served as a positive control for the protocol, which showed only positive staining of vWF in the endothelium.

9.1. Integrin αvβ3 expression in the equine lung and jejunum

(Accepted for publication in the Canadian Journal of Veterinary Research)

Nguyen Phuong Khanh Le[1,2], Volker Gerdts[1,3], and Baljit Singh[1,4]

[1] Western College of Veterinary Medicine, University of Saskatchewan, Canada.

[2] Faculty of Animal Science and Veterinary Medicine, Nong Lam University, Ho Chi Minh City, Vietnam

[3] Vaccine and Infectious Disease Organization-International Vaccine Centre, University of Saskatchewan, Canada.

[4] Faculty of Veterinary Medicine, University of Calgary, Canada.

9.1.1. Abstract

Integrin αvβ3 recognizes arginine-glycine-aspartic acid (RGD) sequences and has important functions in cell adhesion, signalling, and survival. However, the expression of integrin αvβ3 in the equine lung and jejunum is not well understood. In this report, we used the lungs and jejuna of the horse to explore the hitherto unknown expression of integrin αvβ3 with light and electron immunocytochemistry. Immunohistochemistry showed integrin αvβ3 on the epithelium, the immune cells in Peyer's patches, the smooth muscle, and the endothelium of equine jejuna. In equine lungs, we recognized integrin αvβ3 on the endothelium of blood vessels, the alveolar septa, the bronchial lymph nodes, and the cartilages. However, the expression of the integrin αvβ3 was weak on the epithelium of bronchioles. In conclusion, these are the first data to show the expression of integrin αvβ3 in equine lungs and jejuna.

Key Words: integrin αvβ3, horse

9.1.2. Introduction

Integrins are heterodimeric transmembrane receptors, comprised of two subunits, α and β. The integrins are present in many species such as mammals, chicken, zebrafish, sponges, the nematode *Caenorhabditis elegans* (two α and one β subunits, forming two integrins) and the fruit-fly *Drosophila melanogaster* (five α and one β subunits, forming five integrins) (229). The integrin family has 18 α and eight β subunits, forming 24 heterodimeric transmembrane receptors (29, 229). All five integrins αv, two integrins β1 (α5β1, α8β1), and αIIbβ3 can recognize arginine-glycine-aspartic acid (RGD) peptide ligands, known as a general integrin-binding motif (29). Each subunit has an extracellular domain, a single transmembrane region, and a short cytoplasmic domain (8). The extracellular domain, a ligand-binding site, transmits signals from outside into the cell interior and vice versa receives the intracellular signals to regulate back to the affinity of their ligand-binding site (11, 29, 229, 266). Although smaller than the extracellular domains, the cytoplasmic domains up-regulate the activation of integrins by their association with adaptor proteins, including Src, focal adhesion kinase, integrin-linked kinase, kindlin, paxillin, talin, and vinculin (103, 170). Consequently, these interactions rearrange the cytoskeleton, thus affecting the structure and function of extracellular domains (103). The activation state of the integrins is characterized by separation, twisting, pistoning, and hinging of their tails (103). The integrins with a highly bent physiologic conformation have low affinity for binding biological ligands (230).

Integrin αvβ3, known as a vitronectin receptor, plays an essential role in cell adhesion, cell signalling, cell survival, angiogenesis, and leukocyte migration (159, 220). The expression of integrin αvβ3 is increased in neovascular endothelial cells (220). This protein serves as a marker on the cell surface, which recognizes and binds peptides containing RGD (159, 220). Our lab

reported that integrin αvβ3 is expressed on the bronchial vasculature in the lung of the calves and dogs, as well as the small intestine of the calves, dogs, and pigs (213).

Horses suffer from many inflammatory diseases, including some of the infectious origin (49, 192). The mechanisms of inflammatory cell recruitment, cell activation, and changes in vascular permeability underlying diseases such as colic, virus as well as bacterial enteritis, and pneumonia, are not fully understood (49, 140, 146, 183). The occurrence of diarrhea is commonly seen in horses, and the altered gut barrier function underlies in increased secretion of water into the intestine (183). The integrin αvβ3 with roles in fundamental processes such as cell signalling, cell migration and vascular hydraulic conductivity (210, 239), may function in equine inflammatory diseases of the lung and the intestine. Currently, there are no data on the expression of the integrin αvβ3 in equine tissues. Our data showed that integrin αvβ3 was expressed in equine lungs and jejuna.

9.1.3. Materials and methods

Materials

Jejuna and lungs from horses (n = 4 each) were processed and embedded in paraffin blocks at Western College of Veterinary Medicine at the University of Saskatchewan. Mouse monoclonal integrin αvβ3 antibody (clone LM609, Chemicon Inc., Temecula, USA.), polyclonal goat anti-mouse immunoglobulins/HRP secondary antibody (Dako, California, USA.), primary antibody polyclonal rabbit anti-human von Willebrant Factor (vWF) (Dako, Burlington, ON, Canada), Vector® VIP peroxidase substrate kit for peroxidase (Vector laboratories, Burlingame, CA, USA), methyl green (Dako, California, USA.) were purchased commercially.

Immunohistochemical staining integrin αvβ3

Equine lungs and jejuna in paraffin blocks were sectioned at 5µm thickness for immunohistochemistry as per a previous protocol (213). Briefly, sections were de-paraffinized, followed by quenching the endogenous peroxidase activity and treatment with pepsin. Following two hours blocking with 1% BSA, the sections were incubated with monoclonal integrin αvβ3 antibody (clone LM609, Chemicon Inc., Temecula, USA.) and appropriate polyclonal goat anti-mouse immunoglobulins/HRP secondary antibody. The color development was carried out with Vector® VIP peroxidase substrate kit. The controls included staining with the anti-endothelial marker vWF serving as a positive control, or isotype antibody matching control (mouse IgG1) instead of primary antibody or the omission of primary antibody serving as negative controls.

Immuno-gold electron microscopy for integrin αvβ3

Equine lungs and jejuna in LR white resin were sectioned at 100nm thickness on nickel grids. The non-specific bindings were blocked by BSA 1% in Tris-buffered saline before one-hour incubation in the integrin αvβ3 antibody (50µg/ml). A section stained without primary antibody was used as a negative control. After three times being washed in Tris-buffered saline, the sections were incubated for 1 hour in 15–nm gold-conjugated anti-mouse secondary antibody with 1:100 dilution. Following that, samples were incubated in 2% aqueous uranyl acetate, an indicator for negative staining, then Reynold's lead citrate to enhance the electron-scattering properties of biological components inside the cells. The micrographs were imaged using a transmission electron microscope (Hitachi HT7700 - XFlash 6T160, Germany) operated at 80KV.

9.1.4. Results

Integrin αvβ3 was detected on the equine lungs and jejuna. Immunohistochemistry showed integrin αvβ3 on the endothelium of blood vessels, the alveolar septa, the bronchial lymph nodes, the cartilages, the epithelium of bronchioles in equine lungs, neutrophils, type 1 epithelium and pulmonary intravascular macrophages (Figure 9.2). Immuno-electron microscopy yielded data on the detailed subcellular expression of the integrin. We found that the integrin was present in type I alveolar epithelial cells, pulmonary capillary endothelium, and neutrophils (Figure 9.3). The integrin was localized on the plasma membrane, cytoplasm, and the nuclei of these cells. Pulmonary intravascular macrophages also expressed integrin αvβ3 on their surface, cytoplasm, and the nucleus (Figure 9.3).

In equine jejunum, integrin αvβ3 was found in the epithelium, lymphocytes in Peyer's patches, smooth muscles, and endothelium lining lumen (Figure 9.4). Negative controls for the specificity of primary, or secondary antibody include mouse IgG1 isotype control instead of integrin αvβ3 antibody, or the omission of primary antibody or both primary antibody and secondary antibody conjugated HRP. All negative controls show only the green-blue color of methyl green counter staining, but no positive staining reaction (Figure 9.5).

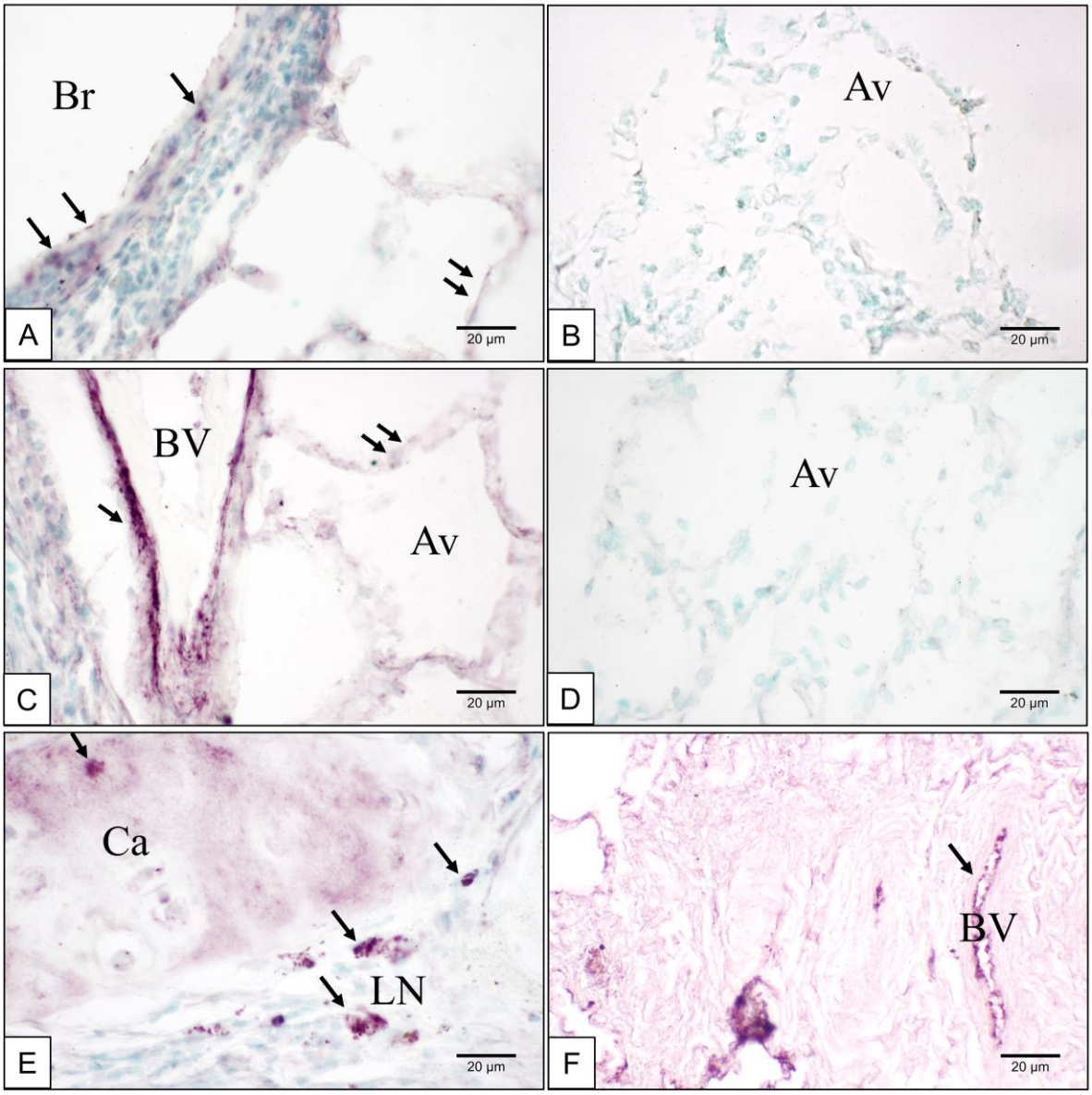

Figure 9.2. Equine lung immunohistochemistry for integrin αvβ3

Lung sections from healthy normal horses, stained with BSA (B), or IgG1 isotype control (D), showed only the green-blue color of methyl green counterstaining while anti-vWF antibody (F) reacts with vascular endothelium (purple-pink color). Integrin αvβ3 staining (arrows to purple-pink patchy deposition) is observed in alveolar (Av) septum (C), bronchiole (Br) epithelium (A), endothelium on blood vessel (BV, C), bronchial lymph node (LN, E), cartilage (Ca, E). Magnification: 400×.

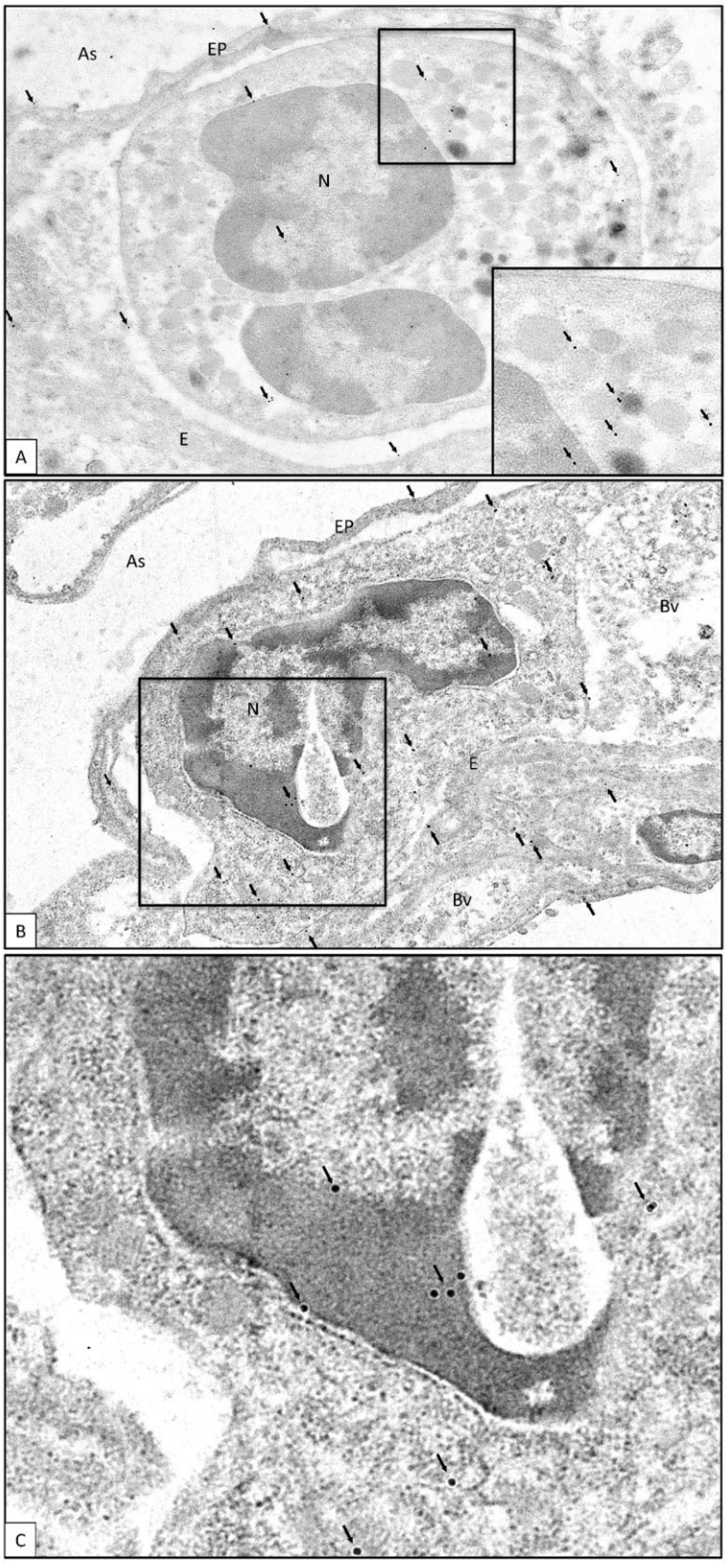
As
EP
N
E
A
EP
As
Bv
N
E
Bv
B
C

Figure 9.3. Immuno-gold electron microscopy for integrin αvβ3 of an equine lung.

The transmission electron micrograph of the normal healthy equine lung showed staining for integrin αvβ3 (arrows) in the plasma membrane, nucleus (N) and cytoplasm of a neutrophil in a capillary (figure A), a pulmonary intravascular macrophages (PIM) (Figure B, and Figure C shows the boxed area highlighted), a type 1 epithelium on alveolar septa (EP, figure A and B), endothelium (E, Figure A and B). The PIM was characterized as a giant and irregularly shaped leukocyte with a kidney bean-shaped nucleus, adhering to the capillary endothelial cell on the thicker side of the alveolar septum. The cytoplasm of PIM contains some vacuoles. Abbreviation: As: Alveolar space, Bv: blood vessel, Br: Bronchiole, E: endothelium, EP: epithelium, N: nucleus. Magnification: (A): 15,000×, (B): 10,000×.

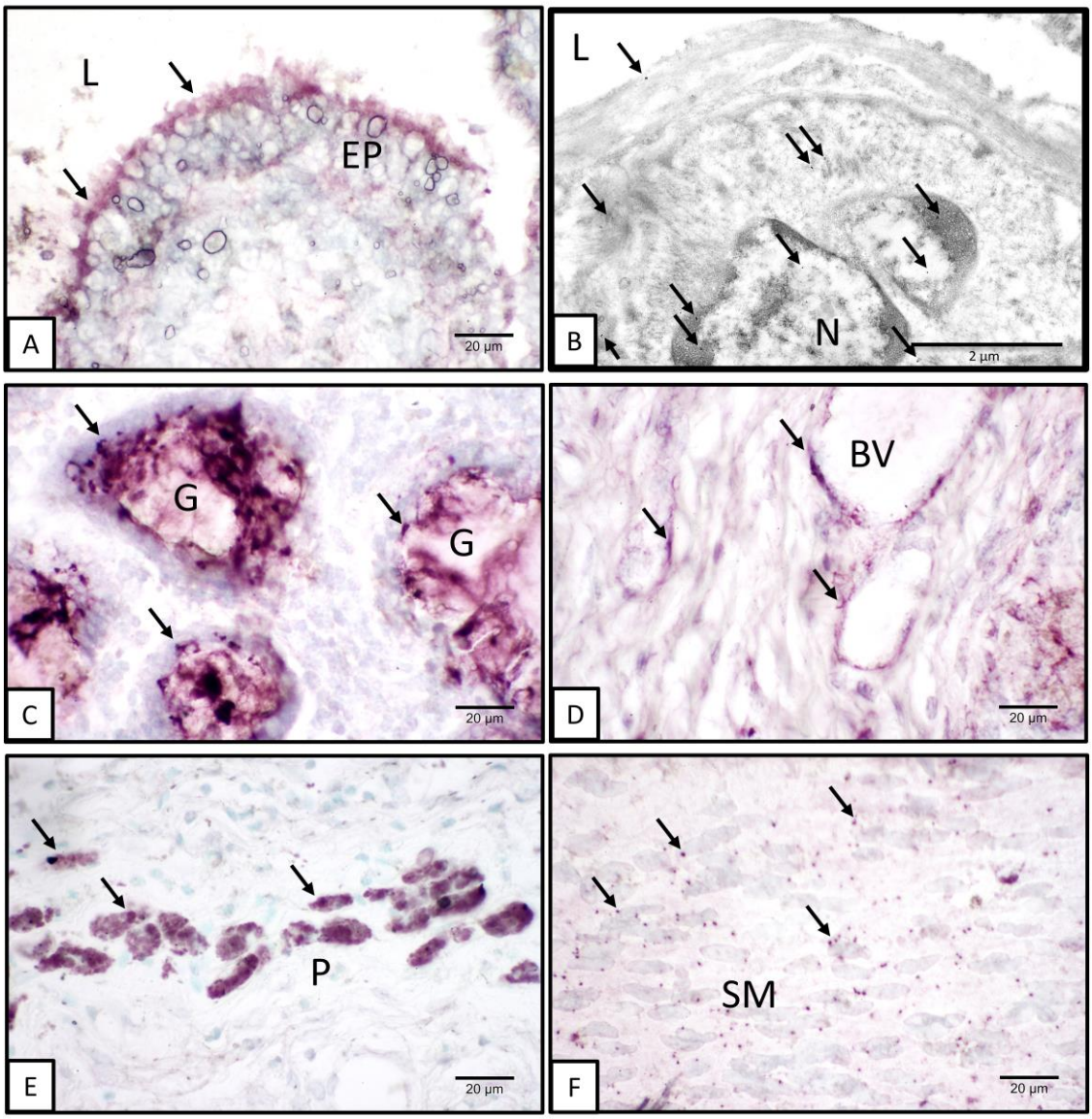

Figure 9.4. Equine jejunum immunohistochemistry and immune-gold for integrin αvβ3 Immunohistochemistry results show positive staining integrin αvβ3 (purple-pink) on epithelium on lumen (A), crypts (C), endothelium (D), cells in Peyer's patches (E), and smooth muscle (F). The immune-gold electron micrograph of integrin αvβ3 expression on the epithelium of normal healthy horse jejunum shows integrin αvβ3 on the nucleus, cytoplasm, and apical surface of the epithelium (B). Abbreviation: L: lumen, EP: epithelium, BV: blood vessel, SM: smooth muscle, G: gland (crypts), P: Peyer's patches, N: Nucleus. Magnification: A, C-F: 400×, B: 20,000×.

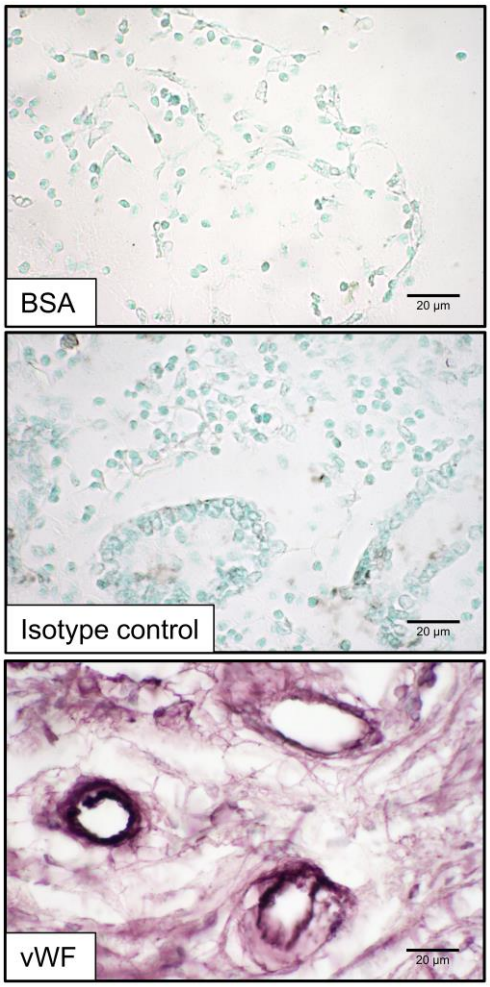

Figure 9.5. Integrin αvβ3 immunohistochemical staining controls of equine jejunum

From top to bottom, the equine jejunal section, stained with bovine serum albumin (BSA) and omitted integrin αvβ3 primary antibody, showed only the green-blue color of methyl green counter staining. The equine jejunal section, stained with IgG1 rabbit isotype control instead of integrin αvβ3 primary antibody, also served as negative control and did not show any positive reaction. The equine jejunal section, stained with anti-vWF antibody, and served as a positive control for the protocol, reacted only with vascular endothelium (pink-violet). Magnification: 400×.

9.1.5. Discussion

The financial losses due to intestinal and respiratory diseases are in the range of billions of dollars every year worldwide (183). The lung and intestine are two organs of the body that interact with the environment through air and food, respectively, all the time and are exposed to pathogens and allergens (140, 146). The unique and heterogenous lining of the epithelium in the intestine and the lungs is the first physical, physiological, and immunological barrier with a well-developed system for handling the bacteria and viruses (140, 146). The epithelia employ a variety of molecular strategies to tackle invading microbes and interaction with the intestinal microbiota. We have previously provided evidence on the expression of integrin αvβ3, which is an important adhesion and signalling molecule in rat, calf, pig, dog, and human (175, 210, 211, 213). In this present study, we continued exploring the specific and detailed expression of integrin αvβ3 on the equine lung and jejunum. We found that integrin αvβ3 was present on the epithelium, endothelium, and immune cells in the lungs, and jejuna of the horse.

We have previously reported the occurrence of the integrin αvβ3 on the porcine intestinal epithelia as well as the airway and alveolar epithelia of the lung of pigs, dogs, and cattle (213). The integrin αvβ3 may play an important role in the adhesion and uptake of bacteria and viruses by the epithelial cells and aid in keeping the epithelium clean (81). Recently, there has been major interest in understanding the formation and ecology of the microbiome in various organs, including the gut and the airways of animals (49, 140, 146, 183). The role of adhesive proteins as integrin αvβ3 in the maintenance of healthy microbiome and the interactions of microbiome with the equine epithelia remains unexplored and may be an area of interest. This could be especially important in species such as horses that have high incidence of intestinal diseases such as colic (49) and virus infection (183), as well as lung diseases such as heaves (192). Similar to these data,

previously we also demonstrated the expression of integrin αvβ3 on the bronchiolar epithelia and alveolar macrophages in normal human lung (211). The expression of integrin αvβ3 in alveolar macrophages was intense in human sepsis lungs (211).

There are differences in the anatomy and physiology of the lung between the horse and other mammal animals as well as humans since the horse lung supports its intense athletic performance (108). The horse lung also has the population of pulmonary intravascular macrophages (PIMs), which humans do not have, in addition to the usual complement of alveolar macrophages (12, 13). These PIMs have electron-dense globular surface-coat (12). The equine PIMs have previously been shown to express TLR4 (214), which potentially may be a reason for enhanced sensitivity of the horse to lipopolysaccharide endotoxin-induced lung injury (172, 173, 214). Here, we show the presence of integrin αvβ3 in PIMs. Considering the role of this integrin in cell signalling, it is possible that the integrin αvβ3 provides another mechanism for the activation of PIMs. It is important to note that depletion of PIMs, even in a spontaneous disease such as heaves, reduces lung inflammation and clinical signs of the disease (3, 212). The PIMs play an essential role in removing circulating particles in the capillaries (25) and the immune system in the lung (92, 201). There are recent data showing induction of PIMs in rodents that normally lack PIMs, and the induced PIMs increase susceptibility of lung inflammation, which is abrogated upon their depletion (82). There is a need for studies to examine the occurrence of PIMs in humans (201). In this study, the expression of integrin αvβ3 in equine PIMs provides a mechanism for their activation. The integrin αvβ3 may play a role in the aggregation of platelets around PIMs in equine lungs, as has been reported previously in the lungs of cattle infected with *Mannheimia hemolytica* (212).

Here, we also found integrin αvβ3 on neutrophils. Some of the earlier data have shown that the integrin αvβ3 is important in the locomotion of neutrophils (14, 15, 133, 188). Moreover,

in this report, the occurrence of integrin αvβ3 on lung vascular endothelium is consistent with previous findings, and it may have a role in maintaining endothelial barrier function as demonstrated previously by Bhattacharya lab and others (149, 218, 239) as well as angiogenesis (141).

Taken together, this is the first elucidation of the cellular and subcellular expression of the integrin αvβ3 in equine lung and jejunum. Considering the role of the integrin αvβ3 in cell biology and signalling, this sets the stage for further studies to understand the expression and biology of the integrin in inflamed lungs and the intestines of the horse.

9.1.6. Acknowledgments

We thank the Saskatchewan Agriculture Development Fund (ADF), the Natural Science and Engineering Research Council (NSERC), the Graduate Student Scholarship program from the Integrated Training Program in Infectious Disease, Food Safety and Public Policy (ITraP), the Devolved Graduate Scholarship program from the Department of Veterinary Biomedical Sciences, and the Graduate Student Scholarship program from the Western College of Veterinary Medicine, the University of Saskatchewan, Canada for supporting this research. We thank LaRhonda Sobchishin for the technical support.

9.1.7. Grants

The study was funded through the Saskatchewan Agriculture Development Fund (ADF) and the Discovery Grant from the Natural Sciences and Engineering Research Council of Canada (NSERC) to Dr. Baljit Singh.

REFERENCES

1. **Abdolahad M, Janmaleki M, Taghinejad M, Taghnejad H, Salehi F, and Mohajerzadeh S**. Single-cell resolution diagnosis of cancer cells by carbon nanotube electrical spectroscopy. *Nanoscale* 5: 3421-3427, 2013.
2. **Abul K. Abbas AHL, Shiv Pillai**. *Cellular and Molecular Immunology - Chapter 4: Innate Immunity*. Elsevier, 2012.
3. **Aharonson-Raz K, Lohmann KL, Townsend HG, Marques F, and Singh B**. Pulmonary intravascular macrophages as proinflammatory cells in heaves, an asthma-like equine disease. *Am J Physiol Lung Cell Mol Physiol* 303: L189-198, 2012.
4. **Ailes E, Budge P, Shankar M, Collier S, Brinton W, Cronquist A, Chen M, Thornton A, Beach MJ, and Brunkard JM**. Economic and health impacts associated with a Salmonella Typhimurium drinking water outbreak-Alamosa, CO, 2008. *PLoS One* 8: e57439, 2013.
5. **Alghisi GC, and Ruegg C**. Vascular integrins in tumor angiogenesis: mediators and therapeutic targets. *Endothelium* 13: 113-135, 2006.
6. **Almond GW**. Research applications using pigs. *Vet Clin North Am Food Anim Pract* 12: 707-716, 1996.
7. **Anderson SL, and Singh B**. Neutrophil apoptosis is delayed in an equine model of colitis: Implications for the development of systemic inflammatory response syndrome. *Equine Vet J* 49: 383-388, 2017.
8. **Andriu A, Crockett J, Dall'Angelo S, Piras M, Zanda M, and Fleming IN**. Binding of alphavbeta3 Integrin-Specific Radiotracers Is Modulated by Both Integrin Expression Level and Activation Status. *Mol Imaging Biol* 20(1): 27-36, 2018 Feb.

9. **Annes JP, Rifkin DB, and Munger JS**. The integrin alphaVbeta6 binds and activates latent TGFbeta3. *FEBS Lett* 511: 65-68, 2002.

10. **Antonov AS, Antonova GN, Munn DH, Mivechi N, Lucas R, Catravas JD, and Verin AD**. alphaVbeta3 integrin regulates macrophage inflammatory responses via PI3 kinase/Akt-dependent NF-kappaB activation. *J Cell Physiol* 226: 469-476, 2011.

11. **Arnaout MA**. Integrin structure: new twists and turns in dynamic cell adhesion. *Immunol Rev* 186: 125-140, 2002.

12. **Atwal OS, McDonell W, Staempfli H, Singh B, and Minhas KJ**. Evidence that halothane anaesthesia induces intracellular translocation of surface coat and Golgi response in equine pulmonary intravascular macrophages. *J Submicrosc Cytol Pathol* 26: 369-386, 1994.

13. **Atwal OS, Singh B, Staempfli H, and Minhas K**. Presence of pulmonary intravascular macrophages in the equine lung: some structuro-functional properties. *Anat Rec* 234: 530-540, 1992.

14. **Aulakh GK, Balachandran Y, Liu L, and Singh B**. Angiostatin inhibits activation and migration of neutrophils. *Cell Tissue Res* 355: 375-396, 2014.

15. **Aziz M, Yang WL, Corbo LM, Chaung WW, Matsuo S, and Wang P**. MFG-E8 inhibits neutrophil migration through alphavbeta(3)-integrin-dependent MAP kinase activation. *Int J Mol Med* 36: 18-28, 2015.

16. **Bagnato GL, Irrera N, Pizzino G, Santoro D, Roberts WN, Bagnato G, Pallio G, Vaccaro M, Squadrito F, Saitta A, Altavilla D, and Bitto A**. Dual alphavbeta3 and alphavbeta5 blockade attenuates fibrotic and vascular alterations in a murine model of systemic sclerosis. *Clin Sci (Lond)* 132: 231-242, 2018.

17. **Barczyk M, Carracedo S, and Gullberg D**. Integrins. *Cell Tissue Res* 339: 269-280, 2010.

18. **Bertschinger HU, Bachmann M, Mettler C, Pospischil A, Schraner EM, Stamm M, Sydler T, and Wild P**. Adhesive fimbriae produced in vivo by Escherichia coli O139:K12(B):H1 associated with enterotoxaemia in pigs. *Vet Microbiol* 25: 267-281, 1990.

19. **Bingula R, Filaire M, Radosevic-Robin N, Berthon JY, Bernalier-Donadille A, Vasson MP, Thivat E, Kwiatkowski F, and Filaire E**. Characterisation of gut, lung, and upper airways microbiota in patients with non-small cell lung carcinoma: Study protocol for case-control observational trial. *Medicine (Baltimore)* 97: e13676, 2018.

20. **Black RE, Cousens S, Johnson HL, Lawn JE, Rudan I, Bassani DG, Jha P, Campbell H, Walker CF, Cibulskis R, Eisele T, Liu L, and Mathers C**. Global, regional, and national causes of child mortality in 2008: a systematic analysis. *Lancet* 375: 1969-1987, 2010.

21. **Blystone SD, Slater SE, Williams MP, Crow MT, and Brown EJ**. A molecular mechanism of integrin crosstalk: alphavbeta3 suppression of calcium/calmodulin-dependent protein kinase II regulates alpha5beta1 function. *J Cell Biol* 145: 889-897, 1999.

22. **Bon H, Hales P, Lumb S, Holdsworth G, Johnson T, Qureshi O, and Twomey BM**. Spontaneous Extracellular Matrix Accumulation in a Human in vitro Model of Renal Fibrosis Is Mediated by alphaV Integrins. *Nephron* 1-23, 2019.

23. **Borges E, Jan Y, and Ruoslahti E**. Platelet-derived growth factor receptor beta and vascular endothelial growth factor receptor 2 bind to the beta 3 integrin through its extracellular domain. *J Biol Chem* 275: 39867-39873, 2000.

24. **Bozzini S, Visai L, Pignatti P, Petersen TE, and Speziale P**. Multiple binding sites in fibronectin and the staphylococcal fibronectin receptor. *Eur J Biochem* 207: 327-333, 1992.

25. **Brain JD, Molina RM, DeCamp MM, and Warner AE**. Pulmonary intravascular macrophages: their contribution to the mononuclear phagocyte system in 13 species. *Am J Physiol* 276: L146-154, 1999.

26. **Brakebusch C, and Fassler R**. The integrin-actin connection, an eternal love affair. *EMBO J* 22: 2324-2333, 2003.

27. **Brilha S, Wysoczanski R, Whittington AM, Friedland JS, and Porter JC**. Monocyte Adhesion, Migration, and Extracellular Matrix Breakdown Are Regulated by Integrin alphaVbeta3 in Mycobacterium tuberculosis Infection. *J Immunol* 199: 982-991, 2017.

28. **Brooks PC, Montgomery AM, Rosenfeld M, Reisfeld RA, Hu T, Klier G, and Cheresh DA**. Integrin alpha v beta 3 antagonists promote tumor regression by inducing apoptosis of angiogenic blood vessels. *Cell* 79: 1157-1164, 1994.

29. **Campbell ID, and Humphries MJ**. Integrin structure, activation, and interactions. *Cold Spring Harb Perspect Biol* 3: 2011.

30. **Caprioli A, Nigrelli A, Gatti R, Zavanella M, Blando AM, Minelli F, and Donelli G**. Characterisation of verocytotoxin-producing Escherichia coli isolated from pigs and cattle in northern Italy. *Vet Rec* 133: 323-324, 1993.

31. **Carlton L. Gyles JFP, Glenn Songer, Charles O. Thoen**. Escherichia coli

In: *Pathogenesis of bacterial infections in animals*Wiley-Blackwell, 2010.

32. **Carlton L. Gyles JFP, Glenn Songer, Charles O. Thoen**. Themes in bacterial pathogenic mechanisms. In: *Pathogenesis of bacterial infections in animals*Wiley-Blackwell, 2010, p. 3-14.

33. **Carmeliet P**. VEGF as a key mediator of angiogenesis in cancer. *Oncology* 69 Suppl 3: 4-10, 2005.

34. **CDC**. Multistate Outbreak of Shiga toxin-producing Escherichia coli O157:H7 Infec-tions Linked to Leafy Greens. *Centers for Disease Control and Prevention* January 25, 2018.

35. **CDC**. Multistate Outbreak of Shiga toxin-producing Escherichia coli O157:H7 Infections Linked to I.M. Healthy Brand SoyNut Butter. *Centers for Disease Control and Prevention* May 4, 2017.

36. **Charbit A, Clement JM, and Hofnung M**. Further sequence analysis of the phage lambda receptor site. Possible implications for the organization of the lamB protein in Escherichia coli K12. *J Mol Biol* 175: 395-401, 1984.

37. **Che L, Xu Q, Wu C, Luo Y, Huang X, Zhang B, Auclair E, Kiros T, Fang Z, Lin Y, Xu S, Feng B, Li J, and Wu**. Effects of dietary live yeast supplementation on growth performance, diarrhoea severity, intestinal permeability and immunological parameters of weaned piglets challenged with enterotoxigenic Escherichia coli K88. *Br J Nutr* 118: 949-958, 2017.

38. **Chen X, Park R, Tohme M, Shahinian AH, Bading JR, and Conti PS**. MicroPET and autoradiographic imaging of breast cancer alpha v-integrin expression using 18F- and 64Cu-labeled RGD peptide. *Bioconjug Chem* 15: 41-49, 2004.

39. **Childs A, Hemraz UD, Castro NJ, Fenniri H, and Zhang LG**. Novel biologically-inspired rosette nanotube PLLA scaffolds for improving human mesenchymal stem cell chondrogenic differentiation. *Biomed Mater* 8: 065003, 2013.

40. **Chou HT, Wen HW, Kuo TY, Lin CC, and Chen WJ**. Interaction of cationic antimicrobial peptides with phospholipid vesicles and their antibacterial activity. *Peptides* 31: 1811-1820, 2010.

41. **Clark AF, Brotchie D, Read AT, Hellberg P, English-Wright S, Pang IH, Ethier CR, and Grierson I**. Dexamethasone alters F-actin architecture and promotes cross-linked actin network formation in human trabecular meshwork tissue. *Cell Motil Cytoskeleton* 60: 83-95, 2005.

42. **Clemmons DR, Maile LA, Ling Y, Yarber J, and Busby WH**. Role of the integrin alphaVbeta3 in mediating increased smooth muscle cell responsiveness to IGF-I in response to hyperglycemic stress. *Growth Horm IGF Res* 17: 265-270, 2007.

43. **Coddens A, Loos M, Vanrompay D, Remon JP, and Cox E**. Cranberry extract inhibits in vitro adhesion of F4 and F18(+)Escherichia coli to pig intestinal epithelium and reduces in vivo excretion of pigs orally challenged with F18(+) verotoxigenic E. coli. *Vet Microbiol* 202: 64-71, 2017.

44. **Cohen E, Dolev S, Frenkel S, Kryzhanovsky B, Palagushkin A, Rosenblit M, and Zakharov V**. Optical solver of combinatorial problems: nanotechnological approach. *J Opt Soc Am A Opt Image Sci Vis* 30: 1845-1853, 2013.

45. **Collinson SK, Doig PC, Doran JL, Clouthier S, Trust TJ, and Kay WW**. Thin, aggregative fimbriae mediate binding of Salmonella enteritidis to fibronectin. *J Bacteriol* 175: 12-18, 1993.

46. **Cota E, Jones C, Simpson P, Altroff H, Anderson KL, du Merle L, Guignot J, Servin A, Le Bouguenec C, Mardon H, and Matthews S**. The solution structure of the invasive tip complex from Afa/Dr fibrils. *Mol Microbiol* 62: 356-366, 2006.

47. **Croxen MA, Law RJ, Scholz R, Keeney KM, Wlodarska M, and Finlay BB**. Recent advances in understanding enteric pathogenic Escherichia coli. *Clin Microbiol Rev* 26: 822-880, 2013.

48. **Cuenca AG, Jiang H, Hochwald SN, Delano M, Cance WG, and Grobmyer SR**. Emerging implications of nanotechnology on cancer diagnostics and therapeutics. *Cancer* 107: 459-466, 2006.

49. **Curtis L, Burford JH, England GCW, and Freeman SL**. Risk factors for acute abdominal pain (colic) in the adult horse: A scoping review of risk factors, and a systematic review of the effect of management-related changes. *PLoS One* 14: e0219307, 2019.

50. **Cuzange A, Chroboczek J, and Jacrot B**. The penton base of human adenovirus type 3 has the RGD motif. *Gene* 146: 257-259, 1994.

51. **Danabassis MS**. The importance of the F4 receptor in post-weaned pigs in eliciting F4 specific immune responses in the intestine. In: *Department of Veterinary Microbiology*University of Saskatchewan, 2006, p. 127.

52. **De Greve H, Wyns L, and Bouckaert J**. Combining sites of bacterial fimbriae. *Curr Opin Struct Biol* 17: 506-512, 2007.

53. **Debordeaux F, Chansel-Debordeaux L, Pinaquy JB, Fernandez P, and Schulz J**. What about alphavbeta3 integrins in molecular imaging in oncology? *Nucl Med Biol* 62-63: 31-46, 2018.

54. **Dijkgraaf I, and Boerman OC**. Radionuclide imaging of tumor angiogenesis. *Cancer Biother Radiopharm* 24: 637-647, 2009.

55. **Donkuru M, Michel D, Awad H, Katselis G, and El-Aneed A**. Hydrophilic interaction liquid chromatography-tandem mass spectrometry quantitative method for the cellular analysis of varying structures of gemini surfactants designed as nanomaterial drug carriers. *J Chromatogr A* 1446: 114-124, 2016.

56. **Donnenberg MS, Tzipori S, McKee ML, O'Brien AD, Alroy J, and Kaper JB**. The role of the eae gene of enterohemorrhagic Escherichia coli in intimate attachment in vitro and in a porcine model. *J Clin Invest* 92: 1418-1424, 1993.

57. **Duong LT, and Rodan GA**. Integrin-mediated signaling in the regulation of osteoclast adhesion and activation. *Front Biosci* 3: d757-768, 1998.

58. **Elgavish A, Pattanaik A, Lloyd K, and Reed R**. Integrin-mediated adhesive properties of uroepithelial cells are inhibited by treatment with bacterial toxins. *Am J Physiol* 266: C1552-1559, 1994.

59. **Ernsberger U, Edgar D, and Rohrer H**. The survival of early chick sympathetic neurons in vitro is dependent on a suitable substrate but independent of NGF. *Dev Biol* 135: 250-262, 1989.

60. **Esmaeili Dooki MR, Rajabnia R, Barari Sawadkohi R, Mosaiebnia Gatabi Z, Poornasrollah M, and Mirzapour M**. Bacterial entropathogens and antimicrobial susceptibility in children with acute diarrhea in Babol, Iran. *Caspian J Intern Med* 5: 30-34, 2014.

61. **Fairbrother JM, Nadeau E, and Gyles CL**. Escherichia coli in postweaning diarrhea in pigs: an update on bacterial types, pathogenesis, and prevention strategies. *Anim Health Res Rev* 6: 17-39, 2005.

62. **Faralli JA, Filla MS, and Peters DM**. Effect of alphavbeta3 Integrin Expression and Activity on Intraocular Pressure. *Invest Ophthalmol Vis Sci* 60: 1776-1788, 2019.

63. **Fenniri H, Deng BL, and Ribbe AE**. Helical rosette nanotubes with tunable chiroptical properties. *J Am Chem Soc* 124: 11064-11072, 2002.

64. **Fenniri H, Mathivanan P, Vidale KL, Sherman DM, Hallenga K, Wood KV, and Stowell JG**. Helical rosette nanotubes: design, self-assembly, and characterization. *J Am Chem Soc* 123: 3854-3855, 2001.

65. **Francis DH, Erickson AK, and Grange PA**. K88 adhesins of enterotoxigenic Escherichia coli and their porcine enterocyte receptors. *Adv Exp Med Biol* 473: 147-154, 1999.

66. **Franke S, Harmsen D, Caprioli A, Pierard D, Wieler LH, and Karch H**. Clonal relatedness of Shiga-like toxin-producing Escherichia coli O101 strains of human and porcine origin. *J Clin Microbiol* 33: 3174-3178, 1995.

67. **Franke TF, Kaplan DR, and Cantley LC**. PI3K: downstream AKTion blocks apoptosis. *Cell* 88: 435-437, 1997.

68. **Friggeri A, Yang Y, Banerjee S, Park YJ, Liu G, and Abraham E**. HMGB1 inhibits macrophage activity in efferocytosis through binding to the alphavbeta3-integrin. *Am J Physiol Cell Physiol* 299: C1267-1276, 2010.

69. **Frydendahl K**. Prevalence of serogroups and virulence genes in Escherichia coli associated with postweaning diarrhoea and edema disease in pigs and a comparison of diagnostic approaches. *Vet Microbiol* 85: 169-182, 2002.

70. **Gaastra W, and de Graaf FK**. Host-specific fimbrial adhesins of noninvasive enterotoxigenic Escherichia coli strains. *Microbiol Rev* 46: 129-161, 1982.

71. **Gagen D, Filla MS, Clark R, Liton P, and Peters DM**. Activated alphavbeta3 integrin regulates alphavbeta5 integrin-mediated phagocytosis in trabecular meshwork cells. *Invest Ophthalmol Vis Sci* 54: 5000-5011, 2013.

72. **Garas LC, Cooper CA, Dawson MW, Wang JL, Murray JD, and Maga EA**. Young Pigs Consuming Lysozyme Transgenic Goat Milk Are Protected from Clinical Symptoms of Enterotoxigenic Escherichia coli Infection. *J Nutr* 147: 2050-2059, 2017.

73. **Garciarena CD, McHale TM, Martin-Loeches I, and Kerrigan SW**. Pre-emptive and therapeutic value of blocking bacterial attachment to the endothelial alphaVbeta3 integrin with cilengitide in sepsis. *Crit Care* 21: 246, 2017.

74. **Garthright WE, Archer DL, and Kvenberg JE**. Estimates of incidence and costs of intestinal infectious diseases in the United States. *Public Health Rep* 103: 107-115, 1988.

75. **Gavrilovskaya IN, Brown EJ, Ginsberg MH, and Mackow ER**. Cellular entry of hantaviruses which cause hemorrhagic fever with renal syndrome is mediated by beta3 integrins. *J Virol* 73: 3951-3959, 1999.

76. **Gavrilovskaya IN, Peresleni T, Geimonen E, and Mackow ER**. Pathogenic hantaviruses selectively inhibit beta3 integrin directed endothelial cell migration. *Arch Virol* 147: 1913-1931, 2002.

77. **Gavrilovskaya IN, Shepley M, Shaw R, Ginsberg MH, and Mackow ER**. beta3 Integrins mediate the cellular entry of hantaviruses that cause respiratory failure. *Proc Natl Acad Sci U S A* 95: 7074-7079, 1998.

78. **Gerdts V, Uwiera RR, Mutwiri GK, Wilson DJ, Bowersock T, Kidane A, Babiuk LA, and Griebel PJ**. Multiple intestinal 'loops' provide an in vivo model to analyse multiple mucosal immune responses. *J Immunol Methods* 256: 19-33, 2001.

79. **Gerdts V, Wilson HL, Meurens F, van Drunen Littel-van den Hurk S, Wilson D, Walker S, Wheler C, Townsend H, and Potter AA**. Large animal models for vaccine development and testing. *ILAR J* 56: 53-62, 2015.

80. **Gerthoffer WT, and Gunst SJ**. Invited review: focal adhesion and small heat shock proteins in the regulation of actin remodeling and contractility in smooth muscle. *J Appl Physiol (1985)* 91: 963-972, 2001.

81. **Gianni T, and Campadelli-Fiume G**. alphaVbeta3-integrin relocalizes nectin1 and routes herpes simplex virus to lipid rafts. *J Virol* 86: 2850-2855, 2012.

82. **Gill SS, Suri SS, Janardhan KS, Caldwell S, Duke T, and Singh B**. Role of pulmonary intravascular macrophages in endotoxin-induced lung inflammation and mortality in a rat model. *Respir Res* 9: 69, 2008.

83. **Gomes ED, Mendes SS, Leite-Almeida H, Gimble JM, Tam RY, Shoichet MS, Sousa N, Silva NA, and Salgado AJ**. Combination of a peptide-modified gellan gum hydrogel with cell therapy in a lumbar spinal cord injury animal model. *Biomaterials* 105: 38-51, 2016.

84. **Gonzalez-Ortiz G, Hermes RG, Jimenez-Diaz R, Perez JF, and Martin-Orue SM**. Screening of extracts from natural feed ingredients for their ability to reduce enterotoxigenic Escherichia coli (ETEC) K88 adhesion to porcine intestinal epithelial cell-line IPEC-J2. *Vet Microbiol* 167: 494-499, 2013.

85. **Gonzalez-Vallina R, Wang H, Zhan R, Berschneider HM, Lee RM, Davidson NO, and Black DD**. Lipoprotein and apolipoprotein secretion by a newborn piglet intestinal cell line (IPEC-1). *Am J Physiol* 271: G249-259, 1996.

86. **Gonzalez AM, Bhattacharya R, deHart GW, and Jones JC**. Transdominant regulation of integrin function: mechanisms of crosstalk. *Cell Signal* 22: 578-583, 2010.

87. **Gonzalez AM, Gonzales M, Herron GS, Nagavarapu U, Hopkinson SB, Tsuruta D, and Jones JC**. Complex interactions between the laminin alpha 4 subunit and integrins regulate endothelial cell behavior in vitro and angiogenesis in vivo. *Proc Natl Acad Sci U S A* 99: 16075-16080, 2002.

88. **Guerrero CA, Mendez E, Zarate S, Isa P, Lopez S, and Arias CF**. Integrin alpha(v)beta(3) mediates rotavirus cell entry. *Proc Natl Acad Sci U S A* 97: 14644-14649, 2000.

89. **Hall ER, Bibby LI, and Slack RJ**. Characterisation of a novel, high affinity and selective alphavbeta6 integrin RGD-mimetic radioligand. *Biochem Pharmacol* 117: 88-96, 2016.

90. **Hamidi H, and Ivaska J**. Every step of the way: integrins in cancer progression and metastasis. *Nat Rev Cancer* 18: 533-548, 2018.

91. **Harburger DS, and Calderwood DA**. Integrin signalling at a glance. *J Cell Sci* 122: 159-163, 2009.

92. **Harrison JM, Quanstrom LM, Robinson AR, Wobeser B, Anderson SL, and Singh B**. Expression of von Willebrand factor, pulmonary intravascular macrophages, and Toll-like receptors in lungs of septic foals. *J Vet Sci* 18: 17-23, 2017.

93. **Hayashida T**. Integrins modulate cellular fibrogenesis at multiple levels; Regulation of TGF-beta signaling. *Endocr Metab Immune Disord Drug Targets* 10: 302-319, 2010.

94. **Henderson NC, Arnold TD, Katamura Y, Giacomini MM, Rodriguez JD, McCarty JH, Pellicoro A, Raschperger E, Betsholtz C, Ruminski PG, Griggs DW, Prinsen MJ, Maher JJ, Iredale JP, Lacy-Hulbert A, Adams RH, and Sheppard D**. Targeting of alphav integrin identifies a core molecular pathway that regulates fibrosis in several organs. *Nat Med* 19: 1617-1624, 2013.

95. **Henson SJ, Majowicz SE, Masakure O, Sockett PN, MacDougall L, Edge VL, Thomas MK, Fyfe M, Kovacs SJ, and Jones AQ**. Estimation of the costs of acute gastrointestinal illness in British Columbia, Canada. *Int J Food Microbiol* 127: 43-52, 2008.

96. **Hong SS, Gay B, Karayan L, Dabauvalle MC, and Boulanger P**. Cellular uptake and nuclear delivery of recombinant adenovirus penton base. *Virology* 262: 163-177, 1999.

97. **Horan GS, Wood S, Ona V, Li DJ, Lukashev ME, Weinreb PH, Simon KJ, Hahm K, Allaire NE, Rinaldi NJ, Goyal J, Feghali-Bostwick CA, Matteson EL, O'Hara C, Lafyatis R, Davis GS, Huang X, Sheppard D, and Violette SM**. Partial inhibition of integrin alpha(v)beta6 prevents pulmonary fibrosis without exacerbating inflammation. *Am J Respir Crit Care Med* 177: 56-65, 2008.

98. **Horton MA**. The alpha v beta 3 integrin "vitronectin receptor". *Int J Biochem Cell Biol* 29: 721-725, 1997.

99. **House JN**. RGDSK-functionalized helical rosette nanotube interactions with integrin αvβ3 – expressing biological milieus. In: *Toxicology Centre*University of Saskatchewan, 2016.

100. **Humphries JD, Byron A, and Humphries MJ**. Integrin ligands at a glance. *J Cell Sci* 119: 3901-3903, 2006.

101. **Hutchinson JH, Halczenko W, Brashear KM, Breslin MJ, Coleman PJ, Duong LT, Fernandez-Metzler C, Gentile MA, Fisher JE, Hartman GD, Huff JR, Kimmel DB, Leu CT, Meissner RS, Merkle K, Nagy R, Pennypacker B, Perkins JJ, Prueksaritanont T, Rodan GA, Varga SL, Wesolowski GA, Zartman AE, Rodan SB, and Duggan ME**. Nonpeptide alphavbeta3 antagonists. 8. In vitro and in vivo evaluation of a potent alphavbeta3 antagonist for the prevention and treatment of osteoporosis. *J Med Chem* 46: 4790-4798, 2003.

102. **Hynes RO**. Integrins: a family of cell surface receptors. *Cell* 48: 549-554, 1987.

103. **Hynes RO**. Integrins: bidirectional, allosteric signaling machines. *Cell* 110: 673-687, 2002.

104. **Isberg RR, and Leong JM**. Multiple beta 1 chain integrins are receptors for invasin, a protein that promotes bacterial penetration into mammalian cells. *Cell* 60: 861-871, 1990.

105. **Janardhan KS, Appleyard GD, and Singh B**. Expression of integrin subunits alphav and beta3 in acute lung inflammation. *Histochem Cell Biol* 121: 383-390, 2004.

106. **Jin LZ, and Zhao X**. Intestinal receptors for adhesive fimbriae of enterotoxigenic Escherichia coli (ETEC) K88 in swine--a review. *Appl Microbiol Biotechnol* 54: 311-318, 2000.

107. **Johnson GA, Burghardt RC, and Bazer FW**. Osteopontin: a leading candidate adhesion molecule for implantation in pigs and sheep. *J Anim Sci Biotechnol* 5: 56, 2014.

108. **Johnson L, Montgomery JB, Schneider JP, Townsend HG, Ochs M, and Singh B**. Morphometric examination of the equine adult and foal lung. *Anat Rec (Hoboken)* 297: 1950-1962, 2014.

109. **Journeay WS, Suri SS, Fenniri H, and Singh B**. High-aspect ratio nanoparticles in nanotoxicology. *Integr Environ Assess Manag* 4: 128-129, 2008.

110. **Journeay WS, Suri SS, Moralez JG, Fenniri H, and Singh B**. Low inflammatory activation by self-assembling Rosette nanotubes in human Calu-3 pulmonary epithelial cells. *Small* 4: 817-823, 2008.

111. **Journeay WS, Suri SS, Moralez JG, Fenniri H, and Singh B**. Macrophage inflammatory response to self-assembling rosette nanotubes. *Small* 5: 1446-1452, 2009.

112. **Journeay WS, Suri SS, Moralez JG, Fenniri H, and Singh B**. Rosette nanotubes show low acute pulmonary toxicity in vivo. *Int J Nanomedicine* 3: 373-383, 2008.

113. **Juliano RL, and Varner JA**. Adhesion molecules in cancer: the role of integrins. *Curr Opin Cell Biol* 5: 812-818, 1993.

114. **Kalcheim C, Barde YA, Thoenen H, and Le Douarin NM**. In vivo effect of brain-derived neurotrophic factor on the survival of developing dorsal root ganglion cells. *EMBO J* 6: 2871-2873, 1987.

115. **Kaper JB, Nataro JP, and Mobley HL**. Pathogenic Escherichia coli. *Nat Rev Microbiol* 2: 123-140, 2004.

116. **Kaser T, Pasternak JA, Delgado-Ortega M, Hamonic G, Lai K, Erickson J, Walker S, Dillon JR, Gerdts V, and Meurens F**. Chlamydia suis and Chlamydia trachomatis induce multifunctional CD4 T cells in pigs. *Vaccine* 35: 91-100, 2017.

117. **Kaser T, Renois F, Wilson HL, Cnudde T, Gerdts V, Dillon JR, Jungersen G, Agerholm JS, and Meurens F**. Contribution of the swine model in the study of human sexually transmitted infections. *Infect Genet Evol* 66: 346-360, 2018.

118. **Katsumoto TR, Violette SM, and Sheppard D**. Blocking TGFbeta via Inhibition of the alphavbeta6 Integrin: A Possible Therapy for Systemic Sclerosis Interstitial Lung Disease. *Int J Rheumatol* 2011: 208219, 2011.

119. **Khan SB, Zou G, Xiao R, Cheng Y, Rehman ZU, Ali S, Memon AM, Fahad S, Ahmad I, and Zhou R**. Prevalence, quantification and isolation of pathogenic shiga toxin Escherichia coli O157:H7 along the production and supply chain of pork around Hubei Province of China. *Microb Pathog* 115: 93-99, 2018.

120. **Kiessling F, Huppert J, Zhang C, Jayapaul J, Zwick S, Woenne EC, Mueller MM, Zentgraf H, Eisenhut M, Addadi Y, Neeman M, and Semmler W**. RGD-labeled USPIO inhibits adhesion and endocytotic activity of alpha v beta3-integrin-expressing glioma cells and only accumulates in the vascular tumor compartment. *Radiology* 253: 462-469, 2009.

121. **Kim C, Ye F, and Ginsberg MH**. Regulation of integrin activation. *Annu Rev Cell Dev Biol* 27: 321-345, 2011.

122. **Kim KK, Kugler MC, Wolters PJ, Robillard L, Galvez MG, Brumwell AN, Sheppard D, and Chapman HA**. Alveolar epithelial cell mesenchymal transition develops in vivo during pulmonary fibrosis and is regulated by the extracellular matrix. *Proc Natl Acad Sci U S A* 103: 13180-13185, 2006.

123. **Kim M, Ogawa M, Fujita Y, Yoshikawa Y, Nagai T, Koyama T, Nagai S, Lange A, Fassler R, and Sasakawa C**. Bacteria hijack integrin-linked kinase to stabilize focal adhesions and block cell detachment. *Nature* 459: 578-582, 2009.

124. **Klemm P, and Schembri MA**. Bacterial adhesins: function and structure. *Int J Med Microbiol* 290: 27-35, 2000.

125. **Kobayashi M, Sawada K, and Kimura T**. Potential of Integrin Inhibitors for Treating Ovarian Cancer: A Literature Review. *Cancers (Basel)* 9: 2017.

126. **Koh SY, George S, Brozel V, Moxley R, Francis D, and Kaushik RS**. Porcine intestinal epithelial cell lines as a new in vitro model for studying adherence and pathogenesis of enterotoxigenic Escherichia coli. *Vet Microbiol* 130: 191-197, 2008.

127. **Kukkonen M, Saarela S, Lahteenmaki K, Hynonen U, Westerlund-Wikstrom B, Rhen M, and Korhonen TK**. Identification of two laminin-binding fimbriae, the type 1 fimbria of Salmonella enterica serovar typhimurium and the G fimbria of Escherichia coli, as plasminogen receptors. *Infect Immun* 66: 4965-4970, 1998.

128. **Kuusela P, Vartio T, Vuento M, and Myhre EB**. Attachment of staphylococci and streptococci on fibronectin, fibronectin fragments, and fibrinogen bound to a solid phase. *Infect Immun* 50: 77-81, 1985.

129. **Kwakwa KA, and Sterling JA**. Integrin alphavbeta3 Signaling in Tumor-Induced Bone Disease. *Cancers (Basel)* 9: 2017.

130. **Laarmann S, and Schmidt MA**. The Escherichia coli AIDA autotransporter adhesin recognizes an integral membrane glycoprotein as receptor. *Microbiology* 149: 1871-1882, 2003.

131. **Lanone S, and Boczkowski J**. Biomedical applications and potential health risks of nanomaterials: molecular mechanisms. *Curr Mol Med* 6: 651-663, 2006.

132. **Laroui H, Rakhya P, Xiao B, Viennois E, and Merlin D**. Nanotechnology in diagnostics and therapeutics for gastrointestinal disorders. *Dig Liver Dis* 45: 995-1002, 2013.

133. **Lawson MA, and Maxfield FR**. Ca(2+)- and calcineurin-dependent recycling of an integrin to the front of migrating neutrophils. *Nature* 377: 75-79, 1995.

134. **Le MH, Suri SS, Rakotondradany F, Fenniri H, and Singh B**. Rosette nanotubes inhibit bovine neutrophil chemotaxis. *Vet Res* 41: 75, 2010.

135. **Leask A**. Scar wars: is TGFbeta the phantom menace in scleroderma? *Arthritis Res Ther* 8: 213, 2006.

136. **Lee KE, Lim SI, Shin SH, Kwon YK, Kim HY, Song JY, and An DJ**. Distribution of Clostridium perfringens Isolates from Piglets in South Korea. *J Vet Med Sci* 2014.

137. **Legate KR, and Fassler R**. Mechanisms that regulate adaptor binding to beta-integrin cytoplasmic tails. *J Cell Sci* 122: 187-198, 2009.

138. **Li C, Su M, Yin B, Guo D, Wei S, Kong F, Feng L, Wu R, and Sun D**. Integrin alphavbeta3 enhances replication of porcine epidemic diarrhea virus on Vero E6 and porcine intestinal epithelial cells. *Vet Microbiol* 237: 108400, 2019.

139. **Li HH, Li YP, Zhu Q, Qiao JY, and Wang WJ**. Dietary supplementation with Clostridium butyricum helps to improve the intestinal barrier function of weaned piglets challenged with enterotoxigenic Escherichia coli K88. *J Appl Microbiol* 125: 964-975, 2018.

140. **Li XV, Leonardi I, and Iliev ID**. Gut Mycobiota in Immunity and Inflammatory Disease. *Immunity* 50: 1365-1379, 2019.

141. **Liao Z, Kasirer-Friede A, and Shattil SJ**. Optogenetic interrogation of integrin alphaVbeta3 function in endothelial cells. *J Cell Sci* 130: 3532-3541, 2017.

142. **Liu C, Xie X, Zhao W, Liu N, Maraccini PA, Sassoubre LM, Boehm AB, and Cui Y**. Conducting nanosponge electroporation for affordable and high-efficiency disinfection of bacteria and viruses in water. *Nano Lett* 13: 4288-4293, 2013.

143. **Louie M, de Azavedo J, Clarke R, Borczyk A, Lior H, Richter M, and Brunton J**. Sequence heterogeneity of the eae gene and detection of verotoxin-producing Escherichia coli using serotype-specific primers. *Epidemiol Infect* 112: 449-461, 1994.

144. **Ly DP, Zazzali KM, and Corbett SA**. De novo expression of the integrin alpha5beta1 regulates alphavbeta3-mediated adhesion and migration on fibrinogen. *J Biol Chem* 278: 21878-21885, 2003.

145. **Ma LJ, Yang H, Gaspert A, Carlesso G, Barty MM, Davidson JM, Sheppard D, and Fogo AB**. Transforming growth factor-beta-dependent and -independent pathways of induction of tubulointerstitial fibrosis in beta6(-/-) mice. *Am J Pathol* 163: 1261-1273, 2003.

146. **Maschirow L, Suttorp N, and Opitz B**. Microbiota-Dependent Regulation of Antimicrobial Immunity in the Lung. *Am J Respir Cell Mol Biol* 61: 284-289, 2019.

147. **Matthys VS, Gorbunova EE, Gavrilovskaya IN, and Mackow ER**. Andes virus recognition of human and Syrian hamster beta3 integrins is determined by an L33P substitution in the PSI domain. *J Virol* 84: 352-360, 2010.

148. **McCarthy RA, and Hay ED**. Collagen I, laminin, and tenascin: ultrastructure and correlation with avian neural crest formation. *Int J Dev Biol* 35: 437-452, 1991.

149. **McDonnell CJ, Garciarena CD, Watkin RL, McHale TM, McLoughlin A, Claes J, Verhamme P, Cummins PM, and Kerrigan SW**. Inhibition of major integrin alphaVbeta3 reduces Staphylococcus aureus attachment to sheared human endothelial cells. *J Thromb Haemost* 2016.

150. **McKee TJ, Perlman G, Morris M, and Komarova SV**. Extracellular matrix composition of connective tissues: a systematic review and meta-analysis. *Sci Rep* 9: 10542, 2019.

151. **Meredith JE, Jr., Fazeli B, and Schwartz MA**. The extracellular matrix as a cell survival factor. *Mol Biol Cell* 4: 953-961, 1993.

152. **Meredith JE, Jr., and Schwartz MA**. Integrins, adhesion and apoptosis. *Trends Cell Biol* 7: 146-150, 1997.

153. **Meurens F, Berri M, Auray G, Melo S, Levast B, Virlogeux-Payant I, Chevaleyre C, Gerdts V, and Salmon H**. Early immune response following Salmonella enterica subspecies enterica serovar Typhimurium infection in porcine jejunal gut loops. *Vet Res* 40: 5, 2009.

154. **Meurens F, Summerfield A, Nauwynck H, Saif L, and Gerdts V**. The pig: a model for human infectious diseases. *Trends Microbiol* 20: 50-57, 2012.

155. **Meyer A, Auernheimer J, Modlinger A, and Kessler H**. Targeting RGD recognizing integrins: drug development, biomaterial research, tumor imaging and targeting. *Curr Pharm Des* 12: 2723-2747, 2006.

156. **Mochizuki S, and Okada Y**. ADAMs in cancer cell proliferation and progression. *Cancer Sci* 98: 621-628, 2007.

157. **Moeser AJ, and Blikslager AT**. Mechanisms of porcine diarrheal disease. *J Am Vet Med Assoc* 231: 56-67, 2007.

158. **Monroe S, and Polk R**. Antimicrobial use and bacterial resistance. *Curr Opin Microbiol* 3: 496-501, 2000.

159. **Morozevich GE, Kozlova NI, Chubukina AN, and Berman AE**. Role of integrin alphavbeta3 in substrate-dependent apoptosis of human intestinal carcinoma cells. *Biochemistry (Mosc)* 68: 416-423, 2003.

160. **Mowat AM, Scott CL, and Bain CC**. Barrier-tissue macrophages: functional adaptation to environmental challenges. *Nat Med* 23: 1258-1270, 2017.

161. **Muller A, Baumann A, Essbauer S, Radosa L, Kruger DH, Witkowski PT, Zeier M, and Krautkramer E**. Analysis of the integrin beta3 receptor for pathogenic orthohantaviruses in rodent host species. *Virus Res* 2019.

162. **Munger JS, Huang X, Kawakatsu H, Griffiths MJ, Dalton SL, Wu J, Pittet JF, Kaminski N, Garat C, Matthay MA, Rifkin DB, and Sheppard D**. The integrin alpha v beta 6 binds and activates latent TGF beta 1: a mechanism for regulating pulmonary inflammation and fibrosis. *Cell* 96: 319-328, 1999.

163. **Mutwiri G, Bowersock T, Kidane A, Sanchez M, Gerdts V, Babiuk LA, and Griebel P**. Induction of mucosal immune responses following enteric immunization with antigen delivered in alginate microspheres. *Vet Immunol Immunopathol* 87: 269-276, 2002.

164. **Neff S, Sa-Carvalho D, Rieder E, Mason PW, Blystone SD, Brown EJ, and Baxt B**. Foot-and-mouth disease virus virulent for cattle utilizes the integrin alpha(v)beta3 as its receptor. *J Virol* 72: 3587-3594, 1998.

165. **Niewold TA, Kerstens HH, van der Meulen J, Smits MA, and Hulst MM**. Development of a porcine small intestinal cDNA micro-array: characterization and functional analysis of the response to enterotoxigenic E. coli. *Vet Immunol Immunopathol* 105: 317-329, 2005.

166. **Oberhammer FA, Pavelka M, Sharma S, Tiefenbacher R, Purchio AF, Bursch W, and Schulte-Hermann R**. Induction of apoptosis in cultured hepatocytes and in regressing liver by transforming growth factor beta 1. *Proc Natl Acad Sci U S A* 89: 5408-5412, 1992.

167. **Okada Y, Copeland BR, Hamann GF, Koziol JA, Cheresh DA, and del Zoppo GJ**. Integrin alphavbeta3 is expressed in selected microvessels after focal cerebral ischemia. *Am J Pathol* 149: 37-44, 1996.

168. **Olsen A, Arnqvist A, Hammar M, Sukupolvi S, and Normark S**. The RpoS sigma factor relieves H-NS-mediated transcriptional repression of csgA, the subunit gene of fibronectin-binding curli in Escherichia coli. *Mol Microbiol* 7: 523-536, 1993.

169. **Orr AW, Ginsberg MH, Shattil SJ, Deckmyn H, and Schwartz MA**. Matrix-specific suppression of integrin activation in shear stress signaling. *Mol Biol Cell* 17: 4686-4697, 2006.

170. **Ozaki I, Hamajima H, Matsuhashi S, and Mizuta T**. Regulation of TGF-beta1-Induced Pro-Apoptotic Signaling by Growth Factor Receptors and Extracellular Matrix Receptor Integrins in the Liver. *Front Physiol* 2: 78, 2011.

171. **Panchatcharam M, Miriyala S, Yang F, Leitges M, Chrzanowska-Wodnicka M, Quilliam LA, Anaya P, Morris AJ, and Smyth SS**. Enhanced proliferation and migration of vascular smooth muscle cells in response to vascular injury under hyperglycemic conditions is controlled by beta3 integrin signaling. *Int J Biochem Cell Biol* 42: 965-974, 2010.

172. **Parbhakar OP, Duke T, Townsend HG, and Singh B**. Depletion of pulmonary intravascular macrophages partially inhibits lipopolysaccharide-induced lung inflammation in horses. *Vet Res* 36: 557-569, 2005.

173. **Parbhakar OP, Duke T, Townsend HG, and Singh B**. Immunophenotypic characterization and depletion of pulmonary intravascular macrophages of horses. *Vet Res* 35: 39-51, 2004.

174. **Parry C, Bell S, Minson T, and Browne H**. Herpes simplex virus type 1 glycoprotein H binds to alphavbeta3 integrins. *J Gen Virol* 86: 7-10, 2005.

175. **Pearce JW, Janardhan KS, Caldwell S, and Singh B**. Angiostatin and integrin alphavbeta3 in the feline, bovine, canine, equine, porcine and murine retina and cornea. *Vet Ophthalmol* 10: 313-319, 2007.

176. **Perez-Lopez A, Behnsen J, Nuccio SP, and Raffatellu M**. Mucosal immunity to pathogenic intestinal bacteria. *Nat Rev Immunol* 16: 135-148, 2016.

177. **Pesavento JB, Crawford SE, Roberts E, Estes MK, and Prasad BV**. pH-induced conformational change of the rotavirus VP4 spike: implications for cell entry and antibody neutralization. *J Virol* 79: 8572-8580, 2005.

178. **Piersanti S, Cherubini G, Martina Y, Salone B, Avitabile D, Grosso F, Cundari E, Di Zenzo G, and Saggio I**. Mammalian cell transduction and internalization properties of lambda phages displaying the full-length adenoviral penton base or its central domain. *J Mol Med (Berl)* 82: 467-476, 2004.

179. **Plow EF, Haas TA, Zhang L, Loftus J, and Smith JW**. Ligand binding to integrins. *J Biol Chem* 275: 21785-21788, 2000.

180. **Poltorak A, He X, Smirnova I, Liu MY, Van Huffel C, Du X, Birdwell D, Alejos E, Silva M, Galanos C, Freudenberg M, Ricciardi-Castagnoli P, Layton B, and Beutler B**. Defective LPS signaling in C3H/HeJ and C57BL/10ScCr mice: mutations in Tlr4 gene. *Science* 282: 2085-2088, 1998.

181. **Poole S, Firtel RA, Lamar E, and Rowekamp W**. Sequence and expression of the discoidin I gene family in Dictyostelium discoideum. *J Mol Biol* 153: 273-289, 1981.

182. **Pottratz ST, and Martin WJ, 2nd**. Mechanism of Pneumocystis carinii attachment to cultured rat alveolar macrophages. *J Clin Invest* 86: 1678-1683, 1990.

183. **Pusterla N, Vin R, Leutenegger CM, Mittel LD, and Divers TJ**. Enteric coronavirus infection in adult horses. *Vet J* 231: 13-18, 2018.

184. **Pytela R, Pierschbacher MD, and Ruoslahti E**. A 125/115-kDa cell surface receptor specific for vitronectin interacts with the arginine-glycine-aspartic acid adhesion sequence derived from fibronectin. *Proc Natl Acad Sci U S A* 82: 5766-5770, 1985.

185. **Qadri F, Svennerholm AM, Faruque AS, and Sack RB**. Enterotoxigenic Escherichia coli in developing countries: epidemiology, microbiology, clinical features, treatment, and prevention. *Clin Microbiol Rev* 18: 465-483, 2005.

186. **Qiu S, Wang Y, Xu X, Li P, Hao R, Yang C, Liu N, Li Z, Wang Z, Wang J, Wu Z, Su W, Yang G, Jin H, Wang L, Sun Y, Yuan Z, Huang L, and Song H**. Multidrug-resistant atypical variants of Shigella flexneri in China. *Emerg Infect Dis* 19: 1147-1150, 2013.

187. **Raab-Westphal S, Marshall JF, and Goodman SL**. Integrins as Therapeutic Targets: Successes and Cancers. *Cancers (Basel)* 9: 2017.

188. **Rainger GE, Buckley CD, Simmons DL, and Nash GB**. Neutrophils sense flow-generated stress and direct their migration through alphaVbeta3-integrin. *Am J Physiol* 276: H858-864, 1999.

189. **Ratliff TL, Palmer JO, McGarr JA, and Brown EJ**. Intravesical Bacillus Calmette-Guerin therapy for murine bladder tumors: initiation of the response by fibronectin-mediated attachment of Bacillus Calmette-Guerin. *Cancer Res* 47: 1762-1766, 1987.

190. **Reynolds LE, Wyder L, Lively JC, Taverna D, Robinson SD, Huang X, Sheppard D, Hynes RO, and Hodivala-Dilke KM**. Enhanced pathological angiogenesis in mice lacking beta3 integrin or beta3 and beta5 integrins. *Nat Med* 8: 27-34, 2002.

191. **Ristow LC, Tran V, Schwartz KJ, Pankratz L, Mehle A, Sauer JD, and Welch RA**. The Extracellular Domain of the beta2 Integrin beta Subunit (CD18) Is Sufficient for Escherichia coli Hemolysin and Aggregatibacter actinomycetemcomitans Leukotoxin Cytotoxic Activity. *MBio* 10: 2019.

192. **Robinson NE, Karmaus W, Holcombe SJ, Carr EA, and Derksen FJ**. Airway inflammation in Michigan pleasure horses: prevalence and risk factors. *Equine Vet J* 38: 293-299, 2006.

193. **Rocha LA, Learmonth DA, Sousa RA, and Salgado AJ**. alphavbeta3 and alpha5beta1 integrin-specific ligands: From tumor angiogenesis inhibitors to vascularization promoters in regenerative medicine? *Biotechnol Adv* 36: 208-227, 2018.

194. **Rognoni E, Ruppert R, and Fassler R**. The kindlin family: functions, signaling properties and implications for human disease. *J Cell Sci* 129: 17-27, 2016.

195. **Rothkotter HJ, Sowa E, and Pabst R**. The pig as a model of developmental immunology. *Hum Exp Toxicol* 21: 533-536, 2002.

196. **Ruoslahti E**. RGD and other recognition sequences for integrins. *Annu Rev Cell Dev Biol* 12: 697-715, 1996.

197. **Rutter JM, Burrows MR, Sellwood R, and Gibbons RA**. A genetic basis for resistance to enteric disease caused by E. coli. *Nature* 257: 135-136, 1975.

198. **Sambrook J, MacCallum P, and Russell D**. *Molecular cloning: a laboratory manual*. Cold Spring Harbor Laboratory Press: Cold Spring Harbor, USA, 2001.

199. **Santulli G, Basilicata MF, De Simone M, Del Giudice C, Anastasio A, Sorriento D, Saviano M, Del Gatto A, Trimarco B, Pedone C, Zaccaro L, and Iaccarino G**. Evaluation of the anti-angiogenic properties of the new selective alphaVbeta3 integrin antagonist RGDechiHCit. *J Transl Med* 9: 7, 2011.

200. **Sartori A, Corno C, De Cesare M, Scanziani E, Minoli L, Battistini L, Zanardi F, and Perego P**. Efficacy of a Selective Binder of alphaVbeta3 Integrin Linked to the Tyrosine Kinase Inhibitor Sunitinib in Ovarian Carcinoma Preclinical Models. *Cancers (Basel)* 11: 2019.

201. **Schneberger D, Aharonson-Raz K, and Singh B**. Pulmonary intravascular macrophages and lung health: what are we missing? *Am J Physiol Lung Cell Mol Physiol* 302: L498-503, 2012.

202. **Schneller M, Vuori K, and Ruoslahti E**. Alphavbeta3 integrin associates with activated insulin and PDGFbeta receptors and potentiates the biological activity of PDGF. *EMBO J* 16: 5600-5607, 1997.

203. **Schroeckh V, Hortschansky P, Fricke S, Luckenbach GA, and Riesenberg D**. Expression of soluble, recombinant alphavbeta3 integrin fragments in Escherichia coli. *Microbiol Res* 155: 165-177, 2000.

204. **Sears CL, and Kaper JB**. Enteric bacterial toxins: mechanisms of action and linkage to intestinal secretion. *Microbiol Rev* 60: 167-215, 1996.

205. **Seipel D, Oliveira BC, Resende TL, Schuindt SH, Pimentel PM, Kanashiro MM, and Arnholdt AC**. Toxoplasma gondii infection positively modulates the macrophages migratory molecular complex by increasing matrix metalloproteinases, CD44 and alpha v beta 3 integrin. *Vet Parasitol* 169: 312-319, 2010.

206. **Shahriar F, Ngeleka M, Gordon JR, and Simko E**. Identification by mass spectroscopy of F4ac-fimbrial-binding proteins in porcine milk and characterization of lactadherin as an inhibitor of F4ac-positive Escherichia coli attachment to intestinal villi in vitro. *Dev Comp Immunol* 30: 723-734, 2006.

207. **Shu Y, Shu D, Haque F, and Guo P**. Fabrication of pRNA nanoparticles to deliver therapeutic RNAs and bioactive compounds into tumor cells. *Nat Protoc* 8: 1635-1659, 2013.

208. **Silveira H, Amaral LGM, Garbossa CAP, Rodrigues LM, Silva CCD, and Cantarelli VS**. Benzoic acid in nursery diets increases the performance from weaning to finishing by reducing diarrhoea and improving the intestinal morphology of piglets inoculated with Escherichia coli K88(). *J Anim Physiol Anim Nutr (Berl)* 102: 1675-1685, 2018.

209. **Simpson KW, Dogan B, Rishniw M, Goldstein RE, Klaessig S, McDonough PL, German AJ, Yates RM, Russell DG, Johnson SE, Berg DE, Harel J, Bruant G, McDonough SP, and Schukken YH**. Adherent and invasive Escherichia coli is associated with granulomatous colitis in boxer dogs. *Infect Immun* 74: 4778-4792, 2006.

210. **Singh B, Fu C, and Bhattacharya J**. Vascular expression of the alpha(v)beta(3)-integrin in lung and other organs. *Am J Physiol Lung Cell Mol Physiol* 278: L217-226, 2000.

211. **Singh B, Janardhan KS, and Kanthan R**. Expression of angiostatin, integrin alphavbeta3, and vitronectin in human lungs in sepsis. *Exp Lung Res* 31: 771-782, 2005.

212. **Singh B, Pearce JW, Gamage LN, Janardhan K, and Caldwell S**. Depletion of pulmonary intravascular macrophages inhibits acute lung inflammation. *Am J Physiol Lung Cell Mol Physiol* 286: L363-372, 2004.

213. **Singh B, Rawlings N, and Kaur A**. Expression of integrin alphavbeta3 in pig, dog and cattle. *Histol Histopathol* 16: 1037-1046, 2001.

214. **Singh Suri S, Janardhan KS, Parbhakar O, Caldwell S, Appleyard G, and Singh B**. Expression of toll-like receptor 4 and 2 in horse lungs. *Vet Res* 37: 541-551, 2006.

215. **Sokurenko EV, Courtney HS, Abraham SN, Klemm P, and Hasty DL**. Functional heterogeneity of type 1 fimbriae of Escherichia coli. *Infect Immun* 60: 4709-4719, 1992.

216. **Sossey-Alaoui K, Pluskota E, Bialkowska K, Szpak D, Parker Y, Morrison CD, Lindner DJ, Schiemann WP, and Plow EF**. Kindlin-2 Regulates the Growth of Breast Cancer Tumors by Activating CSF-1-Mediated Macrophage Infiltration. *Cancer Res* 77: 5129-5141, 2017.

217. **Springer WR, Cooper DN, and Barondes SH**. Discoidin I is implicated in cell-substratum attachment and ordered cell migration of Dictyostelium discoideum and resembles fibronectin. *Cell* 39: 557-564, 1984.

218. **Stewart PL, and Nemerow GR**. Cell integrins: commonly used receptors for diverse viral pathogens. *Trends Microbiol* 15: 500-507, 2007.

219. **Sting R, and Stermann M**. Duplex real-time PCR assays for rapid detection of virulence genes in E. coli isolated from post-weaning pigs and calves with diarrhoea. *Dtsch Tierarztl Wochenschr* 115: 231-238, 2008.

220. **Stromblad S, and Cheresh DA**. Integrins, angiogenesis and vascular cell survival. *Chem Biol* 3: 881-885, 1996.

221. **Sun BO, Fang Y, Li Z, Chen Z, and Xiang J**. Advances in the application of nanotechnology in the diagnosis and treatment of gastrointestinal tumors. *Mol Clin Oncol* 3: 274-280, 2015.

222. **Sun Y, and Kim SW**. Intestinal challenge with enterotoxigenic Escherichia coli in pigs, and nutritional intervention to prevent postweaning diarrhea. *Anim Nutr* 3: 322-330, 2017.

223. **Suri SS, Fenniri H, and Singh B**. Nanotechnology-based drug delivery systems. *J Occup Med Toxicol* 2: 16, 2007.

224. **Suri SS, Fenniri H, and Singh B**. Rosette nanotubes for targeted drug delivery. In: *Nanomaterials for the Life Sciences - Polymeric Nanomaterials*, edited by Kuma CSSR. Weinheim: WILEY-VCH 2011, p. 493-508.

225. **Suri SS, Mills S, Aulakh GK, Rakotondradany F, Fenniri H, and Singh B**. RGD-tagged helical rosette nanotubes aggravate acute lipopolysaccharide-induced lung inflammation. *Int J Nanomedicine* 6: 3113-3123, 2011.

226. **Suri SS, Rakotondradany F, Myles AJ, Fenniri H, and Singh B**. The role of RGD-tagged helical rosette nanotubes in the induction of inflammation and apoptosis in human lung adenocarcinoma cells through the P38 MAPK pathway. *Biomaterials* 30: 3084-3090, 2009.

227. **Suzuki S, Argraves WS, Pytela R, Arai H, Krusius T, Pierschbacher MD, and Ruoslahti E**. cDNA and amino acid sequences of the cell adhesion protein receptor recognizing vitronectin reveal a transmembrane domain and homologies with other adhesion protein receptors. *Proc Natl Acad Sci U S A* 83: 8614-8618, 1986.

228. **Syrkina MS, Shirokov DA, Rubtsov MA, Kadyrova EL, Veiko VP, and Manuvera VA**. Preparation and functional evaluation of RGD-modified streptavidin targeting to integrin-expressing melanoma cells. *Protein Eng Des Sel* 26: 143-150, 2013.

229. **Takada Y, Ye X, and Simon S**. The integrins. *Genome Biol* 8: 215, 2007.

230. **Takagi J, Petre BM, Walz T, and Springer TA**. Global conformational rearrangements in integrin extracellular domains in outside-in and inside-out signaling. *Cell* 110: 599-511, 2002.

231. **Tamkun JW, DeSimone DW, Fonda D, Patel RS, Buck C, Horwitz AF, and Hynes RO**. Structure of integrin, a glycoprotein involved in the transmembrane linkage between fibronectin and actin. *Cell* 46: 271-282, 1986.

232. **Tchesnokova V, Aprikian P, Yakovenko O, Larock C, Kidd B, Vogel V, Thomas W, and Sokurenko E**. Integrin-like allosteric properties of the catch bond-forming FimH adhesin of Escherichia coli. *J Biol Chem* 283: 7823-7833, 2008.

233. **Tenaillon O, Skurnik D, Picard B, and Denamur E**. The population genetics of commensal Escherichia coli. *Nat Rev Microbiol* 8: 207-217, 2010.

234. **Thapar N, and Sanderson IR**. Diarrhoea in children: an interface between developing and developed countries. *Lancet* 363: 641-653, 2004.

235. **The Royal Society tUnaos, and the Royal Academy of Engineering, the UK national academy of engineering,**. Nanoscience and nanotechnologies: opportunities and uncertainties. *Press and Public Relations, The Royal Society, London* 2004.

236. **Thomas DD, Baseman JB, and Alderete JF**. Fibronectin tetrapeptide is target for syphilis spirochete cytadherence. *J Exp Med* 162: 1715-1719, 1985.

237. **Tizard IR**. *Veterinary Immunology - chapter 25: Immunity to bacteria and fungi*. Elsevier, 2013.

238. **Tseng M, Fratamico PM, Manning SD, and Funk JA**. Shiga toxin-producing Escherichia coli in swine: the public health perspective. *Anim Health Res Rev* 15: 63-75, 2014.

239. **Tsukada H, Ying X, Fu C, Ishikawa S, McKeown-Longo P, Albelda S, Bhattacharya S, Bray BA, and Bhattacharya J**. Ligation of endothelial alpha v beta 3 integrin increases capillary hydraulic conductivity of rat lung. *Circ Res* 77: 651-659, 1995.

240. **Turner SM, Scott-Tucker A, Cooper LM, and Henderson IR**. Weapons of mass destruction: virulence factors of the global killer enterotoxigenic Escherichia coli. *FEMS Microbiol Lett* 263: 10-20, 2006.

241. **Van den Broeck W, Cox E, and Goddeeris BM**. Receptor-dependent immune responses in pigs after oral immunization with F4 fimbriae. *Infect Immun* 67: 520-526, 1999.

242. **Van den Broeck W, Cox E, and Goddeeris BM**. Receptor-specific binding of purified F4 to isolated villi. *Vet Microbiol* 68: 255-263, 1999.

243. **van der Flier A, and Sonnenberg A**. Function and interactions of integrins. *Cell Tissue Res* 305: 285-298, 2001.

244. **Vandenbroucke V, Croubels S, Martel A, Verbrugghe E, Goossens J, Van Deun K, Boyen F, Thompson A, Shearer N, De Backer P, Haesebrouck F, and Pasmans F**. The mycotoxin deoxynivalenol potentiates intestinal inflammation by Salmonella typhimurium in porcine ileal loops. *PLoS One* 6: e23871, 2011.

245. **Varner JA, and Cheresh DA**. Integrins and cancer. *Curr Opin Cell Biol* 8: 724-730, 1996.

246. **Vaure C, and Liu Y**. A comparative review of toll-like receptor 4 expression and functionality in different animal species. *Front Immunol* 5: 316, 2014.

247. **Vila J, Saez-Lopez E, Johnson JR, Romling U, Dobrindt U, Canton R, Giske CG, Naas T, Carattoli A, Martinez-Medina M, Bosch J, Retamar P, Rodriguez-Bano J, Baquero F, and Soto SM**. Escherichia coli: an old friend with new tidings. *FEMS Microbiol Rev* 40: 437-463, 2016.

248. **Vuori K, and Ruoslahti E**. Association of insulin receptor substrate-1 with integrins. *Science* 266: 1576-1578, 1994.

249. **Walker RI**. New vaccines against enteric bacteria for children in less developed countries. *Expert Rev Vaccines* 4: 807-812, 2005.

250. **Walmsley GG, McArdle A, Tevlin R, Momeni A, Atashroo D, Hu MS, Feroze AH, Wong VW, Lorenz PH, Longaker MT, and Wan DC**. Nanotechnology in bone tissue engineering. *Nanomedicine* 2015.

251. **Wang B, Dolinski BM, Kikuchi N, Leone DR, Peters MG, Weinreb PH, Violette SM, and Bissell DM**. Role of alphavbeta6 integrin in acute biliary fibrosis. *Hepatology* 46: 1404-1412, 2007.

252. **Wang X, Huang DY, Huong SM, and Huang ES**. Integrin alphavbeta3 is a coreceptor for human cytomegalovirus. *Nat Med* 11: 515-521, 2005.

253. **Wang Y, Fang R, Yuan Y, Hu M, Zhou Y, and Zhao J**. Identification of host proteins interacting with the integrin-like A domain of Toxoplasma gondii micronemal protein MIC2 by yeast-two-hybrid screening. *Parasit Vectors* 7: 543, 2014.

254. **Watarai M, Funato S, and Sasakawa C**. Interaction of ipa proteins of Shigella flexneri with alpha(5)beta(1) integrin promotes entry of the bacteria into mammalian cells. *J Exp Med* 183: 991-999, 1996.

255. **Weis SM, and Cheresh DA**. alphaV integrins in angiogenesis and cancer. *Cold Spring Harb Perspect Med* 1: a006478, 2011.

256. **Weis SM, and Cheresh DA**. Tumor angiogenesis: molecular pathways and therapeutic targets. *Nat Med* 17: 1359-1370, 2011.

257. **Westerlund B, and Korhonen TK**. Bacterial proteins binding to the mammalian extracellular matrix. *Mol Microbiol* 9: 687-694, 1993.

258. **Westerlund B, van Die I, Kramer C, Kuusela P, Holthofer H, Tarkkanen AM, Virkola R, Riegman N, Bergmans H, Hoekstra W, and et al.** Multifunctional nature of P fimbriae of uropathogenic Escherichia coli: mutations in fsoE and fsoF influence fimbrial binding to renal tubuli and immobilized fibronectin. *Mol Microbiol* 5: 2965-2975, 1991.

259. **Wickham TJ, Mathias P, Cheresh DA, and Nemerow GR**. Integrins alpha v beta 3 and alpha v beta 5 promote adenovirus internalization but not virus attachment. *Cell* 73: 309-319, 1993.

260. **Wilder RL**. Integrin alpha V beta 3 as a target for treatment of rheumatoid arthritis and related rheumatic diseases. *Ann Rheum Dis* 61 Suppl 2: ii96-99, 2002.

261. **Wolf MK**. Occurrence, distribution, and associations of O and H serogroups, colonization factor antigens, and toxins of enterotoxigenic Escherichia coli. *Clin Microbiol Rev* 10: 569-584, 1997.

262. **Wu CH, Ko JL, Pan HH, Chiu LY, Kang YT, and Hsiao YP**. Ni-induced TGF-beta signaling promotes VEGF-a secretion via integrin beta3 upregulation. *J Cell Physiol* 2019.

263. **Xia P, Quan G, Yang Y, Zhao J, Wang Y, Zhou M, Hardwidge PR, Zhu J, Liu S, and Zhu G**. Binding determinants in the interplay between porcine aminopeptidase N and enterotoxigenic Escherichia coli F4 fimbriae. *Vet Res* 49: 23, 2018.

264. **Xia Y, Bin P, Liu S, Chen S, Yin J, Liu G, Tang Z, and Ren W**. Enterotoxigenic Escherichia coli infection promotes apoptosis in piglets. *Microb Pathog* 125: 290-294, 2018.

265. **Xia Y, Chen S, Zhao Y, Chen S, Huang R, Zhu G, Yin Y, Ren W, and Deng J**. GABA attenuates ETEC-induced intestinal epithelial cell apoptosis involving GABAAR signaling and the AMPK-autophagy pathway. *Food Funct* 2019.

266. **Xiong JP, Stehle T, Diefenbach B, Zhang R, Dunker R, Scott DL, Joachimiak A, Goodman SL, and Arnaout MA**. Crystal structure of the extracellular segment of integrin alpha Vbeta3. *Science* 294: 339-345, 2001.

267. **Zhang J, Teh M, Kim J, Eva MM, Cayrol R, Meade R, Nijnik A, Montagutelli X, Malo D, and Jaubert J**. A loss-of-function mutation in the integrin alpha L (Itgal) gene contributes to susceptibility to Salmonella Typhimurium infection in Collaborative Cross strain CC042. *Infect Immun* 2019.

268. **Zhang L, Rakotondradany F, Myles AJ, Fenniri H, and Webster TJ**. Arginine-glycine-aspartic acid modified rosette nanotube-hydrogel composites for bone tissue engineering. *Biomaterials* 30: 1309-1320, 2009.

269. **Zhang L, Ramsaywack S, Fenniri H, and Webster TJ**. Enhanced osteoblast adhesion on self-assembled nanostructured hydrogel scaffolds. *Tissue Eng Part A* 14: 1353-1364, 2008.

270. **Zhang L, Rodriguez J, Raez J, Myles AJ, Fenniri H, and Webster TJ**. Biologically inspired rosette nanotubes and nanocrystalline hydroxyapatite hydrogel nanocomposites as improved bone substitutes. *Nanotechnology* 20: 175101, 2009.

271. **Zhang W, Zhao M, Ruesch L, Omot A, and Francis D**. Prevalence of virulence genes in Escherichia coli strains recently isolated from young pigs with diarrhea in the US. *Vet Microbiol* 123: 145-152, 2007.

272. **Zhou BH, Tan PP, Jia LS, Zhao WP, Wang JC, and Wang HW**. PI3K/AKT signaling pathway involvement in fluoride-induced apoptosis in C2C12cells. *Chemosphere* 199: 297-302, 2018.

273. **Zhu C, Ye JL, Yang J, Yang KM, Chen Z, Liang R, Wu XJ, Wang L, and Jiang ZY**. Differential expression of intestinal ion transporters and water channel aquaporins in young piglets challenged with enterotoxigenic Escherichia coli K88. *J Anim Sci* 95: 5240-5252, 2017.